Dimension Dependence of the Critical Phenomena in Gravitational Collapse of Massless Scalar Field

by

Jason Bryan Bland

A Thesis

submitted to the Faculty of Graduate Studies of

The University of Manitoba

in partial fulfilment of the requirements of the degree of

Doctor of Philosophy

DEPARTMENT OF PHYSICS AND ASTRONOMY

THE UNIVERSITY OF MANITOBA

WINNIPEG, MANITOBA

CANADA

THE UNIVERSITY OF MANITOBA

FACULTY OF GRADUATE STUDIES

*****

COPYRIGHT PERMISSION

Dimension Dependence of the Critical

Phenomena in Gravitational Collapse of

Massless Scalar Field

BY

Jason Bryan Bland

A Thesis/Practicum submitted to the Faculty of Graduate Studies of The University of

Manitoba in partial fulfillment of the requirement of the degree

Doctor of Philosophy

ABSTRACT

A study of the critical behaviour which is observed in numerical calculations of spherically symmetric scalar field collapse has been performed. The gravitational collapse calculations are carried out using the field equations of Einstein's general theory of relativity in the context of a two dimensional dilaton gravity theory.

The problem is formulated by considering a spherically symmetric matter distribution in an arbitrary number of space-time dimensions greater than three. A spherical distribution will only depend on two space-time coordinates, therefore, the action of the model can be reduced to a specific case of a $1 + 1$ dilaton gravity theory. The evolution equations of the problem are simplified by carrying out a conformal transformation of the metric field. The number of space-time dimensions then appears as an input parameter of the field equations. Initial data is defined on a discrete space-time grid and numerical simulations of gravitational collapse are carried out. The computer

code is optimized to increase numerical stability near the critical solutions.

Discrete self-similarity and mass scaling in the near critical solutions are observed for each of the dimensions studied. The critical phenomena are described with a high level of confidence by smooth functions of space-time dimension. It is hypothesized that the critical solution of the theory at the limit of large dimension is discretely self-similar with a period of 5/2 and contains critical scaling with a constant of 1/2. Evidence will also be presented which suggests the critical solution in three dimensions with zero cosmological constant is not discretely self-similar but contains a critical scaling constant of approximately 0.11.

ACKNOWLEDGMENTS

I am especially grateful to my supervisor Gabor Kunstatter for his patience, guidance and financial support throughout my PhD studies. Gabor is very knowledgeable and experienced in theoretical physics and is an excellent choice for any physics student looking for an advisor and mentor. It has been a great privilege for me to have worked with Gabor. I'd like to thank my local committee members: Randy Kobes, Balram Bhakar, and Ken Friesen, for their advice and patience in seeing this thesis to its completion. I'd also like to thank my external, David Garfinkle, for his helpful comments and for making the trip to Winnipeg for my thesis defence.

I would like to thank the faculty and staff at the Department of Physics and Astronomy at the University of British Columbia for making me feel very comfortable and welcome during my study in Vancouver. Thank you Roman Petryk for helpful discussions and advice. I'd also like to send a special thank you to Shirin, Dastegir, Mehran and Ali for all those fun nights!

I would like to thank my friend Dave. You've always been there (countless times) to pick me up when I fall down and one could not ask for a better friend. I'd also like to thank Clint, Hani and Tim, and especially Charlie for her encouragement and pep talks throughout these (occasionally) long years. I give my warmest regards to Natasha for her companionship, inspiration, and many interesting conversations. I wish you health and every happiness in the future.

I'd like to thank my big sister Shelley for her encouragement, love and support. Thanks to Charles, Chris, and our newest Sam! You all rock and I wish you the best. Thank you for the time we have shared in Victoria.

No part of this project could have been possible without the love and support of my Mom and Dad. You've always stood behind me, helped me in whatever way you could, and I thank you for making me the most fortunate son in all the world. I love you both very much.

CONTENTS

LIST OF TABLES

LIST OF FIGURES

1. INTRODUCTION

It has long been known that strong field dynamics in gravitational collapse produces universal, or critical, solutions. These critical solutions are interpreted as one parameter attractors in phase space. They have the properties of universality, scaling, as well as discrete and continuous self-similarity, for all varieties of initial matter shapes and profiles. The solutions do, however, have some dependence on initial matter field type (for example, scalar field versus yang-mills field) as well as a dependence on space-time dimension.

In this thesis I examine spherically symmetric scalar field collapse. The system represents one of the most simple dynamical problems available. Despite the simplicity of this system, properties of critical solutions are found. The critical solutions will be analyzed numerically by constructing a discrete grid in space and time and solving the evolution equations at each grid point. In this way the problem is simplified by simultaneously solving a set of linear differential equations. However, the problem is complicated by the

discretization process which introduces a numerical error at each grid point. The numerical errors can lead to instabilities in the evolution procedure. A particular sequence of grid spacing refinements will be used to maintain stability of the evolution for as many iterations necessary to extract useful data.

In d space-time dimensions, the action for the model can be reduced to a $1+1$ dilaton gravity theory. Using an appropriate conformal redefinition of the metric field, the kinetic term in the action (a term bilinear in the dilaton field) is eliminated which will further simplify the field equations derived in the model. The space-time dimension of the fields then appears as a parameter of the evolution equations once a coordinate system is chosen.

Initial data is defined and the values of the fields are calculated at each grid point on the initial hypersurface. The evolution equations and boundary conditions determine the values of the fields on the adjacent hypersurface and the system is allowed to evolve over several iterations to one of two classes of solutions. Initial data can evolve to a final state which contains a black hole or one that does not. Initial data which evolves to a black hole solution are called *supercritical*, whereas, data which do not form a black hole are called *subcritical*. The initial data parameters which lead to the solution separating

these two states are called *critical* parameters.

The scaling constant and discrete self-similarity constant have been measured in supercritical collapse as a function of space-time dimension. Functional forms of the critical constants as functions of d are found for space-time dimension $3 < d \leq 14$. In both cases, these forms will be used to extrapolate a value of the scaling and discrete self-similarity constant for $d = 3$ and $d \to \infty$.

This thesis is divided into five chapters. The second chapter introduces and presents the relevant aspects of numerical relativity in the context of the dimension dependence of critical phenomena observed in gravitational collapse. The field equations and formalism of the model is presented in chapter three by first parameterizing in the context of a $1 + 1$ dilaton gravity theory, then deriving the evolution equations and choosing boundary conditions. In chapter four, the method is described and the results of the numerical analysis are presented together with a hypothesis on the nature of the critical solution at the small and large d limits of the theory. In the concluding chapter a summary of the results of the thesis is presented along with an objective for future research.

1.1 Einstein's Field Equations

Einstein's General Theory of Relativity is a generally covariant theory of gravity based on the principle of relativity [1]. The theory is a generalization of the Special Theory of Relativity to non-Euclidean manifolds. In the General theory the space-time continuum is an m dimensional continuously differentiable Riemannian space-time manifold $\mathcal{M}$ [2]. The manifold is covered with a Lorentz metric field $g_{\mu\nu}$ which divides vectors into three classes: spacelike, timelike, and null. At each point in the manifold $p \in \mathcal{M}$ we can choose locally inertial coordinates so that at p the metric field takes on the Minkowksi values. In general, however, the global structure of the space-time does not remain Minkowski.

The most general field equations which possess general covariance and contain at most second derivatives of the metric are given by the Einstein field equations with cosmological constant [3]:

$$R_{\mu\nu} - \frac{1}{2} g_{\mu\nu} R + \frac{1}{2} g_{\mu\nu} \Lambda = 8\pi T_{\mu\nu}, \tag{1.1}$$

where $R_{\mu\nu}$ is the Ricci curvature tensor, R is the curvature scalar, Λ is the cosmological constant, $T_{\mu\nu}$ is the energy momentum tensor of matter, G is

the Newtonian coupling constant (a number which determines the strength of the gravitational interaction), c is the speed of light, and 8π is the matter coupling constant in relativistic units $G = c = 1$.

Soon after Einstein published his General theory, Schwarzschild [4] found a solution which described the space-time external to a mass point located at the origin of coordinates. In spherical coordinates (r, t), the Schwarzschild line element is given by

$$ds^2 = -\left(1 - \frac{2GM}{r}\right) dt^2 + \left(1 - \frac{2GM}{r}\right)^{-1} dr^2 + r^2 d\Omega^2, \qquad (1.2)$$

where, M is the mass of the matter distribution, and $d\Omega^2$ is the metric on the two-sphere with unit radius.

One of the more intriguing aspects of this solution is the existence of the coordinate singularities in the metric. Specifically, supposing all the mass resides within a sphere of radius $2GM$, what can we expect to observe on the surface $r = 2GM$? And what about below this surface? If one examines the radial light rays in Painlevé-Güllstrand coordinates [5, 6, 7], it is found [8] that

$$\frac{dr}{dt} = -\sqrt{\frac{2GM}{r}} \pm 1, \qquad (1.3)$$

where dr/dt measures the local speed of radial light rays. Thus, at $r = 2GM$ one notices that $dr/dt = 0, -2$. This means that outgoing radial light rays are standing still whereas ingoing light rays continue to approach the coordinate origin. Moreover, for $r < 2GM$, it is seen that $dr/dt < 0$ for both ingoing and outgoing light rays meaning that the surface, or boundary, $r = 2GM$, encloses a volume of space-time which is causally removed from the rest of space-time. This boundary is called the event horizon and is interpreted as the boundary of a black hole.

In the 1960's, the singularity theorems showed that an essential singularity (a point of infinite space-time curvature) must always occur once a closed trapped surface[1] has formed, independent of matter type or symmetry. Prior to these theorems, Oppenheimer and Snyder [10] showed explicitly, in 1939, that a black hole could be formed dynamically as the end point of gravitational collapse. Despite its very interesting properties, gravitational collapse and the black holes which are subsequently formed did not receive very much attention in the 1940's and 1950's on account of the rise of quantum mechanics.

In 1976, Davies, Fulling and Unruh [11] demonstrated using a two dimen-

[1] In 1965, Penrose defined a trapped surface as a closed, spacelike, two-surface with the property that orthogonal null geodesics converge locally in future directions [9].

sional model that, in the case of massless scalar field, black holes evaporate over time by contributing to the thermal flux at infinity. This result was consistent with Hawking's earlier speculations that quantum mechanical effects will cause black holes to radiate away thermal energy in proportion to their surface gravity [12]. In both of these cases, one attempts to include quantum mechanical effects in the gravitational field by only quantizing the matter field in a background stationary solution of the classical gravitational field equations.

The non-linearity of the gravitational field equations often makes analytical solutions difficult or even impossible to obtain. Numerical relativity offers insights to the dynamics of gravitational collapse by solving the field equations iteratively using computer code. For a recent review on numerical relativity, see Gundlach [13] and Lehner [14]. In 1987, Goldwirth and Piran [15] studied the numerical collapse of massless scalar fields in spherical symmetry. They observed that black holes form in the space-time for certain configurations of initial field matter. In other cases, for weaker initial field matter, the matter dispersed to infinity. Unfortunately, the data were not sufficiently accurate for a detailed analysis of the central (physical) singularity. Nevertheless, numerical relativity appeared to be capable of addressing

the issue of the cosmic censorship conjectures.

The weak cosmic censorship conjecture affirms that all singularities arising, generically, from the gravitational collapse of matter must be hidden behind a black hole horizon and are thus hidden from any distant observer. The conjecture has never been proven (nor disproven) [16] but the consequences of its validity would forbid the existence of naked singularities[2].

Intuitively, it seems reasonable to expect that sufficiently small amounts of matter, parameterized by sufficiently small-valued initial data, would, at late evolution times, disperse leaving the space-time free of singularities. Indeed, this has been shown for certain types of matter [17, 18]. On the other hand, sufficiently large-valued initial data would be expected to collapse to form a black hole and a singularity. But even until the early 1990's little was known of the nature of dynamical gravitational collapse nor of what might happen in the collapse of matter which was neither "sufficiently small" or "sufficiently large".

Beginning in the early 1990's, Choptuik began a systematic numerical study of the gravitational collapse of a minimally coupled spherically symmetric massless scalar field [19]. He found several surprising properties in the

[2] A naked singularity is a singular point in a space-time which is visible to distant observers. See, Hawking and Ellis [2] for more on the singularity theorems.

dynamics of collapse including the appearance of naked singularities. This finding appeared to violate the cosmic censorship conjectures.

Penrose describes the cosmic censorship conjecture in the following way: Any generic suitable non-singular initial data which evolves according to the field equations of classical general relativity will not develop any space-time singularity visible from infinity [20]. This would mean that even an observer falling behind the event horizon into a Schwarzschild black hole would not observe the central singularity until they had met their fate. In 1981, Moncrief and Eardley [21] reformulated the cosmic censorship conjectures in the context of a global existence conjecture for solutions of the Einstein field equations.

Some form of cosmic censorship is essential for general relativity because the existence of naked singularities in a space-time would not allow predictions of stable future evolution in regions outside of the horizon. This would happen because arbitrary pieces of information from within the singularity could be visible from infinity thus modifying, in some arbitrary way, the physics of the rest of the universe. Without the censorship conjectures general relativity theory could predict its own demise.

Nevertheless, in 1991, Shapiro and Tuekolsky [22] were one of the first

to numerically observe naked singularities during the collapse of collisionless gas spheroids. The black holes formed in this system where found to be consistent with the hoop conjecture which states that black holes with mass M will always form whenever that mass is compacted within a region whose circumference in every direction is $\leq 4\pi M$. For initial data with sufficiently large valued semi-major axis the authors observed *spindle* singularities without an apparent horizon thus suggesting a violation of the cosmic censorship conjectures.

Christodoulou [23] provided analytic examples of naked singularity formation in scalar field collapse. In an important extension to this earlier work, Christodoulou [24] later argued that because the naked singularities found in scalar field collapse have positive codimension they are necessarily unstable phenomena. This would suggest that, for the case of scalar field, one has not yet lost cosmic censorship.

1.2 Conventions

Einstein summation is implied over repeated indices on tensors, e.g.

$$T^{\mu}_{\nu\mu} = \sum_{a=1}^{m} T^{a}_{\nu a}, \tag{1.4}$$

where m is the number of independent coordinates and $T^{\sigma}_{\nu\mu}$ is an arbitrary mixed tensor. The metric tensor $g_{\mu\nu}$ is defined by

$$ds^2 = g_{\mu\nu}dx^{\mu}dx^{\nu}, \tag{1.5}$$

where ds is the infinitesimal distance measure between adjacent points in the manifold. The metric tensor is also the covariant tensor used to lower contravariant indices, therefore,

$$T_{\mu\nu} = g_{\mu\alpha}g_{\nu\beta}T^{\alpha\beta}. \tag{1.6}$$

The inverse of the metric tensor is the contravariant tensor $g^{\mu\nu}$ defined by

$$g^{\mu\nu}g_{\nu\sigma} = \delta^{\mu}_{\sigma}, \tag{1.7}$$

where δ^{μ}_{σ} is the kronecker delta. For two dimensional spaces, we use a metric signature of $(-+)$. For higher dimensional spaces, the metric signature we use is $(-+\cdots+)$. The length or norm of a vector X^{μ} is given by

$$X^2 = X_{\mu}X^{\mu} = g_{\mu\nu}X^{\mu}X^{\nu}. \tag{1.8}$$

Using our convention: vectors are timelike if $X^2 < 0$, spacelike if $X^2 > 0$, and null if $X^2 = 0$. We also define

$$(\nabla\chi)^2 = \nabla_\mu\chi\nabla^\mu\chi = g^{\mu\nu}\nabla_\mu\chi\nabla_\nu\chi. \tag{1.9}$$

The metric determinant is defined such that

$$\sqrt{-g} = [-\det(\mathbf{g})]^{1/2} \tag{1.10}$$

is a scalar density of weight +1. Therefore, a tensor density for an arbitrary tensor $T^{\mu\nu}$ can be constructed by forming the product $(\sqrt{-g}T^{\mu\nu})$. The Christoffel connection is given by [3]

$$\Gamma^\lambda_{\mu\nu} = \frac{1}{2}g^{\lambda\sigma}\left(\frac{\partial g_{\nu\sigma}}{\partial x^\mu} + \frac{\partial g_{\sigma\mu}}{\partial x^\nu} - \frac{\partial g_{\mu\nu}}{\partial x^\sigma}\right). \tag{1.11}$$

Alternative notation for the partial differentiation of a tensor $T_{\mu\nu}$ is given by

$$\frac{\partial T_{\mu\nu}}{\partial x^\lambda} = \partial_\lambda T_{\mu\nu} = T_{\mu\nu,\lambda}. \tag{1.12}$$

Covariant differentiation of a mixed tensor T^{ν}_{μ} is given by [3]

$$\nabla_{\lambda} T^{\nu}_{\mu} = T^{\nu}_{\mu;\lambda} = T^{\nu}_{\mu,\lambda} + \Gamma^{\nu}_{\lambda\sigma} T^{\sigma}_{\mu} - \Gamma^{\sigma}_{\lambda\mu} T^{\nu}_{\sigma}. \tag{1.13}$$

The d'Alembertian operator is given by

$$\Box = \nabla_{\mu} \nabla^{\mu} = g^{\mu\nu} \nabla_{\mu} \nabla_{\nu}. \tag{1.14}$$

The Riemann-Christoffel curvature tensor is given by [3]

$$R^{\lambda}_{\mu\nu\sigma} = \Gamma^{\lambda}_{\mu\nu,\sigma} - \Gamma^{\lambda}_{\mu\sigma,\nu} + \Gamma^{\eta}_{\mu\nu} \Gamma^{\lambda}_{\sigma\eta} - \Gamma^{\eta}_{\mu\sigma} \Gamma^{\lambda}_{\nu\eta}. \tag{1.15}$$

The Ricci tensor is obtained by contraction of the curvature tensor

$$R_{\mu\nu} = R^{\sigma}_{\mu\sigma\nu} \tag{1.16}$$

and the curvature scalar is given by

$$R = g^{\mu\nu} R_{\mu\nu}. \tag{1.17}$$

2. REVIEW OF THE CRITICAL PHENOMENA IN GRAVITATIONAL COLLAPSE

In this chapter, a review of the critical phenomena observed in numerical calculations of gravitational collapse is presented. The first section focuses on the numerical solution first reported by Choptuik in massless scalar field collapse. Choptuik found a universal critical solution in the numerical collapse of scalar field matter with spherical symmetry in a $3+1$ dimensional space-time. The properties of this critical solution are discussed. Although the focus will remain largely on scalar field matter types, I include in Section 2.1.1 a brief discussion on the critical phenomena observed in gravitational collapse of other matter types.

Scalar field collapse in space-time dimensions other than $3+1$ will be discussed in Section 2.2. The section begins with a review of the BTZ black hole in three dimensions and the interesting properties of this solution. The three dimensional space-time is interesting because it only admits black hole solu-

tions when a constant curvature term, i.e. cosmological constant, is included in the action. In the literature, there exists numerical and analytic evidence that the solution of scalar field collapse in three dimensions with cosmological constant is a universal critical solution with continuous self-similarity.

The chapter is concluded by discussing contemporary theory on critical phenomena (Section 2.3). Critical solutions in gravitational collapse are qualitatively similar to phase transitions and critical phenomena observed in statistical physics. They display symmetry breaking, self-similarity, and power law scaling. These concepts will also be discussed.

2.1 *Choptuik Scalar Field Collapse in* $3+1$

Choptuik was first to discover critical behaviour in the gravitational collapse of a massless scalar field [19]. He evolved one parameter families of initial data and found that the matter field collapsed to form one of two possible end states. The data either formed a black hole solution or dispersed to spatial infinity leaving behind asymptotically flat space. The initial data could, in general, be parameterized by several parameters. If one parameter was allowed to vary while the others remain fixed the end state of the evolution would depend on the initial value of this one parameter.

Choptuik denoted an initial parameter by a and the solution to the evolution equations which depend on a by $\mathcal{S}[a]$. For sufficiently large concentrations of matter, corresponding to sufficiently large values of a, a black hole would form in the space-time. These types of solutions are conventionally referred to as supercritical. On the other hand, for sufficiently small values of a the matter would eventually disperse. These solutions are conventionally referred to as subcritical. Choptuik demonstrated explicitly that there existed a critical value, $a_* \in a$, which separates black hole from dispersion solutions and that the critical solution—i.e., $\mathcal{S}[a_*]$—is a universal solution independent of the family of initial data.

Choptuik considered the evolution of four distinct families of initial data with each family described by two or more parameters. In each case one of the parameters was allowed to vary until the critical value of that parameter was determined (within machine precision). Choptuik found that all supercritical solutions with $a \sim a_*$ contain black holes with mass satisfying a power law with the same critical exponent. Below, we formulate Choptuik's model.

Consider a minimally coupled massless scalar field, χ, coupled to the

gravitational field $g_{\mu\nu}$. The energy-momentum tensor for the field is given by

$$T_{\mu\nu} = \nabla_\mu \chi \nabla_\nu \chi - \frac{1}{2} g_{\mu\nu} \nabla_\sigma \chi \nabla^\sigma \chi, \tag{2.1}$$

where the matter field is subject to the Klein-Gordon equation

$$\Box \chi = 0. \tag{2.2}$$

The Einstein field equations for the system considered by Choptuik are given by

$$G_{\mu\nu} = R_{\mu\nu} - \frac{1}{2} g_{\mu\nu} R = 8\pi T_{\mu\nu}. \tag{2.3}$$

Notice in the above equation that we have dropped the cosmological term from (1.1). In generally covariant form, the massless Klein-Gordon equation is

$$\frac{1}{\sqrt{-g}} \partial_\mu \left(\sqrt{-g} g^{\mu\nu} \partial_\nu \chi \right) = 0. \tag{2.4}$$

Consider further that the system is spherically symmetric so that the following time-dependent Schwarzschild-like, metric tensor can be defined on

the manifold:

$$ds^2 = -\alpha^2(r,t)\,dt^2 + \beta^2(r,t)\,dr^2 + r^2 d\Omega^2, \tag{2.5}$$

where, the radial coordinate r measures the proper surface area, t is a time coordinate, $\alpha(r,t)$ and $\beta(r,t)$ are metric functions dependent on only two coordinates, and $d\Omega^2$ is the metric on the two-sphere with unit radius. The field equations in these coordinates yield four non-vanishing equations [4]. Only three of the field equations are independent due to the Bianchi identities (see page 95). Choptuik chose to evolve initial data via the following two field equations:

$$G_0^0 = \frac{1}{r\beta^2}\left(\frac{2\beta'}{\beta} - \frac{1}{r}\right) + \frac{1}{r^2} = 8\pi T_0^0 \tag{2.6}$$

$$G_0^0 + G_1^1 = \frac{2}{r\beta^2}\left(\frac{\beta'}{\beta} - \frac{\alpha'}{\alpha} - \frac{1}{r}\right) + \frac{2}{r^2} = 8\pi\left(T_0^0 + T_1^1\right), \tag{2.7}$$

where a prime indicates partial differentiation with respect to the coordinate r.

During the calculation, Choptuik monitored the total conserved mass, M,

of the space-time. From (2.6), the total mass is

$$M = \int_0^\infty 4\pi r^2 T_0^0 dr = \int_0^\infty \left(\frac{dm}{dr}\right) dr, \tag{2.8}$$

where the mass aspect function m is related to the metric (2.5) via

$$\left(1 - \frac{2m}{r}\right) = \frac{1}{\beta^2}. \tag{2.9}$$

Choptuik evolved several one parameter families of initial data profiles using finite difference techniques and an adaptive mesh refinement algorithm which varied the local grid spacings in response to the development of solution structure. The mesh refinement technique used by Choptuik was a specialized version of a method developed for hyperbolic partial differential equations and enabled a more accurate analysis of the problem than had been achieved previously.

Choptuik examined the strong field dynamics in the regime of solutions near the critical solution of the model. In this region, he found several interesting results: i) that arbitrarily small black holes could be formed in the space-time as one approaches the critical solution (from supercritical values of a); ii) near the critical solution, the masses of the black holes, M_{BH}, obey

the power law scaling relationship

$$M_{BH} \propto |a - a_*|^\gamma \tag{2.10}$$

where γ is a universal constant independent of the family of initial data; iii) the field profiles "echo", or repeat themselves, on increasingly smaller spatiotemporal scales. That is, the solutions exhibit discrete self-similarity. The results are summarized in more detail below.

Universal Critical Solutions

Some aspects of Choptuik's results were far from unexpected. For example, it had long been known that a black hole could be formed dynamically as the end point of gravitational collapse. This had already been shown explicitly by Oppenheimer and Snyder as we mentioned above. In contrast, it has been shown, at least for certain types of matter, that small amounts of initial matter will disperse leaving the space-time free of singularities [25]. What Choptuik set out to do in his research program was to determine what features gravitational collapse might have in the region separating these two extremes.

Choptuik conjectured that there exists a universal critical solution which

is independent of the family of initial data. Furthermore, that a zero mass black hole is formed in the space-time when the initial parameter is exactly tuned to the critical value. That is, the critical solution acted like a phase transition separating two distinct end states of collapse and as he fine tuned the initial parameter to near the critical value, Choptuik observed that the strong field gravitational dynamics "washed out" any information the fields contained of the initial data profile. Hence, all one-parameter families describing initial matter appeared to be attracted to the critical solution along the same path in phase space[1]. Moreover, the evolution of Choptuik's critical solution concluded in finite central proper time T_0^*. The proper time of a central observer is defined by

$$T_0 = \int_0^t \alpha\left(0, \tilde{t}\right) d\tilde{t}. \tag{2.11}$$

Hamadé and Stewart [26] also examined the gravitational collapse of a massless scalar field in spherical symmetry. Using a double-null coordinate chart and a similar algorithm to Choptuik, Hamadé and Stewart confirmed the critical behaviour in scalar field collapse. Along with verifying the uni-

[1] The phase space picture of critical phenomena in the context of gravitational collapse is treated in more detail below.

versal critical constants, they also showed that the scalar curvature R and scalar field energy density could reach arbitrarily large values in subcritical collapse.

In [27], Garfinkle and Duncan verified that the maximum curvature in subcritical collapse scaled via power law relationship similar to (2.10). They also observed that the scaling constant has the same value as the scaling constant seen in supercritical mass scaling.

In 1995, Garfinkle [28] reported verification of the critical phenomena in the Choptuik model using a null initial value formulation which did not use adaptive mesh refinement. To increase stability in the algorithm, Garfinkle expanded the matter and metric functions in a Taylor series near the center of symmetry and adjusted the grid size iteratively to maximize resolution in the result. In his study, Garfinkle also verified the discrete self-similarity in the critical solution.

Black Hole Mass Scaling

One of the interesting results of Choptuik's work was the discovery of universal black hole mass scaling. The mass of a black hole in dynamical gravitational collapse is estimated by observing the apparent formation of a closed

trapped surface and determining the position of the horizon. Black hole formation is signalled by $2m/r \to 1$ for some r_{BH}. The mass $M_{BH} = 2r_{BH}$ then immediately follows. The parameter value a describing the initial matter field profile which corresponded to the black hole solution with mass M_{BH} was stored in a data file. In the region near the critical solution, Choptuik collated the results (a, M_{BH}) for several a and found all one parameter families of initial data satisfied the power law

$$M_{BH} = c_F \left| a - a_* \right|^{\gamma} \tag{2.12}$$

where, c_F and a_* are family dependent constants, and $\gamma \sim 0.37$. Gundlach [29] later reported, via perturbation calculation, $\gamma = 0.374 \pm 0.001$ in the gravitational collapse of massless minimally coupled spherically symmetric scalar field. Several other authors have reported verification of $\gamma = 0.374$, including those mentioned above.

The initial data families Choptuik considered were:

$$\chi(r) = \chi_0 \, r^3 \exp\left(- \left[\frac{r - r_0}{\delta} \right]^q \right) \tag{2.13}$$

$$\chi(r) = \chi_0 \tanh\left(\frac{r - r_0}{\delta} \right) \tag{2.14}$$

$$\chi(r + r_0) \;=\; \chi_0\, r^{-5}\left[\exp\left(\frac{1}{r}\right) - 1\right]^{-1}. \qquad (2.15)$$

A fourth family was also considered whose initial profile was a weighted combination (weighting parameter η) of late-time fits to the subcritical and supercritical evolution profile of a square barrier pulse shape. In all cases, one of the parameters, either χ_0, r_0, δ, q, or η, were allowed to vary over several runs of the computer code. Critical values of the parameters were determined via binary search of subcritical and supercritical evolutions (to the limit of machine precision which was $|a - a_*|/a \approx 10^{-13}$). In this thesis, I will consider an initial family of data similar to (2.13).

Scale Echoing

Another of the fascinating and unexpected results of Choptuik's work was the discovery of the scale echoing or discrete self-similarity property of the solutions. In order to show the scale echoing of the fields in the critical solution, Choptuik introduced two new logarithmic variables ρ and τ given by

$$\rho = \log(kr) \qquad \tau = \log\left(k\left[T_0^* - T_0\right]\right). \qquad (2.16)$$

The constants k and T_0^* were family dependent constants which represented the scale invariance of the model. If Choptuik characterized a field profile of the critical solution—e.g. the curvature scalar, a metric function, or the matter scalar itself—in terms of the logarithmic variables as $Z^*(\rho, \tau)$ then the scale echoing of the field profiles was demonstrated by the relation:

$$Z^*(\rho - \Delta, \tau - \Delta) = Z^*(\rho, \tau), \tag{2.17}$$

where Δ is the discrete, or periodic, self-similarity constant [30].

The scale echoing relation could be more readily seen by freezing a near critical evolution at a certain time T_0 (which is near T_0^*), advancing the evolution by a time δT_0 and taking a snapshot of the field profiles (say, as a function of r). Then, at a later time $T_0 + \delta T_0(1 + e^{-\Delta})$ an identical profile was observed to repeat itself over a space scale e^{Δ} times smaller than the profile observed at the time $T_0 + \delta T_0$. This process of increasingly smaller scale echoes of field profiles was conjectured to repeat itself indefinitely in the critical solution.

Initially, Choptuik introduced a separate Δ_ρ and Δ_τ into (2.17) because he assumed the self-similarity would be different in the space and time di-

rections. However, after sufficient analysis it was found $\Delta_\rho = \Delta_\tau = \Delta$ (to within numerical accuracy). In his perturbation analysis, Gundlach [29] reported $\Delta = 3.4453 \pm 0.0005$ in the gravitational collapse of massless minimally coupled spherically symmetric scalar field.

The discrete self-similarity constant Δ was also conjectured to be a universal constant in scalar field collapse because each field profile Choptuik compared in his calculations exhibited the echoing property with the same Δ. Furthermore, the periodic nature of the critical solution manifests itself as a wiggle in the mass and curvature scalar power law scaling relationships. The relation between the periodic wiggle in the scaling relationship and the discrete self-similarity will be discussed in Section 2.3.3.

2.1.1 *Other Matter Models in* $3+1$

Since Choptuik's seminal paper on the subject, several other matter models have been used to study dynamical gravitational collapse to black holes. Universality, mass scaling and self-similarity have been shown to exist in the critical solutions of these other matter types.

In 1993, Abrahams and Evans [31] reported critical behaviour in the gravitational collapse of vacuum axisymmetric gravitational wave packets.

The near-critical solutions found in that case were remarkably similar to those found by Choptuik in scalar field collapse. Abrahams and Evans observed evidence of discrete self-similarity in the strong field region as well as black hole mass scaling approximately equal to the case of spherical massless scalar field ($\gamma \approx 0.37$).

Evans and Coleman [32] analyzed the gravitational collapse of radiation fluid[2] in spherical symmetry. They found mass scaling with a universal scaling constant of $\gamma \approx 0.36$ and demonstrated that the critical solution is continuously self-similar. Moreover, the solution they found was only locally self-similar due to the fact the space-time is not asymptotically flat. Koike, Hara and Adachi [33] performed a linear perturbation analysis, by employing a self-similarity ansatz based on the Evans and Coleman solution. They presented a general method of predicting the mass scaling constant using the largest exponent of the perturbation. Using this perturbation method they show that in the case of radiation fluid one should expect a mass scaling constant $\gamma \approx 0.355\,801\,92$ which was in remarkable agreement with the Evans and Coleman result.

[2] Radiation fluid is perfect fluid matter with pressure, p, and energy density, ρ, related by $p = \frac{1}{3}\rho$. The energy-momentum tensor for perfect fluid is given by $T_{\mu\nu} = \rho u_\mu u_\nu + p\,(g_{\mu\nu} + u_\mu u_\nu) = p\,(g_{\mu\nu} + 4u_\mu u_\nu)$ where u^μ is the four-velocity of fluid particles.

In 1996, Maison [34] was one of the first to suggest that *universal* critical solutions found in gravitational collapse may be, in fact, unique for different matter types. He found in the case of a perfect fluid that the mass scaling constant was dependent on the equation of state—i.e., $\gamma = \gamma(k)$ where k is a parameter of the equation of state $p = k\rho$. In his analysis, Maison confirmed the known result for the special case of radiation fluid ($k = 1/3$) using a linear stability analysis as proposed by Evans and Coleman, however, he demonstrated that the mass scaling constant is a very sensitive function of k which monotonically increases from about 0.1 to about 0.8 as k is increased from 0.01 to 0.9. As Maison's analysis depended strongly on a continuous self-similarity ansatz, there was some skepticism on whether the solution was the attractor at criticality [35]. Neilsen and Choptuik [36] and Harada and Maeda [37] would later provide numerical verification of the Maison result.

Hamadé, Horne and Stewart [35] reported strong evidence that a continuously self-similar solution is the attractor in spherically symmetric axion/dilaton collapse. They carried out a numerical evolution in double-null coordinates which supported an analytical argument based on a css ansatz. The near critical solutions appeared to diverge from a css prediction in the critical solution. In order to predict the mass scaling constant, they used a

linear perturbation method similar to that in [33] and found excellent agreement with the numerical estimate $\gamma = 0.264$.

A numerical analysis of critical phenomena in the gravitational collapse of a Yang-Mills field has been carried out by Choptuik, Chmaj and Bizoń [38]. In their model, the authors observed both css and dss solutions. They reported a dss solution mass scaling of $\gamma \approx 0.20$ with self-similarity constant $\Delta \approx 0.74$. The interesting realization of the Einstein-Yang-Mills model is that it appears to admit a critical solution for which certain two-parameter families of initial data separate dispersal solutions from both Type I and Type II solutions[3].

Type I and Type II solutions are also observed in massive scalar field collapse in spherical symmetry [39]. Further evidence of Type I critical phenomena was reported in 1998 by Rein, Rendall and Schaeffer [40] and in 2001 by Olabarrieta and Choptuik [41]. In those cases, numerical studies of spherically symmetric collisionless matter in the Vlasov-Einstein system were carried out.

Critical phenomena were also found in the gravitational collapse of com-

[3] Type I critical solutions with black hole mass as an order parameter contain a mass gap. Hence, black holes "turn on" at some finite mass in the supercritical region. In contrast, Type II critical solutions have a continuous order parameter meaning a zero mass black hole resides at the critical solution.

plex massless scalar field in [42, 43] and [44]. Analytic work on massive scalar field collapse in a Schwarzschild background has also been performed in [45, 46].

To this point, our review of the literature reporting critical gravitational collapse of various matter types has been restricted to four dimensional space-times. In the following section, we begin a discussion of scalar field collapse in three dimensional and higher dimensional space-times.

2.2 Gravitational Collapse in Other Dimensions

We first review the three dimensional black hole and the interesting properties of the space-time in this solution. We will also discuss numerical and analytic solutions of gravitational collapse of scalar field in three dimensions. The numerical calculations we consider include a cosmological constant term in the action and the results indicate a Type II critical solution with black hole mass scaling. An analytic solution in three dimensions performed by Garfinkle [47] will also be shown to produce black hole solutions. In that case, however, a scalar field css ansatz was used which assumed the cosmological constant could be tuned to zero.

In the section following the three dimensional black hole, a summary of

numerical calculations of scalar field collapse in higher dimensional space-times is presented. Included in the literature presented in this section, are results initially reported Bland, Preston, Becker, Kunstatter and Husain [48] which are also included in the results of this thesis. In [48] it was shown that the critical constants observed in gravitational collapse can be described using smooth functions of space-time dimension. It will also be shown, in higher dimensional collapse, that the critical solution does not depend on the value of a cosmological constant.

2.2.1 The Three Dimensional Black Hole

The Einstein field equations in vacuum are given by

$$G_{\mu\nu} = R_{\mu\nu} - \frac{1}{2}g_{\mu\nu}R + \frac{1}{2}g_{\mu\nu}\Lambda = 0. \tag{2.18}$$

Consider the case where $\Lambda = 0$ in three dimensions. In this case, contracting the above equation yields $R = 0$, which in turn gives

$$R_{\mu\nu} = 0. \tag{2.19}$$

In three dimensions, there are six independent components of both $R^{\lambda}_{\mu\nu\kappa}$ and $R_{\mu\nu}$. Thus, we can assume the Riemann tensor components are linear combinations of the Ricci tensor components and the Ricci scalar. Indeed, the relation between the two tensors is given by [3]

$$R_{\lambda\mu\nu\kappa} = g_{\lambda\nu}R_{\mu\kappa} - g_{\lambda\kappa}R_{\mu\nu} - g_{\mu\nu}R_{\lambda\kappa} + g_{\mu\kappa}R_{\lambda\nu} - \frac{1}{2}\left(g_{\lambda\nu}g_{\mu\kappa} - g_{\lambda\kappa}g_{\mu\nu}\right)R. \quad (2.20)$$

Therefore,

$$R_{\lambda\mu\nu\kappa} = 0. \quad (2.21)$$

Thus, it is seen that there is no curvature in three dimensions if $\Lambda = 0$. With no curvature there are no black hole solutions.

Consider now the case where $\Lambda \neq 0$. We find, using (2.18), $R = 3\Lambda$ and $R_{\mu\nu} = \Lambda g_{\mu\nu}$. Inserting these relations into (2.20) gives

$$R_{\lambda\mu\nu\kappa} = \frac{1}{2}\left(g_{\mu\kappa}g_{\lambda\nu} - g_{\lambda\kappa}g_{\mu\nu}\right)\Lambda, \quad (2.22)$$

and we find that the space now contains non-zero curvature. In fact, a space with these properties is called a space of constant curvature [3].

In 1992, Bañados, Teitelboim and Zanelli (BTZ) [49] examined the Ein-

stein equations with negative cosmological constant. They considered the following action:

$$S = \int d^3x\sqrt{-g}\left(R + \frac{1}{l^2}\right) + B \tag{2.23}$$

wherein the above equation B is a surface term. Applying the minimum action principle to (2.23) and dropping the overall surface term indeed yields the Einstein field equations (2.18) with $-\Lambda = 1/l^2$.

BTZ considered a Schwarzschild-like line element in three dimensions:

$$ds^2 = -\alpha\,(t,r)\,dt^2 + \beta\,(t,r)\,dr^2 + r^2 d\theta^2, \tag{2.24}$$

where θ is the angular coordinate. Inserting (2.24) into the field equations gives the (non-rotating) solution

$$ds^2 = -\left(-M + \frac{r^2}{l^2}\right)dt^2 + \left(-M + \frac{r^2}{l^2}\right)^{-1} dr^2 + r^2 d\theta^2 \tag{2.25}$$

where, the integration constant M is the total mass of the space-time measured at spacelike infinity, and l is a scale factor with units of length. The

metric becomes singular for values of the radius given by the condition

$$r = \pm\sqrt{Ml^2} \tag{2.26}$$

with $r = \sqrt{Ml^2}$ being the black hole horizon radius.

We now point out some interesting properties of this solution. The first is that the black hole mass M is dimensionless, therefore, Λ provides a length scale with which to measure the horizon distance. Namely, if Λ is tuned to zero the horizon radius is pushed to infinity and we are left only with the interior (not to mention the lack of curvature). Secondly, and unlike it's $3+1$ counterpart, there is no curvature singularity at the origin. This second fact is made evident by examining the Riemann scalar invariant which is given by

$$R^{\lambda\mu\nu\kappa}R_{\lambda\mu\nu\kappa} = 3\Lambda^2. \tag{2.27}$$

Perhaps the most interesting aspect of the BTZ solution is that the space-time is asymptotically anti-de Sitter, not asymptotically flat. This is seen by setting $M = -1$ in (2.25). For an excellent review of the $2+1$ black hole cf. Carlip [50].

The zero point of energy is usually chosen so that $M = 0$ when the horizon

radius vanishes. BTZ considered this state as the vacuum, which has line element

$$ds^2_{vac} = -\left(\frac{r}{l}\right)^2 dt^2 + \left(\frac{r}{l}\right)^{-2} dr^2 + r^2 d\theta^2. \tag{2.28}$$

The black hole spectrum lies above this state. For $M < 0, M \neq -1$, a sequence of conical singularities exist at the origin which are excluded from the physical spectrum. Thus, the BTZ space-time contains a mass gap, of one unit, separating an anti-de Sitter "bound state" from the continuous black hole spectrum.

In 2000, Pretorius and Choptuik [51] presented the results of a numerical study of non-rotating massless scalar field collapse in $(2+1)$-dimensional AdS space-time. They observed the collapse and formation of BTZ black holes and found critical behaviour similar to that found in four dimensional collapse. One striking difference between scalar field collapse in $3+1$ and the observed collapse in $2+1$ AdS was the appearance of a continuously self-similar critical solution. Pretorius and Choptuik did not observe a discrete self-similarity in the critical solution.

Pretorius and Choptuik reported a Type II critical solution with a black hole mass scaling constant of approximately 1.2 ± 0.05. In order to determine the scaling exponent, they collated the maximum values of the Ricci scalar

(at $r = 0$) with subcritical values of a keeping l fixed. As the Ricci scalar has dimensions of inverse length-squared, it was assumed that the scaling exponent obtained in this way would be related directly to the black hole mass scaling exponent in supercritical collapse.

In 2001, Husain and Olivier [52] independently studied the collapse of massless scalar field in a three dimensional space-time with negative cosmological constant. They used a double-null formulation of the Einstein-scalar equations in circular symmetry (similar to the method used in [28] for the four dimensional case) and verified the scaling behaviour observed by Pretorius and Choptuik. For supercritical collapse, they reported a critical exponent of 0.81.

Soon after publication of the Pretorius and Choptuik result, Garfinkle [47] performed an analytic study of critical collapse in 2+1 AdS. Garfinkle found an exact solution for the line element using a scalar field css ansatz that required the vanishing of the cosmological constant. The method is outlined below.

Following the work of Christodoulou [25], Garfinkle defined the metric

$$ds^2 = -\exp(2\nu)\,du^2 - 2\exp(\nu+\lambda)\,dudr + r^2 d\theta^2, \qquad (2.29)$$

where $\nu = \nu(u, r)$, $\lambda = \lambda(u, r)$, u is the proper time of an observer at the origin, and r is the proper radius of a circle of circumference $2\pi r$ centered at the origin.

Garfinkle considered the Einstein-scalar field equations with cosmological constant. These equations are given by (1.1) with energy-momentum tensor (2.1). He defined the new quantities

$$g = \exp(\nu + \lambda) \tag{2.30}$$

$$\bar{g} = \exp(\nu - \lambda). \tag{2.31}$$

Solving the field equations gives

$$g = \exp\left[4\pi \int_0^r \tilde{r} \left(\frac{\partial \chi(\tilde{r})}{\partial \tilde{r}}\right) d\tilde{r}\right] \tag{2.32}$$

$$\bar{g} = 1 - 2\Lambda \int_0^r \tilde{r} g(\tilde{r}) d\tilde{r}. \tag{2.33}$$

Note that in order to match the result of Garfinkle we have changed the coupling in the field equations from 8π to 4π.

The scalar wave equation for this system is given by

$$2\frac{\partial^2\chi}{\partial u\partial r}+\frac{1}{r}\frac{\partial\chi}{\partial u}-\frac{1}{r}\frac{\partial}{\partial r}\left(r\bar{g}\frac{\partial\chi}{\partial r}\right)=0. \tag{2.34}$$

Garfinkle used the scalar field css ansatz

$$\chi = cT+\psi(R), \tag{2.35}$$

where the two new variables T and R are defined by

$$u = -\exp(-T) \tag{2.36}$$

$$r = \exp(-T)\,R. \tag{2.37}$$

The constant of proportionality, c, is normally chosen so that the solution best matches the numerical collapse result of Pretorius and Choptuik.

The ansatz required that the cosmological constant in (2.33) be neglected which in turn reduced (2.34) to the flat space wave equation. Putting (2.35) into (2.34) with $\bar{g}=1$ yields

$$R(1-2R)\,\psi''+(1-3R)\,\psi'-c=0, \tag{2.38}$$

where the primes indicate partial derivatives with respect to R. The solution of the above differential equation gave the exact form of the field equation (2.32):

$$g = \left[\frac{\left(1+\sqrt{1-2R}\right)^2}{4\sqrt{1-2R}}\right]^{8\pi c^2}. \tag{2.39}$$

The reader will notice that the line element in these coordinates is singular when $R = 1/2$. After a change of coordinates, Garfinkle demonstrated that this singularity is not physical and that the metric is smooth for values of c given by

$$c^{(n)} = \pm\sqrt{\frac{1}{4\pi}\left(1-\frac{1}{2n}\right)}, \tag{2.40}$$

where n was a positive integer. After comparison with the numerical results of Pretorius and Choptuik, Garfinkle determined $n = 4, c = -0.2443$. However, Garfinkle was unable to determine γ.

2.2.2 Black Holes in Higher Dimensions

Garfinkle, Cutler, and Duncan [53] performed numerical simulations of critical gravitational collapse of massless minimally-coupled scalar field in spherical symmetry in six space-time dimensions. They found a Type II critical solution with discrete self-similarity.

The authors began by defining a Schwarzschild-like metric in d dimensions [54, 55, 56]:

$$\begin{aligned} ds^2 = & - \left(1 - \frac{16\pi}{(d-2)A_{(d-2)}} \frac{M}{r^{d-3}}\right) dt^2 \\ & + \left(1 - \frac{16\pi}{(d-2)A_{(d-2)}} \frac{M}{r^{d-3}}\right)^{-1} dr^2 + r^2 d\Omega^2_{(d-2)}. \end{aligned} \tag{2.41}$$

In the above line element, M is an ADM-like mass [57] and

$$A_{(d-2)} = 2\pi^{(d-1)/2}/\Gamma[(d-1)/2] \tag{2.42}$$

is the area of the unit $(d-2)$-sphere with metric $d\Omega^2_{(d-2)}$. The mass M has dimension $(\text{length})^{d-3}$ so it was expected that the mass scaling relationship in supercritical collapse will approach the scaling law

$$M_{BH} \propto |a - a_*|^{(d-3)\gamma}, \tag{2.43}$$

where it was assumed $\gamma = \gamma(d)$. In [58], naked singularities were found in d-dimensional static spherically symmetric gravity coupled to a massless scalar field.

In generic d-dimensional space-time, the Ricci scalar will always have

units of inverse length squared. Together with the observation that the maximal curvature scales in subcritical collapse just as the black hole mass does in Choptuik's $3+1$ collapse it is conventional to define the scaling relation in d-dimensional collapse as

$$R_{MAX} \propto |a - a_*|^{-2\gamma}. \tag{2.44}$$

Assuming quantities with dimension length scale with the same critical constant we can define a new scaling constant γ_{mass} such that

$$M_{BH} \propto |a - a_*|^{\gamma_{mass}} \tag{2.45}$$

and immediately make the identification

$$\gamma_{mass} = (d-3)\,\gamma. \tag{2.46}$$

The matter field stress-energy tensor for this model was given by (2.1), subject to the metric (2.29) with $d\theta^2$ replaced by $d\Omega^2_{(d-2)}$. To help stabilize

the collapse simulations, the following new matter variable was defined:

$$h = \frac{1}{6r}\frac{\partial^2}{\partial r^2}\left(r^3\chi\right). \tag{2.47}$$

Using this new matter variable, the wave equation for χ became

$$Dh = \frac{3}{r}\left(g-\bar{g}\right)\left(h+\bar{s}-2s\right)+\frac{27\pi g}{2r}\left(s-\bar{s}\right)^3, \tag{2.48}$$

where,

$$s = \frac{2}{r^2}\int_0^r \tilde{r}h(\tilde{r})d\tilde{r}, \tag{2.49}$$

$$\bar{s} = \frac{3}{r^3}\int_0^r \tilde{r}^2 s(\tilde{r})d\tilde{r}, \tag{2.50}$$

$$g = \exp(\nu+\lambda) = \exp\left[18\pi\int_0^r \frac{\left(s(\tilde{r})-\bar{s}(\tilde{r})\right)^2}{\tilde{r}}d\tilde{r}\right], \tag{2.51}$$

$$\bar{g} = \exp(\nu-\lambda) = \frac{3}{r^3}\int_0^r \tilde{r}^2 g(\tilde{r})d\tilde{r}, \tag{2.52}$$

and,

$$D = \frac{\partial}{\partial u}-\frac{1}{2}\bar{g}\frac{\partial}{\partial r} \tag{2.53}$$

is a derivative operator along ingoing light rays.

The initial value of the matter field was chosen to be

$$\chi(0,r) = pr^2 \exp\left[-\frac{(r-r_0)^2}{\sigma^2}\right]. \tag{2.54}$$

With constant r_0 and σ, discrete self-similarity of the matter field near criticality was observed with a period $\Delta = 3.03$. The critical exponent reported was $\gamma = 0.424$.

In 1999, Frolov [59] examined scalar field collapse in d dimensions. He finds exact solutions for $d = 3, 4, 5, 6$ using a css ansatz (which we will see below is not valid for the case of massless scalar field).

A method of obtaining the mass-scaling exponent for any finite dimension $d \geq 4$ with arbitrary cosmological constant Λ, for the case of minimally-coupled massless scalar field in spherical symmetry was first presented by Birukou, Husain, Kunstatter, Vaz and Olivier [60]. The method involved a conformal redefinition of the metric which was used to simplify the field equations of the model. A double null formalism was used which resulted in a similar set of field equations to [52]. As we shall see below, the formalism presented by Birukou et al. [60] will serve as the main content of the formalism presented in this thesis. In that paper, d and Λ appear as input parameters.

The authors verified universality and scaling in the four and six dimensional cases with zero cosmological constant. The critical exponent measured in supercritical collapse for $d = 4$ and $d = 6$ agreed well with the results we have quoted above and the solutions exhibited discrete self-similarity, however, the self-similarity constant was not measured. They presented new results in five dimensions with zero and negative cosmological constant. See Table 2.1 for a summary of the results in five dimensions. It should be noted

Initial data profile	$\Lambda = 0$	$\Lambda = -1$
Gaussian	0.52	0.49
Tanh	0.41	n/a

Tab. 2.1: Critical exponent γ in numerical scalar field collapse in five dimensions as reported by Birukou, Husain, Kunstatter, Vaz, and Olivier [60].

that the results quoted in the $d = 5$ case had low precision but seemed to indicate that γ was independent of Λ.

In 2003, following the work of [60], Husain, Kunstatter, Preston and Birukou [61] presented new evidence that the critical exponent in gravitational collapse of scalar field in AdS space-time was *independent* of cosmological constant Λ.

In that model, and more generally in dilaton gravity, the dependence of the field equations on Λ appear only in the definition of a scalar dilaton po-

tential function. Moreover, the Λ-dependent term in the dilaton potential is a second order correction term which vanishes at the origin for all finite values of Λ. As near critical solutions will always have support very near the origin it is not unreasonable to expect the critical solution to be generically independent of Λ. Table 2.2 presents convincing evidence that γ is not a function of Λ. The authors verified the universality of their result by mea-

Λ	γ	γ (cosh data)
-0.001	$0.370 - 0.375$	
-5	$0.37 - 0.38$	$0.37 - 0.38$
-10	$0.37 - 0.39$	
-20	$0.36 - 0.38$	$0.36 - 0.38$
-50		$0.37 - 0.40$

Tab. 2.2: Mass-scaling exponent in critical scalar field collapse in four dimensions demonstrating the independence of Λ as reported by Husain, Kunstatter, Preston and Birukou [61]. The initial data profiles considered were a Gaussian shell and cosh pulse. The calculated values for the exponent clearly showed the universality of the result and that γ was independent of Λ.

suring the critical exponent for cosh initial data and finding the same scaling constant γ.

Bland et al. [48] expanded on the work of [60, 61]. Similar to the previous work, a conformal redefinition of the metric had been carried out, motivated by two-dimensional dilaton gravity. The work composes the first systematic study of the dimension dependence of critical phenomena in scalar field

gravitational collapse and will serve as the main content of this thesis.

Preliminary results of that analysis were originally presented in 2004 by Kunstatter [62]. In that presentation, however, the nature of the limiting solution in the limit of large dimension remained uncertain. The numerical code had adjusted the cosmological constant to zero but in most other ways had been kept the same as [60, 61]. Several changes to the code, which considerably increased stability, were implemented later in 2004 and throughout 2005.

As it will be seen, the key new difference in the present formalism was the use of an integration by parts of the dilaton evolution equation. This change amounted to an additional few lines of code and as a result of this procedure, substantial stability of the evolution was achieved. The accuracy of the scaling constants was greatly improved and a clear picture of the dependence of γ on d began to emerge ultimately leading to the results presented in [48].

In [48], it was determined that γ monotonically increased to an asymptotic value at large d. The numerical results were well fit by the simple relationship

$$\gamma = 0.467\,(1 - \exp\,[-0.408d])\,. \tag{2.55}$$

The data had been analyzed over the range $3.5 \leq d \leq 14$. Universality of the critical solutions was verified and low precision estimates of Δ were also calculated. Table 2.3 summarizes the critical constants reported in [48, 63].

d	Δ [63]	γ [63]	Δ [48]	γ [48]
3.5				0.349 ± 0.003
4	3.37 ± 0.07	0.372 ± 0.004	3.40 ± 0.1	0.374 ± 0.002
4.5			3.30 ± 0.1	0.398 ± 0.002
5	3.19 ± 0.06	0.408 ± 0.008	3.10 ± 0.1	0.412 ± 0.004
6	3.01 ± 0.06	0.422 ± 0.008	2.98 ± 0.1	0.430 ± 0.003
7	2.83 ± 0.06	0.429 ± 0.009	2.96 ± 0.1	0.441 ± 0.004
8	2.70 ± 0.08	0.436 ± 0.009	2.77 ± 0.1	0.446 ± 0.004
9	2.61 ± 0.08	0.442 ± 0.009	2.63 ± 0.1	0.453 ± 0.003
10	2.55 ± 0.08	0.447 ± 0.013	2.50 ± 0.1	0.456 ± 0.004
11	2.51 ± 0.08	0.44 ± 0.01	2.46 ± 0.1	0.459 ± 0.004
12			2.44 ± 0.1	0.462 ± 0.005
13			2.40 ± 0.1	0.463 ± 0.004
14				0.465 ± 0.004

Tab. 2.3: The echoing periods Δ and scaling exponents γ as reported by Sorkin and Oren [63] and Bland et al. [48]. The initial data profiles were massless scalar Gaussian shells placed in a d-dimensional space-time metric with spherical symmetry. The critical constants reported in [63] were calculated by measuring the maximal scalar curvature in subcritical collapse. In [48], calculations were performed in supercritical collapse. It is expected that both methods will produce the same critical exponent and, as it can be seen in the table, both sets of results agree within uncertainty.

An independent numerical study of the space-time dependence of γ and Δ in gravitational collapse was reported by Sorkin and Oren [63]. In that paper, the authors studied massless minimally coupled scalar field collapse

in spherical symmetry as a function of space-time dimension d. In each dimension examined, they observed the same qualitative behaviour as that originally reported by Choptuik [19], however, the scaling exponent γ was determined to a larger uncertainty then in [48].

Sorkin and Oren used the double null coordinates

$$ds^2 = -\alpha\left(u,v\right)^2 du dv + r\left(u,v\right)^2 d\Omega^2_{(d-2)}. \tag{2.56}$$

They evolved the field equations for a Gaussian initial data using the coordinate u like a time coordinate. A series-smoothing procedure was implemented for points near the center of symmetry. The procedure updated the field values, on a given u-slice, by taking a weighted average of the predicted evolution value of the field with the value of the field on a past light cone. This procedure had the effect of lowering the numerical errors at grid points near $r = 0$ especially in the higher dimensions where numerical stability was most difficult to achieve.

Discrete self-similarity and mass-scaling was observed for integer dimensions $4 \leq d \leq 11$. Sorkin and Oren determined that if the values of γ were extrapolated to higher dimension then γ appeared to have a maximum in

the dimension range $11 \leq d \leq 13$. However, the increase of relative error in γ for $d = 10$ and $d = 11$ might have led to a numerical artifact.

2.3 Theory of Critical Collapse

The simplest example of critical phenomena in statistical physics is the phase transition at the liquid-gas boundary of a fluid. Figure 2.1 shows a typical phase transition diagram for a fluid. It is seen that a discontinuity in the fluid density occurs as one crosses the boiling curve. Define the difference in density as

$$\Delta\rho = \rho_{liquid} - \rho_{gas}. \tag{2.57}$$

As the temperature increases from the triple point, $\Delta\rho$ decreases along the boiling curve. The boiling curve ends at the critical point (p_*, T_*) where $\Delta\rho = 0$. For temperatures larger than the critical temperature T_* the fluid no longer boils and as a result one can no longer distinguish between liquid and gas phases.

In 1938, Landau and Lifshitz [64] showed that the critical point in a fluid transition is an isolated point in the phase space. That is, there can be no continuous series of critical points. Moreover, they showed that the specific

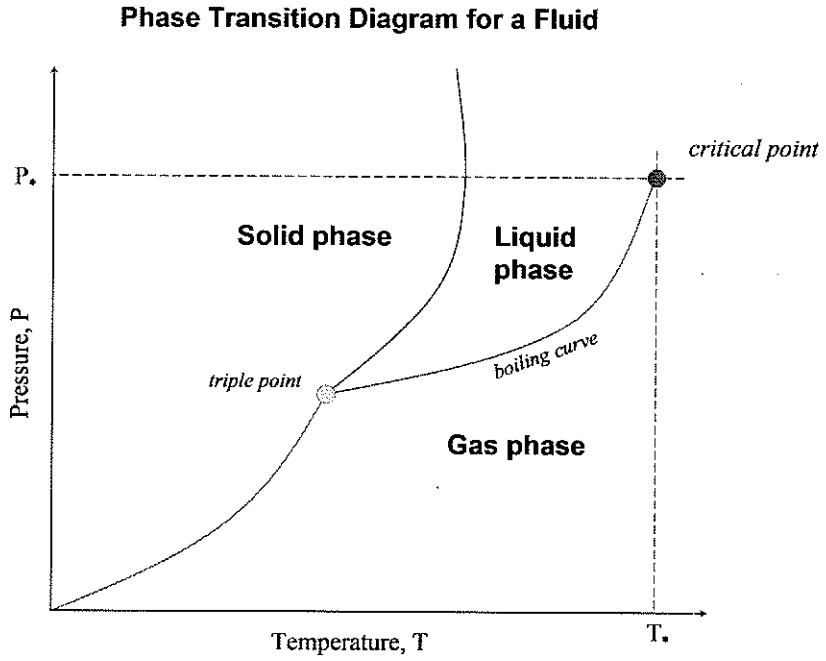

Fig. 2.1: A phase transition diagram for a typical fluid. All three phases coexist at the triple point. Along the boiling curve, the difference in fluid density decreases as one moves toward the critical point. At the critical point there is no difference in fluid density between the liquid and gas phases and so it is not possible to distinguish between these two phases. At all other points along the boiling curve, a discontinuity in fluid density exists between the liquid and gas phases.

heat of a fluid at constant pressure is allowed to become indeterminate at a critical point. These facts suggest that there is no analytic function of the order parameter at such a critical point[4]. It is observed that the density difference varies as a non-integer power of temperature along the boiling curve. That is,

$$\Delta\rho = \rho_{liquid} - \rho_{gas} = |T_* - T|^\gamma \,, \tag{2.58}$$

where γ is a critical exponent.

Another example of a critical phase transition is the spontaneous magnetization of a ferromagnetic material at low temperature [13]. At high temperatures, a ferromagnetic material will exhibit an average magnetization $\mathbf{m}$ which is determined by the presence of an external magnetic field. However, at low temperatures, and in the absence of an external field, the material may spontaneously magnetize according to

$$|\mathbf{m}| = |T_* - T|^\gamma \,, \tag{2.59}$$

where T_* represents the Curie temperature of the material and γ is a new critical exponent.

[4] For more information on Landau theory the reader may also consult, for example, Plischke and Bergersen [65].

In the ferromagnetic case, the phase transition is symmetry breaking and continuous. At temperatures higher than the Curie temperature, the spontaneous magnetization vanishes leaving the system in rotational symmetry (when the external field is zero). This is in contrast to the spontaneous magnetization state which has a random direction even when the external field is zero. Once the direction of $\mathbf{m}$ is determined, the system has a preferred direction.

Phase transitions which break a symmetry are classified as Type II or second order critical phase transitions and require a continuous *order parameter* which vanishes at the critical point. For the ferromagnetic case, the order parameter is the average spontaneous magnetization $\mathbf{m}$ which vanishes continuously as the temperature increases to the Curie temperature.

In the case of the liquid-gas phase transition of a fluid, the density of the fluid, at constant pressure, changes discontinuously across the boiling curve. There is no change in the symmetry of the system and so transitions of this type are classified as Type I or first order critical phase transitions.

The analogy that can be used for critical phenomena in gravitational systems now seems more obvious. In the case of the spherical collapse of scalar field to a black hole, symmetry is broken when crossing the black

hole threshold. In the reflection solution, where no black hole is formed, one is left with Minkowski space-time which is maximally symmetric. In four dimensions this space will contain 10 Killing vectors. On the other hand, the black hole solution will have a Schwarzschild metric possessing a reduced number of symmetries. Thus, crossing the black hole threshold changes the dimension of the Killing algebra of the space-time. Moreover, as we saw above, Choptuik found that the critical solution in scalar field collapse contained a zero mass black hole. Thus, gravitational collapse of scalar field is a Type II critical phenomena with black hole mass being the order parameter.

The black hole mass M_{BH} vanishes continuously at the critical value of an initial parameter[5] and varies according to the power law relation

$$M_{BH} \propto |a - a_*|^{\gamma_{mass}}, \tag{2.60}$$

where, a is a parameter describing the initial data, a_* is the critical value of a, and γ_{mass} is a universal exponent. The scale invariance of Type II phenomena is associated with self-similarity of the matter and gravitational

[5] There are, of course, many functions which can characterize the initial data in gravitational collapse. Choptuik [19] conjectured that in spherical scalar field collapse, the critical behaviour of the system is universal for all one parameter families of initial data.

fields. As discussed above, the spherical collapse of scalar field gives rise to a discretely self-similar critical solution. The collapse of perfect fluid has a continuously self-similar critical solution. So it is seen that Type II phenomena can be associated with either a discrete or a continuous self-similarity. In the following section we will describe these phenomena in terms of a phase space picture.

2.3.1 Phase Space Picture

The critical solution can be thought of as a point in an infinite dimensional phase space [13]. The phase space, or manifold, consists of the set of all possible smooth, asymptotically flat, initial data. The space of initial data is a function space and is therefore infinite dimensional. As the system evolves with respect to time, integral curves in the phase space represent solutions to the Einstein equations.

Each point in this phase space represents one possible state corresponding to the evolution of the set of parameters describing the initial matter profile at one particular time. In the phase space of the spherically symmetric scalar field data, two fixed points exist: the black hole attractor and the reflection (or flat space) attractor. Also in the phase space is an unstable

critical solution hypersurface (which contains the zero mass black hole or naked singularity). The hypersurface is the boundary representing the phase transition from supercritical to subcritical collapse.

For a given set of initial parameters, the system will evolve along an integral curve in the phase space for some period of time before the evolution ends at one of these fixed points[6]. Thus, the evolution proceeds for a finite time (see Figure 2.2).

Choptuik showed in 1993 that, for massless scalar field, the black hole threshold is universal for *one parameter families* of initial data[7]. Thus, it is assumed the critical solution fixed point exists in a (critical solution) hypersurface of codimension one in the phase space. Any critical set of initial parameters will exist within this surface and, as the evolution proceeds, remain in this surface until evolution is terminated at the critical point. All smooth one parameter initial data profiles intersect the critical surface at exactly one point.

Initial data which are tuned to near the critical value of a given parameter set will initially be near to the critical surface in phase space. Evolution of the

[6] Unless, of course, the initial data reside within the critical hypersurface. In those cases the evolution will remain in this surface, eventually terminating at the critical point.

[7] Of course, as we have seen above, several authors have since demonstrated the universality of critical solutions for a variety of matter types.

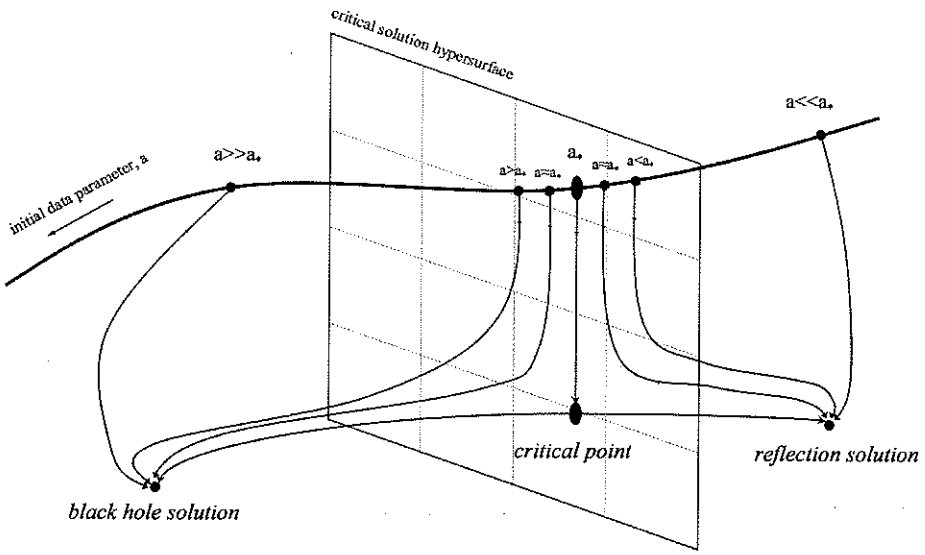

Fig. 2.2: The phase space picture in critical gravitational collapse [29]. The critical point is embedded in a critical hypersurface of codimension one in an infinite dimensional initial value function space. The solid line represents a one parameter family of initial data which intersects the critical surface at exactly $a = a_*$. The directed lines are examples of the evolution of initial data which eventually terminate on either the black hole solution point, the critical point, or the reflection solution point depending on the initial value of a. For initial data very near the critical surface, the evolution approximates the critical solution for some time before being repelled toward the black hole or reflection solutions.

data will proceed for awhile along an integral curve which is nearly parallel to the critical hypersurface. Because the critical hypersurface is unstable, however, the evolution will eventually be repelled toward either a black hole or reflection solution depending on which side of the critical surface the initial data reside. Physically, if the initial data reside in the subcritical part of the phase space then the matter distribution will never become dense enough to form a black hole during the evolution.

When viewed in this way, $|a - a_*|$ is simply the first order measurement of the distance from the critical surface during the time the evolution approximates the critical solution. Let P be a smooth function of the parameter a on phase space such that data sets with $P > 0$ form black holes while those with $P < 0$ do not. Then, the black hole threshold corresponds to $P = 0$. If P is analytic in a neighbourhood of this threshold then

$$P(p) = C\,|a - a_*| + \mathcal{O}((a - a_*)^2), \tag{2.61}$$

where C and a_* are family dependent constants. The black hole mass scaling relation in $3+1$ is given (to first order) by

$$M_{BH} \sim P^{\gamma_{mass}} \sim C\,|a - a_*|^{\gamma_{mass}}. \tag{2.62}$$

We will use a dimensional argument in the next section to show that all quantities with units of length will scale with the critical exponent γ.

2.3.2 Mass Scaling Derivation

Gundlach [13] provides an elegant summary of a derivation of the mass scaling exponent using dimensional arguments and a perturbation analysis originally proposed in [33, 34]. The method is outlined below.

Consider the css case. Define a solution to the evolution equations by $Z(r,t)$. In a css solution, the metric depends on only one coordinate, therefore, let us denote the critical solution by $Z_*(x)$, where x is a some new coordinate adapted to the css solution. An example of suitable new coordinates (x,τ) are given by

$$x = -\frac{r}{t} \tag{2.63}$$

$$\tau = -ln\left(-\frac{t-t_*}{l}\right), \tag{2.64}$$

where l is an overall space-time scale factor with units of length and t_* is the time elapsed in the evolution of the critical solution.

For initial data very near the critical hypersurface, the solution Z will

approximate the critical solution Z_* for an intermediate time. Gundlach calls this region the *intermediate linear region* where the general solution can be determined using a linear perturbation of the critical solution. A general linear perturbation is given by the polynomial expansion in $(t - t_*)$

$$\delta Z = \sum_{i=0}^{\infty} C_i \exp(\lambda_i \tau) Z_i(x), \tag{2.65}$$

where, the C_i are dependent on a, and τ is in some sense a measure of the lifetime of the perturbed solution. We assume the perturbation spectrum is discrete and that there is one growing mode, corresponding, say, to λ_0 being the only real and positive λ_i. At exactly the critical value a_*, we require $C_0(a_*) = 0$ in order to completely suppress the growing mode at the critical solution. For all other finite values of $|a - a_*|$, the exponential function will eventually dominate as $\tau \to \infty$ (hence, as $t \to t_*$), thus rendering the linear perturbation invalid. Nevertheless, for intermediate times the lowest non-zero eigenvalue λ_0 will dominate and we can linearize the perturbation. Therefore, the solution will approximate

$$Z(x, \tau) \sim Z_*(x) + \frac{dC_0}{da} |a - a_*| \exp(\lambda_0 \tau) Z_0(x). \tag{2.66}$$

Koike, Hara and Adachi [33, 66] divide the evolution of a near critical solution into two parts. During early times for which τ is $\leq$ a particular value, say, τ_a, (2.66) is valid. Soon after τ_a the evolution becomes non-linear and the solution quickly becomes a black hole (or not, depending on the sign of $a - a_*$). It is during this non-linear stage where (2.66) is no longer valid. The time τ_a is considered the lifetime of the perturbation and is defined by

$$\epsilon = \exp(\lambda_0 \tau_a) \frac{dC_0}{da} |a - a_*|, \tag{2.67}$$

where ϵ is a small, fixed, positive constant. Therefore

$$\tau_a = \frac{-1}{\lambda_0} \log |a - a_*| + C, \tag{2.68}$$

where C is a fixed constant. The perturbation is given by

$$Z(x, \tau_a) \sim Z_*(x) \pm \epsilon Z_0(x), \tag{2.69}$$

where the sign in front of ϵ corresponds to the sign of $(a - a_*)$.

It is now possible to redefine the adapted coordinates by scaling (r, t) by

a function of τ_a. We define the new scaled coordinates by

$$r \rightarrow \frac{r}{L_a} \tag{2.70}$$

$$t \rightarrow \frac{t}{L_a} \tag{2.71}$$

$$L_a = L\exp\left(-\tau_a\right). \tag{2.72}$$

The dimensional argument is now made as follows. In d dimensions the black hole mass has units $[L]^{d-3}$ and because the only length scale in the system is given by L_a we assume the black hole mass is proportional to an integer power of this scale. Therefore,

$$M_{BH} \propto L_a^{(d-3)} \propto |a - a_*|^{\frac{(d-3)}{\lambda_0}} \tag{2.73}$$

and we make the identification: $\gamma = 1/\lambda_0 = \gamma_{mass}/(d-3)$. Furthermore, any field quantity which has units related to length can be expected to scale like the black hole mass. For example, the curvature scalar R has units $[L]^{-2}$ and so we expect

$$R \propto L_a^{-2} \propto |a - a_*|^{\frac{-2}{\lambda_0}} \tag{2.74}$$

One advantage to measuring the power law scaling of the curvature scalar is

that it can be measured in both the subcritical and supercritical regions.

2.3.3 Self Similar Solutions

Type II critical phenomena have either continuously or discretely self-similar solutions. This is due to the scale-invariance of critical solutions in Type II phenomena. Continuously self-similar solutions are invariant under a small re-scaling of both the space and time coordinates (by a factor of $1 + \epsilon$). Discretely self-similar solutions are invariant under a re-scaling by integer multiples of a discrete factor. The discrete factor is, in general, unique for the space and time coordinates[8]. Figure 2.3 shows a phase space picture of scale invariant or self-similar critical solutions.

Continuous Self-Similarity

In 1971, Cahill and Taub [67] defined a geometric version of css as a spherically symmetric solution which admits a vector field ξ^μ such that

$$\mathcal{L}_\xi g_{\mu\nu} = \xi_{\mu;\nu} + \xi_{\nu;\mu} = 2g_{\mu\nu}. \tag{2.75}$$

[8] However, it was noted above that the dss scaling constant is the same for both coordinates in the massless scalar field case, see page 26.

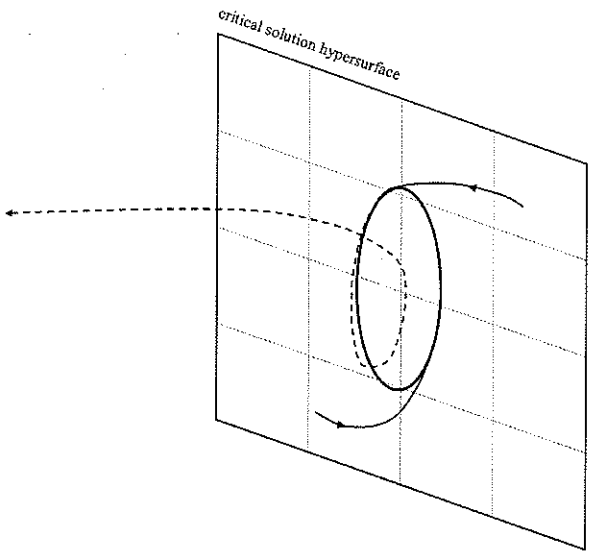

Fig. 2.3: Self-similar solutions in critical gravitational collapse [29]. The critical solution, or limit cycle, is represented by the darkened circle in the critical solution hypersurface. The two solid, directed lines are embedded in the critical surface and are attracted to the limit cycle. The broken line shows an evolution of initial data near the critical surface. For some time, the solution approximates the limit cycle but is eventually repelled by the unstable critical surface.

It can then be shown that the metric depends only on the adapted coordinate $x = r/t$. This reduces the field equations to ordinary differential equations.

A relevant application of this method to scalar field collapse was performed by Hirschmann, Wang and Wu [68]. In that case, the authors analyzed critical gravitational collapse of spherically symmetric scalar field matter in $2 + 1$ space-time dimensions. They obtained a critical solution which asymptotically approached a css critical solution by using a linear perturbation and a css ansatz in the limit of vanishing cosmological constant.

They confirmed the $n = 4$ single unstable mode of the css solution as first found by Garfinkle [47], however, they do not determine a mass-scaling exponent consistent with earlier findings reported in [51, 52, 69]. It is likely that some of the differences in predicted mass-scaling exponents arise due to a variation of boundary conditions used in the analyses.

In 1996, Soda and Hirata [70] reported an analytic study of the dimension dependence of the mass-scaling exponent in critical gravitational collapse of spherically symmetric massless scalar field. They began with a d-dimensional line element using advanced Bondi coordinates in spherical symmetry:

$$ds^2 = -g(v,r)\bar{g}(v,r)dv^2 + 2g(v,r)dudr + r^2 d\Omega^2_{(d-2)}. \qquad (2.76)$$

The matter field that Soda and Hirata studied was given by the action

$$S = \int d^4x\sqrt{-g}\left[R - \frac{1}{2}g^{\mu\nu}\partial_\mu\chi\partial_\nu\chi\right]. \tag{2.77}$$

The authors then impose a css ansatz (2.75) given by

$$\xi = r\partial_r + v\partial_v. \tag{2.78}$$

If a new coordinate $x = r/v$ is defined then, as above, the metric coefficients and the scalar field became functions only of x. Therefore,

$$g = g(x) \tag{2.79}$$

$$\bar{g} = \bar{g}(x) \tag{2.80}$$

$$\chi = \chi(x). \tag{2.81}$$

As a result of the imposition of this ansatz, the set of field equations which Soda and Hirata derived from (2.77) lead to a set of ordinary differential equations which can be solved exactly via linear perturbation. The eigenvalue of the relevant mode was found and the following expression for the black

hole mass-scaling exponent was predicted:

$$\gamma_{BH} = \frac{d-3}{\sqrt{2\,(d-2)}}. \tag{2.82}$$

Table 2.4 shows the predicted values of the mass-scaling constant for a number of integer dimensions. The table also shows the corresponding horizon radius scaling exponent.

Dimension d	γ_{BH}	γ	γ [48]
4	0.5	0.5	0.374 ± 0.002
5	0.81650	0.40825	0.412 ± 0.004
6	1.06066	0.35355	0.430 ± 0.003
7	1.26491	0.31623	0.441 ± 0.004
8	1.44338	0.28868	0.446 ± 0.004
9	1.60357	0.26726	0.453 ± 0.003
10	1.75	0.25	0.456 ± 0.004
11	1.88561	0.23570	0.459 ± 0.004
12	2.01246	0.22361	0.462 ± 0.005

Tab. 2.4: Scaling exponent in massless scalar field collapse as predicted by Soda and Hirata [70]. The centre column contains predicted values of the black hole mass-scaling exponent based on a css ansatz and linear perturbation. The right most column contains the horizon radius scaling exponent, recall that $\gamma_{BH} = (d-3)\gamma$. Unfortunately, the theoretical values do not match observation. For comparison, the results from Bland et al. [48] are shown.

The Soda and Hirata result, although a useful exercise, does not predict values of the scaling exponent which are consistent with observation. This is

due to the fact that critical solutions in massless scalar field collapse exhibit discrete self-similarity thereby invalidating the css ansatz.

Discrete Self-Similarity

Gundlach [29] defines a discretely self-similar space-time as an invariance under a discrete isomorphism on a re-scaled metric. Geometrically, this is equivalent to requiring the existence of a discrete diffeomorphism[9] Φ such that, for any integer n,

$$(\Phi^*)^n g_{ab} = \exp(2n\Delta) g_{ab}, \tag{2.83}$$

where Φ^* is the pullback of g_{ab} under the diffeomorphism Φ and Δ is a real dimensionless constant. In coordinate terms, consider a coordinate system (σ, x^α) such that at a point p with coordinates (σ, x^α) the image of the diffeomorphism, $\Phi(p)$, has coordinates $(\sigma + \Delta, x^\alpha)$. Then, in these coordinates, the dss is equivalent to

$$g_{\mu\nu}(\sigma, x^\alpha) = \exp(2\sigma) \tilde{g}_{\mu\nu}(\sigma, x^\alpha), \tag{2.84}$$

[9] A diffeomorphism is a differentiable map between two manifolds which also has a differentiable inverse.

where

$$\tilde{g}_{\mu\nu}\left(\sigma, x^{\alpha}\right) = \tilde{g}_{\mu\nu}\left(\sigma + \Delta, x^{\alpha}\right). \tag{2.85}$$

In the context of a spherically symmetric collapse of scalar field, a dss symmetry will manifest itself in a dynamical field, say $Z(r,t)$, in the following way:

$$Z\left(r,t\right) = Z\left(e^{n\Delta}r, e^{n\Delta}t\right). \tag{2.86}$$

A suitable set of adapted coordinates for this symmetry is given by

$$\tau = \log\left(\frac{t}{t_0}\right) \tag{2.87}$$

$$x = \log\left(\frac{r}{t}\right) - x_0\left(\tau\right), \tag{2.88}$$

where t_0 is an arbitrary scale factor and x_0 is a periodic function with period Δ. The dss symmetry is then imposed by assuming the ansatz (2.86) on, for example, the scalar field.

The dss symmetry also affects the mass-scaling relationship. Hod and Piran [71] conjectured (and verified numerically) that discrete self-similarity adds a periodic wiggle to the power law behaviour of the black hole mass

formed during collapse. They show that

$$\left(\frac{1}{d-3}\right)\log\left(M_{BH}\right) = \gamma \log|a - a_*| + \Psi\left[\log|a - a_*|\right] + c_k, \tag{2.89}$$

where c_k is a family-dependent constant, and Ψ is a periodic function with period

$$\delta = \frac{\Delta}{2\gamma}. \tag{2.90}$$

The above relationship will be used in this thesis to determine the discrete self-similarity constant in the higher dimensions.

3. D-DIMENSIONAL SPHERICAL SYMMETRY AND DILATON GRAVITY

In this chapter, the field equations of the model studied in this thesis are derived in the context of dilaton gravity. Due to the symmetry in the metric under consideration, it is possible to reduce the d-dimensional action for the theory to a $1+1$ effective theory. The introduction of a dilaton field and conformal redefinition of the metric will simplify the reduced action, thus, leading to a set of field equations which can be used to numerically evolve initial data.

The chapter begins with a brief discussion of dilaton gravity theory. It is then shown why dilaton theory is useful when analyzing higher dimensional gravity theories with symmetries. The method to construct a dilaton field with conformal redefinition of the metric is then introduced. In the final section of the chapter, the relevant field equations of the model are derived and a coordinate system is chosen.

3.1 Gravity in Two Dimensions

Beginning in the late 1980's and early 1990's, two dimensional theories of gravity attracted attention in the physics community due to their tractability and consequential utility as a model for quantum gravity. They are more than just toy models. Dilaton gravity can also be directly linked to higher dimensional gravity theories with spherical symmetries. The content of this thesis is the examination of a classical theory using dilaton gravity as a tool to simplify the numerical evolution equations.

Consider the vacuum Einstein equations with cosmological constant

$$R_{\mu\nu} - \frac{1}{2}g_{\mu\nu}R + \frac{1}{2}g_{\mu\nu}\Lambda = 0. \tag{3.1}$$

In two dimensions, the Riemann curvature tensor has only one independent component given by [3]

$$R_{\lambda\mu\nu\kappa} = \frac{1}{2}R\left(g_{\lambda\nu}g_{\mu\kappa} - g_{\lambda\kappa}g_{\mu\nu}\right) \tag{3.2}$$

which on contraction yields

$$\begin{aligned} R_{\mu\nu} &= \frac{1}{2} g^{\lambda\rho} R \left(g_{\lambda\rho} g_{\mu\nu} - g_{\lambda\nu} g_{\mu\rho} \right) \\ &= \frac{1}{2} R \left(\delta^{\rho}_{\rho} g_{\mu\nu} - \delta^{\rho}_{\nu} g_{\mu\rho} \right) \\ &= \frac{1}{2} R \left(2 g_{\mu\nu} - g_{\mu\nu} \right) \\ &= \frac{1}{2} g_{\mu\nu} R. \end{aligned} \tag{3.3}$$

Inserting (3.3) into (3.1) yields the two dimensional Einstein field equations

$$\Lambda g_{\mu\nu} = 0. \tag{3.4}$$

For non-zero Λ, (3.4) yields the unacceptable result of a vanishing metric, whereas, for $\Lambda = 0$ the field equations yield a trivial solution with no dynamical content. Thus, for any meaningful theory of gravity in two dimensions, the action must contain at least an auxiliary field.

Jackiw, Teitelboim, Banks and Susskind [72, 73] considered a constant curvature ($R = \Lambda$) two dimensional theory of gravity coupled to an auxiliary

dilaton field ϕ. The action for this theory is given by

$$S = \int d^2x\sqrt{-g}\phi\left(R - \Lambda\right). \tag{3.5}$$

Applying the minimum action principle to (3.5) yields the following field equations

$$\nabla_\mu\nabla_\nu\phi = \tfrac{1}{2}g_{\mu\nu}\phi\Lambda \tag{3.6}$$

$$R = \Lambda. \tag{3.7}$$

In 1993, Achúcarro and Ortiz [74] showed that these equations are equivalent to a dimensionally reduced three dimensional action on a metric with axial symmetry. Thus, the constant curvature dilaton theory was equivalent to a dimensionally reduced BTZ theory with no spin. Recall that the BTZ line element yields anti-de Sitter black hole solutions (see Section 2.2.1).

In 1992, Callan, Giddings, Harvey and Strominger analyzed the two dimensional gravitational action coupled to conformal matter [75]

$$S = \int d^2x\sqrt{-g}\left[e^{-2\phi}\left(R + 4g^{\mu\nu}\nabla_\mu\phi\nabla_\nu\phi + 4\lambda^2\right) - \frac{1}{2}g^{\mu\nu}\nabla_\mu f\nabla_\nu f\right]. \tag{3.8}$$

They analyzed the system classically and found it is exactly solvable with solutions that yield black holes. The black hole solutions can correspond to either extremal higher dimensional black holes found in [76, 77], or to the two dimensional quantum black hole found in [78]. In vacuum, the CGHS action is

$$S = \int d^2x\sqrt{-g}e^{-2\phi}\left(R + 4g^{\mu\nu}\nabla_\mu\phi\nabla_\nu\phi + 4\lambda^2\right). \tag{3.9}$$

If the dilaton field in (3.9) is redefined according to

$$\bar{\phi} = 2\sqrt{2}e^{-\phi} \tag{3.10}$$

the new CGHS action is obtained:

$$S = \int d^2x\sqrt{-g}\left(\frac{1}{8}\bar{\phi}^2R + \frac{1}{2}g^{\mu\nu}\nabla_\mu\bar{\phi}\nabla_\nu\bar{\phi} + \frac{1}{2}\bar{\phi}^2\lambda^2\right). \tag{3.11}$$

The kinetic term in the action can be eliminated by the following conformal redefinition of the metric (see Section 3.2.1):

$$g_{\mu\nu} \rightarrow \bar{\phi}^2 g_{\mu\nu}. \tag{3.12}$$

Thus reducing (3.11) to

$$S = \int d^2x\sqrt{-g}\left(\phi R + \frac{1}{2}\lambda^2\right), \tag{3.13}$$

where we have performed a final redefinition of the dilaton field according to

$$\frac{1}{8}\bar{\phi}^2 \to \phi. \tag{3.14}$$

Bose, Parker and Peleg [79] analyzed the CGHS action in the semi-classical approximation using an effective one loop quantum correction for the matter field (they neglected quantum corrections for the gravitational and dilaton fields). In order to find exact solutions they included a counter term in the action. They found black hole solutions which evaporate to a naked singularity. Bose, Luoko, Parker and Peleg [80, 81, 82, 83, 84] have produced a series of papers on the quantum mechanics and black hole thermodynamics of the CGHS system.

Other two dimensional dilaton theories which have been studied are equivalent to higher dimensional gravity theories with symmetry. For example, several authors [85, 86, 87, 88] have considered the reduction of higher dimensional spherically symmetric $3+1$ gravity to a two dimensional action.

The resulting action is given by

$$S = \int d^2x\sqrt{-g}e^{-2\phi}\left(R + 2g^{\mu\nu}\nabla_\mu\phi\nabla_\nu\phi + 2e^{2\phi}\right), \tag{3.15}$$

with the dilaton defined by

$$r = \exp\left(-\phi\right). \tag{3.16}$$

All of the above two dimensional dilaton gravity theories are specific examples of the most general dilaton gravity theory given by the action [89, 90, 91, 92]:

$$S = \int d^2x\sqrt{-g}\left[D\left(\phi\right)R + \frac{1}{2}g^{\mu\nu}\nabla_\mu\phi\nabla_\nu\phi + V\left(\phi\right)\right], \tag{3.17}$$

where $V(\phi)$ is an arbitrary function of ϕ and R is the Ricci scalar associated with $g_{\mu\nu}$. The action (3.17) is the most general diffeomorphism invariant action functional dependent on $g_{\mu\nu}$ and a dilaton scalar field ϕ in two dimensions, such that it contains at most first and second derivatives of the fields [93]. In the following two subsections, a specific case of (3.17), corresponding to a d-dimensional metric with spherical symmetry, will be

presented and which will serve as the model of study.

3.2 Action Functional and Field Equations in Spherical Symmetry

Consider the action for Einstein gravity with cosmological constant in d space-time dimensions, given by

$$S_G^{(d)} = \frac{1}{16\pi G^{(d)}} \int d^d x \sqrt{-g^{(d)}} \left(R^{(d)} \left[g^{(d)} \right] - \hat{\Lambda} \right). \tag{3.18}$$

In the above expression, $G^{(d)}$ is the d-dimensional Newton's coupling constant and $\hat{\Lambda}$ is the cosmological constant.

Spherical symmetry is imposed by assuming the d-dimensional metric can be decomposed into a Kronecker sum (matrix direct product) of a 2×2 metric and a $d-2 \times d-2$ metric (representing the S^{d-2}-sphere submanifold of the complete Riemannian manifold):

$$\mathbf{g}^{(d)} = \bar{\mathbf{g}}^{(2)} \oplus \mathbf{S}^{(d-2)} \tag{3.19}$$

where the components of the 2×2 metric $\bar{g}_{\alpha\beta}$ are only dependent on the two

coordinates x^α, $\alpha = 1, 2$. We also define

$$n = d - 2 \tag{3.20}$$

for notational compactness.

In spherical polar coordinates, with $r = r(x^\alpha)$ representing the proper radial distance from the origin, the metric of the $\mathbf{S}^{(n)}$-sphere takes the usual diagonal form with determinant

$$\det\left(\mathbf{S}^{(n)}\right) = r^{2n} \prod_{i=1}^{(n-1)} \sin^{2(n-i)}\theta_i. \tag{3.21}$$

Thus, the spherically symmetric d-dimensional metric has determinant

$$g^{(d)} = \det\left(\mathbf{g}^{(d)}\right) = \det\left(\bar{\mathbf{g}}^{(2)}\right) \det\left(\mathbf{S}^{(n)}\right). \tag{3.22}$$

Using (3.21) and (3.22), the metric determinant in the d-dimensional action is given by

$$\sqrt{-g^{(d)}} = \sqrt{-\bar{g}^{(2)}} r^n \prod_{i=1}^{(n-1)} \sin^{(n-i)}\theta_i. \tag{3.23}$$

An equivalent way of expressing the symmetry of the metric can, of course, be given by the line element

$$ds^2_{(d)} = \bar{g}_{\alpha\beta}dx^\alpha dx^\beta + r^2(x^\alpha)\, d\Omega_{(n)}, \tag{3.24}$$

where $d\Omega_{(n)}$ is the metric on the subspace $\mathbf{S}^{(n)}$.

An exact expression for the Ricci curvature scalar, in terms of the spherically symmetric metric $\bar{g}$, can be calculated directly. Inserting (3.24) into (1.11) and using (1.15), (1.16) and (1.17), the d-dimensional curvature scalar in spherically symmetric gravity is given by

$$R^{(d)}\left[g^{(d)}\right] = R^{(2)}(\bar{g}) + \frac{n\,(n-1)}{r^2} + \frac{n\,(n-1)}{r^2}\bar{g}^{\alpha\beta}\bar{\nabla}_\alpha r\bar{\nabla}_\beta r \tag{3.25}$$

where $\bar{\nabla}$ is the covariant derivative associated with $\bar{g}_{\alpha\beta}$ and $R^{(2)}$ is used to denote the $d = 2$ curvature scalar which is only dependent on $\bar{g}_{\alpha\beta}$.

Inserting (3.23) and (3.25) into (3.18) and integrating over $d\Omega_{(n)}$ it is found for the dimensionally reduced gravitational action:

$$S_G = \frac{A^{(n)}}{16\pi G^{(d)}}\int d^2x\sqrt{-\bar{g}^{(2)}}\, r^n\Bigg(R^{(2)}(\bar{g}) + \frac{n\,(n-1)}{r^2} + \frac{n\,(n-1)}{r^2}\bar{g}^{\alpha\beta}\bar{\nabla}_\alpha r\bar{\nabla}_\beta r - \hat{\Lambda}\Bigg) \tag{3.26}$$

where

$$A^{(n)} = \frac{2\pi^{(n+1)/2}}{\Gamma\left(\frac{n+1}{2}\right)} \tag{3.27}$$

is the volume of the unit n-sphere [94].

3.2.1 Dilaton Gravity Form

In this section, a dilaton field is defined and a conformal re-parameterization of the metric is carried out in order to simplify the gravitational action of the theory. Begin by defining a dimensionless dilaton field:

$$\bar{\phi} = \left(\frac{r}{\hat{l}}\right)^{n/2} \tag{3.28}$$

$$\hat{l}^n = G^{(d)}. \tag{3.29}$$

Dropping the overall area term $A^{(n)}$, the gravitational action becomes

$$S_G = \frac{1}{2G}\int d^2x\sqrt{-\bar{g}^{(2)}}\,\bar{\phi}^2\left(\frac{n}{8(n-1)}R^{(2)}(\bar{g}) + \frac{n^2}{8\hat{l}^2\bar{\phi}^{4/n}} + \frac{1}{2}\left(\frac{\bar{\nabla}\bar{\phi}}{\bar{\phi}}\right)^2 - \frac{n}{8(n-1)}\hat{\Lambda}\right) \tag{3.30}$$

where

$$\frac{1}{2G} = \frac{8\,(n-1)}{16\pi n}. \tag{3.31}$$

The expression (3.30) can now be more easily identified as a specific case of the general two dimensional dilaton gravity theory (3.17)

$$S_G = \frac{1}{2G}\int d^2x\sqrt{-\bar{g}^{(2)}}\left(\bar{D}(\bar{\phi})R^{(2)}(\bar{g}) + \frac{1}{\hat{l}^2}\bar{V}(\bar{\phi}) + \frac{1}{2}\bar{g}^{\mu\nu}\bar{\nabla}_\mu\bar{\phi}\bar{\nabla}_\nu\bar{\phi}\right) \tag{3.32}$$

with the following identifications:

$$\bar{D}(\bar{\phi}) = \frac{n}{8\,(n-1)}\bar{\phi}^2 \tag{3.33}$$

$$\bar{V}(\bar{\phi}) = \frac{n^2\bar{\phi}^{(2n-4)/n}}{8} - \frac{n\hat{l}^2\bar{\phi}^2\hat{\Lambda}}{8(n-1)}. \tag{3.34}$$

Conformal Re-parameterization

The following conformal re-parameterization of the two dimensional part of the physical metric is considered:

$$g_{\alpha\beta} = \Omega^2(\bar{\phi})\bar{g}^{(2)}_{\alpha\beta}$$

$$g^{\alpha\beta} = \frac{1}{\Omega^2(\bar{\phi})}\bar{g}^{(2)\alpha\beta} \tag{3.35}$$

which affects the metric determinant

$$\sqrt{-\bar{g}^{(2)}} = \frac{\sqrt{-g}}{\Omega^2(\bar{\phi})}. \tag{3.36}$$

Using (3.35), the conformally related curvature scalar becomes

$$R^{(2)}(\bar{g}) = \Omega^2(\bar{\phi})R^{(2)}(g) - 2g^{\mu\nu}\nabla_\mu\Omega\nabla_\nu\Omega + 2\Omega g^{\mu\nu}\nabla_\mu\nabla_\nu\Omega. \tag{3.37}$$

Inserting (3.35)-(3.37) into (3.32) we obtain

$$S_G = \frac{1}{2G}\int d^2x\sqrt{-g}\Big[\bar{D}(\bar{\phi})R^{(2)}(g) + \frac{\bar{V}(\bar{\phi})}{\hat{l}^2\Omega^2} + \frac{1}{2}g^{\mu\nu}\bar{\nabla}_\mu\bar{\phi}\bar{\nabla}_\nu\bar{\phi} - \frac{2\bar{D}(\bar{\phi})g^{\mu\nu}\nabla_\mu\Omega\nabla_\nu\Omega}{\Omega^2} + \frac{2\bar{D}(\bar{\phi})g^{\mu\nu}\nabla_\mu\nabla_\nu\Omega}{\Omega}\Big]. \tag{3.38}$$

Let us now redefine the dilaton field

$$\phi = \bar{D}(\bar{\phi}) = \frac{n}{8\,(n-1)}\bar{\phi}^2. \tag{3.39}$$

Therefore,

$$\bar{\nabla}_\mu\bar{\phi}\bar{\nabla}_\nu\bar{\phi} = \left(\frac{d\bar{D}(\bar{\phi})}{d\bar{\phi}}\right)^{-2}\nabla_\mu\phi\nabla_\nu\phi = \frac{n\phi}{2(n-1)}\nabla_\mu\phi\nabla_\nu\phi. \tag{3.40}$$

In the above line, we have explicitly used the equivalence of the covariant derivatives $\bar{\nabla}_\mu$ and ∇_μ when they are used to differentiate scalar fields. It is also found that

$$\nabla_\mu\Omega\nabla_\nu\Omega = \left(\frac{d\Omega}{d\bar{\phi}}\right)^2\left(\frac{d\bar{D}(\bar{\phi})}{d\bar{\phi}}\right)^{-2}\nabla_\mu\phi\nabla_\nu\phi \tag{3.41}$$

$$\begin{aligned}\nabla_\mu\nabla_\nu\Omega &= \frac{d\Omega}{d\bar{\phi}}\left(\frac{d\bar{D}}{d\bar{\phi}}\right)^{-1}\nabla_\mu\nabla_\nu\phi \\ &+ \left[\frac{d^2\Omega}{d\bar{\phi}^2} - \frac{d\Omega}{d\bar{\phi}}\left(\frac{d\bar{D}}{d\bar{\phi}}\right)^{-1}\frac{d^2\bar{D}}{d\bar{\phi}^2}\right]\left(\frac{d\bar{D}(\bar{\phi})}{d\bar{\phi}}\right)^{-2}\nabla_\mu\phi\nabla_\nu\phi.\end{aligned} \tag{3.42}$$

After inserting (3.39)-(3.42) into (3.37), integrating by parts and dropping surface terms, the new expression for the reduced gravitational action is obtained

$$\begin{aligned}S_G = \frac{1}{2G}\int d^2x\sqrt{-g}\Big[&\phi R^{(2)}(g) + V(\phi) \\ &+ \left(\frac{1}{2} - \frac{2}{\Omega}\frac{d\Omega}{d\bar{\phi}}\frac{d\phi}{d\bar{\phi}}\right)\left(\frac{d\phi}{d\bar{\phi}}\right)^{-2}g^{\mu\nu}\nabla_\mu\phi\nabla_\nu\phi\Big],\end{aligned} \tag{3.43}$$

with the additional redefinition of the scalar dilaton potential

$$V(\phi) = \frac{\bar{V}(\bar{\phi}(\phi))}{\hat{l}^2\Omega^2(\bar{\phi}(\phi))}. \tag{3.44}$$

The main advantage in considering the action functional in the above form is seen after a conformal function which eliminates the kinetic term $g^{\mu\nu}\nabla_\mu\phi\nabla_\nu\phi$ is chosen. The field equations which are derived from the that action are then also simplified. This is achieved whenever the differential equation in (3.43) is satisfied [90, 91]

$$\frac{1}{2}\left(\frac{d\phi}{d\bar{\phi}}\right)^{-1} = \frac{d\log\Omega^2}{d\bar{\phi}}. \tag{3.45}$$

The solution to this differential equation is

$$\Omega^2(\bar{\phi}) = C\exp\left[\frac{1}{2}\int\left(\frac{d\phi}{d\bar{\phi}}\right)^{-1}d\bar{\phi}\right], \tag{3.46}$$

where C is an arbitrary integration constant. Recall, from (3.39),

$$\phi = \frac{n}{8\,(n-1)}\bar{\phi}^2, \tag{3.47}$$

therefore

$$\frac{d\phi}{d\bar{\phi}} = \frac{n}{4\,(n-1)}\bar{\phi}. \tag{3.48}$$

Inserting (3.48) into (3.46) will give the appropriate conformal factor to eliminate the kinetic term from the action:

$$\Omega^2(\bar{\phi}) = C\bar{\phi}^{\frac{2(n-1)}{n}} = C\left[\frac{8(n-1)}{n}\phi\right]^{\left(\frac{n-1}{n}\right)}. \tag{3.49}$$

Without loss of generality the constant C is defined according to

$$C = \frac{n}{\sqrt{8}\,(n-1)}\left(\frac{8(n-1)}{n}\right)^{1/2n}, \tag{3.50}$$

for reasons which will be seen below (see Section 3.3.3). Hence, the final form for the gravitational action becomes

$$S_G = \frac{1}{2G}\int d^2x\sqrt{-g}\,[\phi R + V(\phi)] \tag{3.51}$$

with

$$\phi = \frac{n}{8(n-1)}\left(\frac{r}{\hat{l}}\right)^n \tag{3.52}$$

$$V(\phi) = \frac{1}{C\hat{l}^2}\left(\frac{n}{8(n-1)}\right)^{1/n}\phi^{-1/n}\left[\frac{n^2}{8} - \hat{l}^2\left(\frac{n}{8(n-1)}\right)^{\frac{n-2}{n}}\phi^{2/n}\hat{\Lambda}\right] \tag{3.53}$$

$$R = R^{(2)}(g)\,. \tag{3.54}$$

To simplify the expression for the dilaton potential, let us redefine the scale in the problem. In addition, we redefine the cosmological constant so that it becomes dimensionless. Let us choose

$$\Lambda = \frac{8\hat{l}^2}{n^2}\left(\frac{n}{8(n-1)}\right)^{\frac{n-2}{n}}\hat{\Lambda} \tag{3.55}$$

$$l^2 = \frac{8}{n^2}\left(\frac{8(n-1)}{n}\right)^{1/n}\hat{l}^2. \tag{3.56}$$

Therefore,

$$\phi = \frac{8^{n/2}}{n^n}\left(\frac{n}{8(n-1)}\right)^{1/2}\left(\frac{r}{l}\right)^n \tag{3.57}$$

$$V(\phi) = \frac{1}{Cl^2}\phi^{-1/n}\left[1 - \phi^{2/n}\Lambda\right]. \tag{3.58}$$

3.2.2 The Matter Action

Consider the case of a minimally coupled Klein-Gordon scalar field χ. The field satisfies the well known Klein-Gordon differential equation [95]

$$g^{\mu\nu}\nabla_\mu\nabla_\nu\chi - m^2\chi = 0 \tag{3.59}$$

and is associated with the stress-energy-momentum tensor

$$T_{\mu\nu} = \nabla_\mu\chi\nabla_\nu\chi - \frac{1}{2}g_{\mu\nu}\left(\nabla_\sigma\chi\nabla^\sigma\chi + m^2\chi^2\right). \tag{3.60}$$

The Einstein equations with cosmological constant for a minimally coupled massive scalar field are given by

$$G_{\mu\nu} = R_{\mu\nu} - \frac{1}{2}g_{\mu\nu}R + \frac{1}{2}g_{\mu\nu}\Lambda = 16\pi G^{(d)}T_{\mu\nu} \tag{3.61}$$

Contracting (3.61) we obtain an expression for the scalar curvature in the presence of matter

$$R^{(d)} = 16\pi G^{(d)}\left[(\nabla\chi)^2 + \left(\frac{n+2}{n}\right)m^2\chi^2\right] + \left(\frac{n+2}{n}\right)\Lambda. \tag{3.62}$$

The matter action functional corresponding to the Klein-Gordon field in d-dimensions is given by [95]

$$S_M = -\frac{1}{2}\int d^d x\sqrt{-g^{(d)}}\left(g^{(d)\mu\nu}\nabla_\mu\chi\nabla_\nu\chi + m^2\chi^2\right). \tag{3.63}$$

Consider the case of a spherically symmetric massless ($m = 0$) scalar field $\tilde{\chi}$. Therefore, assume the scalar field is dependent on only the two coordinates x^α. Integrating over the angular dependence in the matter action, it is found

$$S_M = -\frac{1}{2}\int d^2 x\sqrt{-\bar{g}^{(2)}}r^n\bar{g}^{(2)\mu\nu}\bar{\nabla}_\mu\tilde{\chi}\bar{\nabla}_\nu\tilde{\chi}. \tag{3.64}$$

As above, the unit n-sphere volume term is dropped from the action functional. Inserting (3.29), (3.31), (3.35), (3.36), and (3.52), into (3.64), and re-scaling the scalar field $\tilde{\chi} = \chi/\sqrt{8\pi G^{(d)}}$, the following expression gives for the matter action in the conformally related space-time:

$$S_M = -\frac{1}{2G}\int d^2 x\sqrt{-g}\phi g^{\mu\nu}\nabla_\mu\chi\nabla_\nu\chi. \tag{3.65}$$

The reduced total action functional used to derive the field equations for the case of a minimally coupled massless scalar field is found by adding (3.51)

and (3.65):

$$S = S_G + S_M = \frac{1}{2G}\int d^2x\sqrt{-g}\Big[\phi R + V(\phi) - \phi g^{\mu\nu}\nabla_\mu\chi\nabla_\nu\chi\Big]. \quad (3.66)$$

3.2.3 Field Equations

The field equations of the problem are derived by examining the extremum of the total action (3.66) using the minimum action principle. The extremum of the fields are given by the condition:

$$\delta S = 0. \quad (3.67)$$

Formally,

$$\begin{aligned}
\delta S &= \frac{1}{2G}\int d^2x\delta\left[\sqrt{-g}\phi R + \sqrt{-g}V - \sqrt{-g}\phi g^{\mu\nu}\nabla_\mu\chi\nabla_\nu\chi\right] \\
&= \frac{1}{2G}\int d^2x\left[\delta\left(\sqrt{-g}R\right)\phi + \delta\left(\sqrt{-g}\right)\left\{V - \phi g^{\mu\nu}\nabla_\mu\chi\nabla_\nu\chi\right\}\right] \\
&\quad + \frac{1}{2G}\int d^2x\sqrt{-g}\left[R + \frac{dV}{d\phi} - g^{\mu\nu}\nabla_\mu\chi\nabla_\nu\chi\right]\delta\phi \\
&\quad - \frac{1}{2G}\int d^2x\sqrt{-g}\left[\phi\nabla_\mu\chi\nabla_\nu\chi\delta g^{\mu\nu} + 2\phi g^{\mu\nu}\nabla_\mu\chi\left(\nabla_\nu\delta\chi\right)\right]. \quad (3.68)
\end{aligned}$$

To simplify the expression in the final line, it is noted that:

$$\begin{aligned}\nabla_\nu \left(\phi g^{\mu\nu} \nabla_\mu \chi \delta\chi\right) &= \left(g^{\mu\nu}\nabla_\nu\phi\nabla_\mu\chi + \phi g^{\mu\nu}\nabla_\mu\nabla_\nu\chi\right)\delta\chi \\ &\quad + \phi g^{\mu\nu}\nabla_\mu\chi\left(\nabla_\nu\delta\chi\right), \end{aligned} \tag{3.69}$$

where the following identity [3] is used

$$\nabla_\nu g^{\sigma\omega} = 0. \tag{3.70}$$

We also make use of the identity [3]

$$\delta\left(\sqrt{-g}\right) = -\frac{1}{2}\sqrt{-g}g_{\mu\nu}\delta g^{\mu\nu}. \tag{3.71}$$

Inserting (3.69) and (3.71) into (3.68) and integrating out surface terms yields

$$\begin{aligned}\delta S &= -\frac{1}{2G}\int d^2x\sqrt{-g}\left[\nabla_\mu\nabla_\nu\phi - g_{\mu\nu}\Box\phi\right]\delta g^{\mu\nu} \\ &\quad -\frac{1}{2G}\int d^2x\sqrt{-g}\left[\frac{1}{2}g_{\mu\nu}V - \frac{1}{2}\phi g_{\mu\nu}\left(\nabla\chi\right)^2 + \phi\nabla_\mu\chi\nabla_\nu\chi\right]\delta g^{\mu\nu} \\ &\quad +\frac{1}{2G}\int d^2x\sqrt{-g}\left[R + \frac{dV}{d\phi} - \left(\nabla\chi\right)^2\right]\delta\phi \\ &\quad +\frac{1}{2G}\int d^2x\sqrt{-g}\left[2g^{\mu\nu}\nabla_\nu\phi\nabla_\mu\chi + 2\phi g^{\mu\nu}\nabla_\mu\nabla_\nu\chi\right]\delta\chi, \end{aligned} \tag{3.72}$$

where we have used the identity (A.10) in the first line.

The minimum action principle requires that each of the fields $g^{\mu\nu}$, ϕ, and χ, be varied independently while ensuring (3.67) remains valid over the entire solution space. This requirement demands that all three expressions in square brackets identically vanish at the minimum of action. Hence, the three simultaneous field equations are found:

$$\left(\nabla_\mu\nabla_\nu - g_{\mu\nu}\Box\right)\phi + \tfrac{1}{2}g_{\mu\nu}V - \tfrac{1}{2}\phi g_{\mu\nu}g^{\sigma\omega}\nabla_\sigma\chi\nabla_\omega\chi + \phi\nabla_\mu\chi\nabla_\nu\chi = 0 \quad (3.73)$$

$$R + \tfrac{dV}{d\phi} - g^{\mu\nu}\nabla_\mu\chi\nabla_\nu\chi = 0 \quad (3.74)$$

$$g^{\mu\nu}\nabla_\nu\phi\nabla_\mu\chi + \phi g^{\mu\nu}\nabla_\mu\nabla_\nu\chi = 0 \quad (3.75)$$

The expression (3.73) can be simplified by contracting both sides with the metric tensor. This gives the equality

$$\Box\phi = V. \quad (3.76)$$

The matter field constraint equation (3.75) can also be simplified by noting

$$\begin{aligned} g^{\mu\nu}\nabla_\nu\phi\nabla_\mu\chi + \phi g^{\mu\nu}\nabla_\mu\nabla_\nu\chi &= g^{\mu\nu}\left(\nabla_\nu\phi\nabla_\mu\chi + \phi\nabla_\nu\nabla_\mu\chi\right) \\ &= g^{\mu\nu}\left(\nabla_\nu\phi + \phi\nabla_\nu\right)\nabla_\mu\chi \end{aligned}$$

$$= g^{\mu\nu}\nabla_\nu\left(\phi\nabla_\mu\chi\right)$$

$$= \nabla^\mu\left(\phi\nabla_\mu\chi\right). \tag{3.77}$$

Using (3.76) and (3.77) the final form of the field equations with $m = 0$ are given by[1]:

$$\nabla_\mu\nabla_\nu\phi = \tfrac{1}{2}g_{\mu\nu}V - \phi T_{\mu\nu} \tag{3.78}$$

$$R = -\tfrac{dV}{d\phi} + (\nabla\chi)^2 \tag{3.79}$$

$$\nabla^\mu\left(\phi\nabla_\mu\chi\right) = 0. \tag{3.80}$$

3.3 Evolution Equations and Boundary Conditions

In this section, a coordinate system is chosen from which the evolution equations of the model are defined. A double null coordinate grid (u and v coordinates) will be chosen and a gauge choice specified. Boundary conditions are then imposed which ensure Cauchy data on the initial null hypersurface.

[1] Normally, one should perform the dimensional reduction process at the level of the field equations in order to ensure the correct solution space has been found. In spherically symmetric gravity, however, it is well known that the field equations derived here (from the reduced action) are equivalent to the reduced field equations [92, 96].

3.3.1 Coordinate Choice

Notation representing partial differentiation of a function with respect to the u coordinate is indicated using an overdot. A prime indicates differentiation with respect to the v coordinate. Hence,

$$\dot{f} = \frac{\partial f}{\partial u} \tag{3.81}$$

$$f' = \frac{\partial f}{\partial v}. \tag{3.82}$$

The coordinate system chosen is the same as in [28]. The metric is parameterized as follows:

$$ds^2 = -2lg(u,v)\phi'(u,v)dudv. \tag{3.83}$$

The physical metric can also be expressed in terms of an (r,t) coordinate system. Let $x^\alpha = (u,v)$ and $\bar{x}^\alpha = (r,t)$ then

$$\bar{g}_{\mu\nu}(\bar{x}) = \frac{1}{\Omega^2} g_{\alpha\beta}(x) \frac{\partial x^\alpha}{\partial \bar{x}^\mu} \frac{\partial x^\beta}{\partial \bar{x}^\nu}. \tag{3.84}$$

Using the characteristic definition of double null coordinates in flat space

$$u = t - r \tag{3.85}$$

$$v = t + r, \tag{3.86}$$

gives the physical metric in (r, t) coordinates in flat space:

$$\bar{\mathbf{g}} = -\frac{2lg\phi'}{\Omega^2}\begin{pmatrix} 1 & 0 \\ 0 & -1 \end{pmatrix} \tag{3.87}$$

$$\bar{\mathbf{g}}^{-1} = -\frac{\Omega^2}{2lg\phi'}\begin{pmatrix} 1 & 0 \\ 0 & -1 \end{pmatrix}. \tag{3.88}$$

3.3.2 Evolution Equations

Inserting our preferred coordinate system (3.83) into (3.78)-(3.80) yields the following five field equations:

$$\frac{\partial\dot{\phi}}{\partial u} = \frac{\dot{g}\dot{\phi}}{g} + \frac{\dot{\phi}'\dot{\phi}}{\phi'} - \phi\left(\dot{\chi}\right)^2 \tag{3.89}$$

$$g'\phi' = g\phi\left(\chi'\right)^2 \tag{3.90}$$

$$\dot{\phi}' = -\tfrac{1}{2}lg\phi' V \tag{3.91}$$

$$\frac{\partial}{\partial u}\left(\frac{g'}{g}\right) + \frac{\partial}{\partial v}\left(\frac{\dot{\phi}'}{\phi'}\right) = -\tfrac{1}{2}lg\frac{\partial V}{\partial v} - \dot{\chi}\chi' \tag{3.92}$$

$$\frac{\partial}{\partial v}\left(\phi\dot{\chi}\right)+\frac{\partial}{\partial u}\left(\phi\chi'\right)=0. \tag{3.93}$$

By virtue of the Bianchi identities, only three of the field equations (3.89)-(3.93) are independent. The identities reduce the number of independent field equations by two—one for each dimension of the space-time. The Bianchi identities are given by [3]

$$\nabla_\lambda G^\lambda_\mu = 0, \tag{3.94}$$

where $G_{\mu\nu}$ is the Einstein tensor. For our model, the following tensor plays the role of the Einstein tensor

$$G_{\mu\nu} = \nabla_\mu\nabla_\nu\phi - \frac{1}{2}g_{\mu\nu}V. \tag{3.95}$$

Thus, the Bianchi identities can be quickly verified by inserting (3.95) into (3.94)

$$\begin{aligned}\nabla_\lambda G^\lambda_\mu &= \nabla_\lambda\left(g^{\nu\lambda}\nabla_\mu\nabla_\nu\phi\right)-\frac{1}{2}\nabla_\lambda\left(\delta^\lambda_\mu V\right)\\ &= \nabla_\mu\left(\Box\phi - V\right)\\ &= 0,\end{aligned} \tag{3.96}$$

where we have used (3.70), (3.76), and the commutativity of the covariant derivative. Indeed, the Bianchi identities can be shown explicitly by inserting (3.90) and (3.91) into (3.92):

$$\frac{\partial}{\partial u}\left[\frac{\phi}{\phi'}\left(\chi'\right)^2\right] - \frac{l}{2}\frac{\partial}{\partial v}\left(gV\right) = -\frac{lg}{2}\frac{\partial V}{\partial v} - \dot{\chi}\chi', \tag{3.97}$$

which gives,

$$\frac{\chi'}{\phi'}\left(\dot{\phi}\chi' + 2\phi\dot{\chi}' - \frac{\dot{\phi}'}{\phi'}\phi\chi'\right) - \frac{l}{2}g'V = -\dot{\chi}\chi'. \tag{3.98}$$

We can simplify (3.98) by inserting (3.93), which gives the identity

$$g'V = g'V. \tag{3.99}$$

The other Bianchi identity can be seen by inserting (3.91) into (3.89) and differentiating with respect to v. Thus,

$$\begin{aligned} \frac{\partial}{\partial v}\left(\frac{\partial\dot{\phi}}{\partial u}\right) &= \frac{\partial}{\partial v}\left[\frac{\dot{g}\dot{\phi}}{g} - \frac{l}{2}g\dot{\phi}V - \phi\left(\dot{\chi}\right)^2\right] \\ = \dot{\phi}\left[\frac{\partial}{\partial u}\left(\frac{g'}{g}\right) + \frac{\partial}{\partial v}\left(\frac{\dot{\phi}'}{\phi'}\right)\right] &+ \frac{\dot{g}\dot{\phi}'}{g} - \frac{lg}{2}\dot{\phi}'V - \dot{\chi}\left(\phi'\dot{\chi} + 2\phi\dot{\chi}'\right). \end{aligned} \tag{3.100}$$

Inserting (3.92) and (3.93) into (3.100) and simplifying yields

$$\frac{\partial}{\partial v}\left(\frac{\partial\dot{\phi}}{\partial u}\right) = \frac{\dot{g}\dot{\phi}'}{g} - \frac{lg}{2}\dot{\phi}V' - \frac{lg}{2}\dot{\phi}'V. \tag{3.101}$$

Equating the right hand side of the above expression to the u derivative of (3.91) gives the result

$$\dot{\phi}V' = \phi'\dot{V}. \tag{3.102}$$

Recall that $V = V(\phi)$, therefore,

$$V' = \frac{dV}{d\phi}\phi'. \tag{3.103}$$

Inserting (3.103) into (3.102) yields the identity

$$\dot{\phi}\frac{dV}{d\phi}\phi' = \phi'\frac{dV}{d\phi}\dot{\phi} \tag{3.104}$$

thus proving the Bianchi identities hold.

Two other useful quantities to calculate are the two dimensional Ricci scalar, R, and the d-dimensional Ricci scalar, $R^{(d)}$. From (3.79), the Ricci

scalar is given by

$$R = \frac{\phi^{\frac{-n-1}{n}}}{Cnl^2}\left[1+\phi^{2/n}\Lambda\right] - \frac{2}{lg\phi'}\dot{\chi}\chi'. \tag{3.105}$$

From (3.62) with $m = 0$, the d-dimensional Ricci scalar is given by

$$\begin{aligned} R^{(d)} &= \left(\frac{n+2}{n}\right)\hat{\Lambda} + 16\pi G^{(d)}\left(\bar{\nabla}\tilde{\chi}\right)^2 \\ &= \left(\frac{n+2}{n}\right)\left(\frac{8(n-1)}{n}\right)^{\frac{n-1}{n}}\frac{\Lambda}{l^2} + 2\Omega^2 g^{\mu\nu}\nabla_\mu\chi\nabla_\nu\chi \\ &= \left(\frac{8(n-1)}{n}\right)^{\frac{n-1}{n}}\left[\left(\frac{n+2}{n}\right)\frac{\Lambda}{l^2} - \frac{4C}{lg\phi'}\phi^{\frac{n-1}{n}}\dot{\chi}\chi'\right]. \end{aligned} \tag{3.106}$$

Without loss of generality, the following three field equations are used to evolve initial data:

$$g'\phi' = g\phi\left(\chi'\right)^2 \tag{3.107}$$

$$\dot{\phi}' = -\tfrac{1}{2}lg\phi' V \tag{3.108}$$

$$\tfrac{\partial}{\partial v}\left(\phi\dot{\chi}\right) + \tfrac{\partial}{\partial u}\left(\phi\chi'\right) = 0. \tag{3.109}$$

Define the new function

$$\tilde{g} = \int g\phi' V^{(n)}(\phi)\, dv. \tag{3.110}$$

Integrating (3.108) with respect to v gives the *dilaton evolution function*

$$\dot{\phi} = -\frac{l\tilde{g}}{2}. \tag{3.111}$$

Integrating (3.107) with respect to v gives the *metric function*

$$g(u,v) = C_1(u) \exp\left[\int \frac{\phi(\chi')^2}{\phi'} dv\right]. \tag{3.112}$$

As shown by Christodoulou [25, 97] and as implemented by Garfinkle [28], the scalar field constraint equation (3.109) can be decoupled by the introduction of the auxiliary scalar field

$$h = \frac{2\sqrt{\phi}}{\phi'} \frac{\partial}{\partial v}\left(\sqrt{\phi}\chi\right), \tag{3.113}$$

which gives,

$$h = \chi + \frac{2\phi\chi'}{\phi'}. \tag{3.114}$$

The matter field is, therefore, defined explicitly in terms of this new parameterization by

$$\chi = \frac{1}{2\sqrt{\phi}} \int \frac{h\phi'}{\sqrt{\phi}}\, dv + \frac{C_2(u)}{\sqrt{\phi}}. \tag{3.115}$$

Differentiating (3.114) with respect to u and inserting (3.109) gives the *matter evolution function* which, in terms of the new matter parameter h, is given by

$$\begin{aligned} \dot{h} &= -\left(\frac{h-\chi}{\phi'}\right)\left[\dot{\phi}' - \frac{\dot{\phi}\phi'}{2\phi}\right] \\ &= l\left(\frac{h-\chi}{2\phi}\right)\left[g\phi V(\phi) - \frac{\tilde{g}}{2}\right]. \end{aligned} \tag{3.116}$$

Treating the u coordinate like a time coordinate and the v coordinate like a space coordinate, the equations (3.111) and (3.116) can be used to evolve initial data and simulate gravitational collapse by numerical iteration. In the next subsection, a new function which stabilizes the numerical calculations

will be defined.

Integration By Parts

If one examines the dilaton evolution function (3.110), it is noticed that the integrand is singular at the origin due to the dilaton potential term (recall, $V \propto r^{-1}$). During the evolution, field values are integrated outward from the origin in the v direction (for a given value of u). For points near the center of symmetry, where r is small, the dilaton potential becomes nearly singular and creates numerical inaccuracies during the calculation of the integrand in (3.110). The numerical errors are then added to each grid point on the u slice as the functions are integrated, thereby, propagating the error throughout the entire grid.

Fortunately, the neighbourhood of the origin, where the integrand is not well behaved, is small and typically contains only a few grid points. Moreover, the range of integration is very small so it is assumed the result of the integration is finite. This can be seen explicitly by calculating (3.110) via integration by parts[2]. Once the problematic function is redefined it is seen that, indeed, $\tilde{g}$ approaches zero as one approaches the origin.

[2] It should be noted that prior to implementation of this procedure the numerical evolution was highly sensitive near the origin for most space-time dimensions studied. In fact, the sensitivity of $\tilde{g}$ will grow very rapidly with increasing n near the origin. .

Notice

$$\tilde{g} = \int g\phi' V^{(n)}(\phi)\, dv = \frac{1}{Cl^2}\int g\phi' \left(\phi^{-1/n} - \phi^{1/n}\Lambda\right) dv.$$

Therefore,

$$\begin{aligned}\tilde{g} &= \frac{1}{l^2}\left(\frac{n}{n-1}\right)\int g d\left(\phi^{1-1/n}\right) - \frac{\Lambda}{Cl^2}\left(\frac{n}{n+1}\right)\int g d\left(\phi^{1+1/n}\right) \\ &= \frac{ng\phi^{1-1/n}}{Cl^2}\left(\frac{n+1-\Lambda(n-1)\phi^{2/n}}{(n+1)(n-1)}\right) \\ &- \frac{n}{C\,(n-1)\,(n+1)\,l^2}\int\left[(n+1)\,\phi^{1-1/n} - \Lambda\,(n-1)\,\phi^{1+1/n}\right] dg. \quad (3.117)\end{aligned}$$

From (3.112)

$$dg = g\frac{\phi\,(\chi')^2}{\phi'}dv = \frac{g\phi'}{4\phi}\,(h-\chi)^2\, dv. \quad (3.118)$$

Define

$$\tilde{h} = \frac{n}{4l^2}\int\left[\frac{\phi^{-1/n}}{n-1} - \Lambda\frac{\phi^{1/n}}{n+1}\right] g\phi'\,(h-\chi)^2\, dv. \quad (3.119)$$

Then

$$\tilde{g} = \frac{ng\phi}{Cl^2}\left(\frac{\phi^{-1/n}}{n-1} - \frac{\Lambda\phi^{1/n}}{n+1}\right) - \frac{\tilde{h}}{C}. \tag{3.120}$$

Viewed in this way it is also immediately seen that the evolution equations are unavoidably singular in the $d = 3$ $(n = 1)$ case. On the other hand, for space-time dimensions greater than three, $\tilde{g} \to \phi^{1-1/n}$ as $\phi \to 0$. This is due to the fact that the correction term $\tilde{h}$ approaches zero faster than the leading order term in $\tilde{g}$. As a result, the functions are well behaved near the origin.

In the limit of large n, these functions become

$$\tilde{g}_\infty = \lim_{n\to\infty} \tilde{g} = \frac{g\phi}{Cl^2}(1-\Lambda) - \frac{\tilde{h}_\infty}{C}. \tag{3.121}$$

$$\tilde{h}_\infty = \lim_{n\to\infty} \tilde{h} = \left(\frac{1-\Lambda}{4l^2}\right)\int g\phi'(h-\chi)^2\, dv. \tag{3.122}$$

3.3.3 Residual Gauge and Boundary Conditions

It is required that the initial matter profile be a collapsing spherically symmetric shell of matter with no black hole in the interior [60]. Thus, the metric should be flat, initially, until an asymptotically flat spherical shell of matter "appears" on the initial time slice. Exterior to the matter distribution, the

metric will approach the Minkowski metric at spatial infinity. In addition, even at late times, a flat space-time metric in the vicinity of the coordinate origin ($r = 0$) is maintained.

As discussed above, the Bianchi identities reduce the number of independent field equations. This is due to the general covariance of the Einstein equations. The field equations derived under the metric (3.83) are only unique up to a general coordinate transformation of the form

$$\tilde{u} = \sigma(u) \tag{3.123}$$

$$\tilde{v} = \omega(v). \tag{3.124}$$

To fix this residual gauge freedom, I set $u = 0$ on the initial surface and $v = 0$ at the center of symmetry ($r = 0$). Then, using the characteristic definition of double null coordinates given by (3.86), it is found that on the initial $u = 0$ null surface, $r = v/2$. This gauge choice also fixes the origin on the initial surface at $u = v = 0$. Furthermore, at the origin,

$$\frac{\partial r}{\partial u}(r = 0; u = v) = -\frac{1}{2} \tag{3.125}$$

$$\frac{\partial r}{\partial v}(r = 0; u = v) = +\frac{1}{2}. \tag{3.126}$$

The boundary conditions at the origin should be examined in more detail. I have required that the metric be flat for $u < 0$ throughout the entire manifold. To ensure continuity at $u = 0$, we need to solve the vacuum dilaton equations for zero mass and show that they can be smoothly connected to a flat space-time at the position of the origin.

For general $V(\phi)$, with $\Lambda = \chi = 0$, the action (3.66) is that of generic vacuum dilaton gravity. The theory has been studied in great detail [90, 92, 96, 98] and the vacuum equations can be solved exactly. The action for the theory is given by

$$S = \frac{1}{2G} \int d^2\sqrt{-g}\,[\phi R + V(\phi)]\,. \tag{3.127}$$

The field equations derived from this action are given by

$$R + \tfrac{dV}{d\phi} = 0 \tag{3.128}$$

$$\nabla_\mu \nabla_\nu \phi - \tfrac{1}{2} g_{\mu\nu} V = 0. \tag{3.129}$$

It is possible to choose an adapted coordinate system in which the metric is locally time-independent. In this case, the exterior solution to (3.128)-(3.129)

is given by

$$ds^2 = -\left[j\left(\phi\right) - 2GM\right]dt^2 + \left[j\left(\phi\right) - 2GM\right]^{-1}dx^2, \tag{3.130}$$

where,

$$\frac{dj\left(\phi\right)}{d\phi} = l^2 V\left(\phi\right), \tag{3.131}$$

$x = l\phi$, and M plays the role of a mass point located at the origin.

In the model studied here, the initial null surface contains no black hole in the interior, therefore, it is required to set $M = 0$ in (3.130). Consider a coordinate transformation to the null coordinates

$$\begin{aligned} u &= t - \phi^* \\ v &= t + \phi^*, \end{aligned} \tag{3.132}$$

where ϕ^* is the generalized tortoise coordinate

$$\phi^* = l\int_0^{\phi} \frac{d\tilde{\phi}}{j\left(\tilde{\phi}\right)}. \tag{3.133}$$

The line element for generic dilaton gravity with $\Lambda = M = \chi = 0$ then

becomes

$$ds^2 = -j(\phi)\, dudv. \tag{3.134}$$

Solving (3.131) for the specific case of d-dimensional spherically symmetric gravity with $\Lambda = 0$ gives

$$j^{(n)}(\phi) = \int_0^{\phi} \tilde{\phi}^{-1/n} d\tilde{\phi} = \left(\frac{n}{n-1}\right) \phi^{(n-1)/n}. \tag{3.135}$$

Hence, from (3.133) and (3.132),

$$\phi^* = l(n-1)\phi^{1/n} = \frac{1}{2}(v-u). \tag{3.136}$$

Therefore,

$$\phi' = \frac{\partial \phi}{\partial v} = \frac{j(\phi)}{2l}. \tag{3.137}$$

Using the above relation and comparing (3.134) to (3.83) it is seen that the boundary condition at the origin is equivalent to the requirement

$$g = 1. \tag{3.138}$$

Demanding also that the physical metric approach the Minkowski metric

near the origin, it is found, by (3.87):

$$\frac{2lg\left(u,u\right)\phi'\left(u,u\right)}{\Omega^2\left(u,u\right)}=1. \tag{3.139}$$

Therefore,

$$\begin{aligned} g\left(u,u\right) &= \frac{C\sqrt{8}\left(n-1\right)}{2nr'}\left(\frac{n}{8(n-1)}\right)^{1/2n} \\ &= 1, \end{aligned} \tag{3.140}$$

which agrees with (3.138) and justifies the choice for the integration constant C first defined in Section (3.2.1). Also, from (3.112),

$$C_1\left(u\right)=g\left(u,u\right)=1. \tag{3.141}$$

To determine the integration constant $C_2(u)$ in (3.115) it is necessary to examine how the term $2\phi\chi'/\phi'$ behaves near the origin. From the definition of the scalar dilaton,

$$\phi'=\frac{n\phi r'}{r}, \tag{3.142}$$

therefore,

$$\frac{2\phi\chi'}{\phi'} = \frac{2r\chi'}{nr'}. \tag{3.143}$$

As $r \to 0$, $r' \to 1/2$, therefore,

$$\lim_{r\to 0} \frac{2\phi\chi'}{\phi'} = \lim_{r\to 0} \frac{4r\chi'}{n} = 0. \tag{3.144}$$

Thus, $h = \chi$ at the origin which, in turn, requires

$$C_2(u) = 0. \tag{3.145}$$

Let us denote the d-dimensional Ricci scalar at the origin by $R_0^{(d)}$ then, using the boundary conditions at the origin and (3.106), we find

$$R_0^{(d)} = \left(\frac{n+2}{n}\right)\left(\frac{n}{8(n-1)}\right)^{1/n}\frac{\Lambda}{l^2} - 8\dot{\chi}_0\chi_0', \tag{3.146}$$

where $\dot{\chi}_0$ and χ_0' denote the partial derivatives of the matter field (evaluated at the origin).

4. NUMERICAL SIMULATIONS OF CRITICAL SCALAR FIELD COLLAPSE IN D DIMENSIONS

In this chapter, the results of the numerical analysis of the d dimensional spherically symmetric collapse of massless minimally coupled scalar field matter will be presented. In the previous chapter, a coordinate formalism was chosen and the evolution equations derived. Coordinate conditions were then imposed and the boundary conditions of the model calculated. Focus will now change to the details of the particular method used to extract data. Numerical simulations of gravitational collapse are inherently unstable due to the non-linearity of the field equations and as a result several particular techniques needed to be used. These techniques will be discussed throughout the chapter.

The primary focus of research has been on determining the dependence of space-time dimension on the critical scaling phenomena. As discussed above, these phenomena have already been observed in a few particular cases in

the massless scalar field system. The research program presented here will expand to include results from several new dimensions and the data will be used to determine properties of the critical solutions in the limiting cases of large and small numbers of dimension.

The results section of this chapter is divided into three main subsections. The first subsection is a case study of the well known $3+1$ dimensional case and it is where the validity and stability of the method is confirmed with the known results. The second subsection presents the results of collapse simulations for $d \geq 4$ as first reported in [48]. The third subsection presents the results of new simulations for $d \leq 4$ [99]. The chapter is concluded by presenting a hypothesis on the relationship between critical phenomena and space-time dimension.

4.1 Numerical Method

A grid is constructed in (u, v) space as shown in Figure 4.1.

On the initial $u = 0$ surface, the specification $\phi(0, v) = v$ was used. The initial grid size ranged between $6,000$ and $12,000$ grid points along the v axis. The initial v spacing (Δv) was set at 0.0005 for the $d \geq 4$ supercritical collapse simulations. For the $d \leq 4$ simulations, Δv ranged between 0.00029

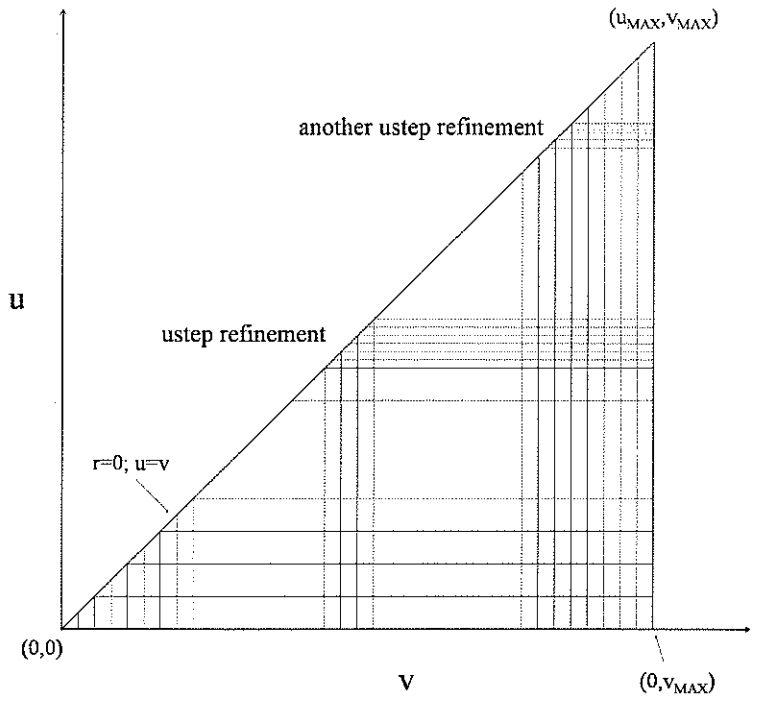

Fig. 4.1: The (u, v) domain of integration for the collapse simulations. At $u = 0$, the initial values of the scalar functions are calculated from the origin $(v = 0)$ to v_{MAX}. The fields are recalculated after each iteration from $u = v$ to v_{MAX} on each u slice according to the evolution equations and boundary conditions. Occasionally, depending upon certain conditions, the u step is reduced to increase resolution in the final result. This may happen several times before the collapse is terminated. The spacing in the v coordinate, however, remains unchanged throughout the collapse.

and 0.0015[1]. To avoid placing the first grid point on the coordinate origin, the first grid point was offset by 0.000001. Let v_0 denote this offset. Let ϕ_0^i denote the dilaton value at the i^{th} grid point on the $u = 0$ initial surface and let N denote the total number of grid points on this surface. Then, the initial values of the dilaton field were specified as follows

$$\phi_0^i = v_0 + i\Delta v \quad i = 0, 1, \ldots, (N-2), (N-1). \tag{4.1}$$

Using this specification: $v_{MAX} = v_0 + (N-1)\Delta v$. In the lower dimensional studies, N was kept fixed and Δv was adjusted so that v_{MAX} was just beyond the apparent horizon in supercritical collapse. This was a similar technique to that used in [28] for the case of subcritical collapse. And was implemented to maximize resolution in the near critical solutions.

The initial values of the remaining functions were calculated as functions of ϕ_0^i. The initial matter field was defined as a Gaussian shell of matter with profile centered at radius ϕ_0

$$\chi = a\phi^{2/n} \exp\left\{ -\left(\frac{\phi - \phi_0}{\sigma} \right)^2 \right\}, \tag{4.2}$$

[1] The numerical method was slightly modified for the lower dimensional collapse studies. Some of the changes to the code included modifying the initial grid spacing in the v direction.

where a was the amplitude of the shell and σ was the width of the profile. For the supercritical collapse data, $\sigma = 0.3$ and $\phi_0 = 1.0$. Once the critical value of a was determined for a given dimension, a check for the universality of the critical phenomena could be carried out by varying one of σ or ϕ_0.

Given the value of the dilaton ϕ^i_j and the dilaton evolution function $\dot{\phi}^i_j$ at grid point (i, j), the lowest order evolved value of the dilaton on the next u slice (at constant v) is given by

$$\phi^i_{j+1} = \phi^i_j + \dot{\phi}^i_j \Delta u_j, \tag{4.3}$$

where Δu_j is the spacing between adjacent u slices. The initial spacing in u was set at 0.001 for all of the collapse runs. However, the collapse code was written to allow for refinements in Δu as solution structure developed. The numerical error in (4.3) is of the order of the correction term involving Δu_j. The accuracy of ϕ^i_{j+1}, however, can be considerably improved by using a higher order evolution (or time step) procedure. To improve the overall accuracy of the calculations reported here a higher order evolution procedure was implemented.

Once the values of the fields were determined on the initial surface, evolu-

tion proceeded via fourth order Runge-Kutta procedure. The Runge-Kutta method of order four uses a set of four derivative estimates to determine the value of a given function at the endpoint of a discrete step. The method combines derivative estimates at the initial point of the step, two estimates at the midpoint of the step, and the derivative at the end point of the step.

The Runge-Kutta method of order four is given by

$$\phi^i_{j+1} = \phi^i_j + \frac{1}{6}\left(k_1 + 2k_2 + 2k_3 + k_4\right), \tag{4.4}$$

where

$$\begin{aligned}
k_1 &= \dot{\phi}\left(u_j, \phi^i_j\right)\Delta u_j \\
k_2 &= \dot{\phi}\left(u_j + \frac{\Delta u_j}{2}, \phi^i_j + \frac{1}{2}k_1\right)\Delta u_j \\
k_3 &= \dot{\phi}\left(u_j + \frac{\Delta u_j}{2}, \phi^i_j + \frac{1}{2}k_2\right)\Delta u_j \\
k_4 &= \dot{\phi}\left(u_{j+1}, \phi^i_j + k_3\right)\Delta u_j \\
u_j &= \int_0^u d\tilde{u} = \sum_{k=0}^{k=j}\Delta u_k \\
u_{j+1} &= u_j + \Delta u_j.
\end{aligned}$$

The local truncation error in this method is $\mathcal{O}((\Delta u_j)^4)$. The Runge-Kutta

order four method is derived from the fourth order Taylor polynomial expansion in two variables. The method indeed requires four calculations per step, however, the approximation error is smaller than a double order single variable Taylor technique at one-half step size [100]. For this reason, Runge-Kutta methods are popular because they offer both efficiency and accuracy for cpu-intensive calculations. The Runge-Kutta method was used throughout the calculations. During each Runge-Kutta step, ϕ and h were evolved simultaneously according to the field equations (3.111) and (3.116).

In double null coordinates, all fields are determined as functions of incoming and outgoing wave fronts. Thus, as the evolution proceeded, some of the ingoing wave packets passed through the origin. The computer code did not track reflected wave pulses, therefore, as grid points reached the origin the overall grid became smaller.

If the evolved value of the dilaton ϕ_j^i was less than zero (hence, the incoming null wave had reached the origin during the j^{th} iteration) then the point was removed from the grid. In the cases where all the v slices were removed from the grid it was assumed that the solution had reflected enough or all of the matter to infinity without the formation of an apparent horizon surface. These solutions were considered subcritical and the initial parameter values

stored as such.

After each iteration, the new ϕ values were scanned and the origin shifted to the first grid point with non-zero ϕ. All of the other functions on the u slice were calculated using the evolved values of ϕ and h.

So long as evolution proceeded, a check throughout the grid for the conditions of an apparent horizon surface was performed. The apparent horizon is the outermost surface from which outgoing null geodesics stand still. In dynamical gravitational collapse the event horizon expands as external matter is contracting. In the case of spherical collapse, the event horizon will asymptotically expand until its surface coincides with the apparent horizon. Thus, in numerical relativity, it is useful to check for an apparent horizon as one always knows an event horizon will be contained within it.

If an apparent horizon was observed, the evolution would be terminated and all information about the fields on the grid surface just prior to apparent horizon formation would be dumped into data files. The signal for horizon formation is given by the vanishing of the following function

$$\sigma_{AH} = g^{\alpha\beta}\partial_\alpha\phi\partial_\beta\phi = -2\frac{\dot{\phi}}{lg}. \tag{4.5}$$

The function σ_{AH} vanishes at finite radius where outgoing null rays don't expand. In practice, however, evolution was terminated when the above function fell below some predetermined threshold value[2].

Partial derivatives of functions with respect to the null coordinate v were calculated via the four point central difference scheme:

$$\phi'^{i}_{j} = \frac{1}{12\Delta v}\left(8\phi^{i+1}_{j} - 8\phi^{i-1}_{j} - \phi^{i+2}_{j} + \phi^{i-2}_{j}\right). \tag{4.6}$$

The computer code uses a five point forward, and backward, difference scheme to calculate derivatives at the first two, and last two, grid points, respectively. These calculations ensured that an equal order of truncation error existed for all grid points. The error in these derivative approximations are of the order $O((\Delta v)^4)$.

Numerical integration on constant u slices was carried out via simple trapezoid method which begins *near* the coordinate origin[3] and then integrating outward. The method of integration is also called a composite

[2] The value of the apparent horizon threshold used to terminate evolution was dependent on the space-time dimension analyzed. Often, when a horizon was nearly pinched off, σ_{AH} changed very rapidly and passed through the threshold and become negative during a single iteration. The evolution was, nevertheless, terminated at that point.

[3] Numerical integration did not begin exactly at the coordinate origin as will be seen below. The values of the fields for the first few grid points near the origin were estimated using a Taylor series expansion and analytic integration.

Newton-Cotes formula for N equally spaced points [94]. In symbols, the composite Newton-Cotes formula for the integral of the function $f(x)$ between the interval $x_b - x_a$ is given by

$$\int_a^b f(x)dx = \frac{h}{2}\left[f(a) + 2\sum_{j=1}^{N-1} f(x_j) + f(b)\right], \tag{4.7}$$

where h is the spacing between grid points. The numerical error of (4.7) is of the order $\mathcal{O}(h^2)$. Higher order methods of integration were found to lead to bifurcations in the solution after multiple iterations and it was concluded that, in the case of integration, a simple trapezoid approximation was the most stable method.

4.1.1 Small ϕ Approximation

To improve numerical accuracy near the origin, a similar procedure to [28] was employed in which the matter field constraint is expanded in a power series in ϕ near $\phi = 0$. On each u slice the matter field is fit (using a least squares fitting procedure) to

$$h = h_0 + h_1\phi + h_2\phi^2 \tag{4.8}$$

for the first n grid points from the origin[4]. All other field values for the first n grid points were calculated analytically using the values of the fitting constants. This procedure elegantly handled the problematic $1/\phi$ factor in the matter evolution equation, $\dot{h}$, for small values of the dilaton.

The remaining values of the fields for the first n grid points are given by:

$$\chi = h_0 + \frac{1}{3}h_1\phi + \frac{1}{5}h_2\phi^2 \tag{4.9}$$

$$g = 1 + \frac{1}{18}h_1^2\phi^2 + \frac{4}{45}h_1h_2\phi^3 + \frac{1}{25}h_2^2\phi^4 \tag{4.10}$$

$$\tilde{h} = \frac{n^2h_1^2}{9l^2}\phi^3\left[\frac{\phi^{-1/n}}{(n-1)(3n-1)} - \frac{\Lambda\phi^{1/n}}{(n+1)(3n+1)}\right] \tag{4.11}$$

$$\tilde{g} = \frac{ng}{Cl^2}\left(\frac{\phi^{1-1/n}}{n-1} - \frac{\Lambda\phi^{1+1/n}}{n+1}\right) - \frac{\tilde{h}}{C} \tag{4.12}$$

$$\dot{h} = \frac{1}{Cl}\left(\frac{1}{6}h_1 + \frac{1}{5}h_2\phi\right)\left[\left(\frac{n-2}{n-1}\right)g\phi^{1-1/n} - \Lambda\left(\frac{n+2}{n+1}\right)g\phi^{1+1/n} + l^2\tilde{h}\right] \tag{4.13}$$

$$\dot{\phi} = -\frac{ng}{2Cl}\left(\frac{\phi^{1-1/n}}{n-1} - \frac{\Lambda\phi^{1+1/n}}{n+1}\right) + \frac{l\tilde{h}}{2C}. \tag{4.14}$$

It should be noted that the lowest order term in the evolution function $\dot{h}$ vanishes if $n = 2$ which corresponds to $d = 4$. As a result, the numerical evolution is considerably more stable in four space-time dimensions. In the

[4] For the higher dimensional study, $d \geq 4$, the fit was performed on the first 8 grid points. For the lower dimensional study the number of grid points used in the fit was reduced to 4.

next subsection, the method of determining uncertainty in the calculations of the critical phenomena will be presented.

4.1.2 Determining Error Estimates

For any given set of initial parameters, either a black hole will form under gravitational contraction, or not. As stated previously, it is assumed that for massless scalar field collapse there exists one universal critical solution $\mathcal{S}[a_*]$ for all one parameter families of initial data. In the collapse code, two extremal values of the parameter which lead, in the one case, to a supercritical collapse and a black hole solution, and in the other, to a subcritical or reflection solution are first determined. Once these two extremal values have been determined, a binary search is carried out which narrows the range separating the two phases. This method of determining a_* is called the *direct observation.*

The sensitivity of the evolution equations to numerical errors has been found to be very significant as the space-time dimension is increased. This was due to the decreasing fractional power of the dilaton in the evolution equations. The effect this has on the evolution of initial data is to create instability near criticality and a subsequent loss of accuracy. Often, in the

large dimensional study the range of possible critical values of a exceeded the limit of machine precision[5]. The code became increasingly unstable as the space-time dimension increased and eventually broke down after 14 dimensions. It was not possible to extract stable results beyond this limit. In the lower dimensional study, however, the numerical scheme was stable enough to reduce the range of possible critical values to the level of machine code precision.

Once the smallest range of a_* had been determined by direct observation the code would be run again for several supercritical values of a and the horizon radius information at collapse would be collated into a data file along with the initial parameter information. Let $\phi_{AH}(a)$ denote the value of ϕ corresponding to the position of the apparent horizon for a given value of the initial matter pulse amplitude a. From the definition of the dilaton field, the radius of the apparent horizon is, therefore,

$$r_{AH} \propto \phi_{AH}^{1/n}. \tag{4.15}$$

From (2.43) and the above relation, it is expected in the case of super-

[5] The code was written in C using double precision real numbers. Thus, the level of machine code precision is roughly one part in 10^{15}.

critical collapse

$$\frac{1}{n}\log\left(\phi_{AH}\right) = \gamma\log\left(a - a_*\right) + c_f, \tag{4.16}$$

where c_f is a family dependent constant. For each dimension studied, the results $\{\phi_{AH}(a), a\}$ are collated and the function (4.16) is plotted. The data is fit to a line using a least squares fit and the r-squared goodness of fit is calculated. The goodness of fit is given by

$$R^2 = 1 - \frac{\sum\left(y_i - a - bx_i\right)^2}{\sum\left(y_i - \bar{y}\right)^2}. \tag{4.17}$$

In practice, the fit is a very sensitive function of the estimated value of the critical parameter.

The critical parameter a_* is then adjusted within the observed range (of direct observation) in order to maximize R^2. For the supercritical collapse data, this would result in maximal values of R^2 of between 0.9998 and 1.0000 indicating a high quality of fit. The value of a_* which would produce the maximum value of R^2 would then become the best estimate of the critical value of a. Refitting (4.16) with the best estimate of a_* produced the best estimate of the scaling exponent γ.

To determine an uncertainty in the best estimate of a_*, the data is plotted

and the maximum value of R^2 is allowed to drop by 0.0001 by varying the input value of a_*. It was found that this method of determining a range of a_* would reduce the overall range of possible values of a_* as compared to the range observed by direct observation. The uncertainty in γ was determined by calculating the range of fit results γ which corresponded to this new reduced range of values of a_*. In the higher dimensional study, the relative error of gamma remained roughly constant using this method. It should also be noted that this method of determing error estimates for the critical constants is consistent with the method used to quote the results in [48].

4.2 Results

The numerical code was first tested in four dimensions with zero cosmological constant. This was done to verify known results in four dimensions as well as to debug the code and establish the validity of our method. The results of collapse simulations in four dimensions are presented as a case study in order to show they are in agreement with previous work on this system.

As discussed above and shown in [61], it was expected that the critical solution of massless scalar field collapse in spherical symmetry is independent of any finite cosmological constant term in the action. Henceforth, these

results are quoted with the cosmological constant tuned to zero. Without loss of generality, the length scale in the problem was fixed by setting $l = 1$.

In the remaining subsections of this chapter, the results of numerical calculations of the critical solutions in other finite dimensions are presented in detail. The chapter is concluded after a speculation on the nature of the dimension dependence of scaling and self-similarity in critical gravitational collapse.

4.2.1 Critical Collapse in Four Dimensions: Case Study

The evolution equations for the case of four dimensions are ideal in the sense that they are naturally more stable[6]. The evolution equations near $\phi = 0$ with $n = 2$, $\Lambda = 0$ and $C = l = 1$ are given by

$$h = h_0 + h_1\phi + h_2\phi^2 \tag{4.18}$$

$$\chi = h_0 + \frac{1}{3}h_1\phi + \frac{1}{5}h_2\phi^2 \tag{4.19}$$

$$g = 1 + \frac{1}{18}h_1^2\phi^2 + \frac{4}{45}h_1h_2\phi^3 + \frac{1}{25}h_2^2\phi^4 \tag{4.20}$$

$$\tilde{g} = 2\phi^{1/2} + \frac{1}{45}h_1^2\phi^{5/2} + \frac{8}{315}h_1h_2\phi^{7/2} + \frac{2}{225}h_2^2\phi^{9/2} \tag{4.21}$$

[6] It should be noted that the supercritical numerical solution in four dimensions did not involve the integration by parts procedure discussed above. All the other collapse simulations did, however, incorporate the function $\tilde{h}$.

$$\dot{h} = \frac{2}{135}h_1^3\phi^{5/2} + \frac{16}{525}h_1^2h_2\phi^{7/2} + \frac{8}{189}h_1h_2^2\phi^{9/2} + \frac{16}{1125}h_2^3\phi^{11/2} \quad (4.22)$$

$$\dot{\phi} = -\phi^{1/2} - \frac{1}{90}h_1^2\phi^{5/2} - \frac{4}{315}h_1h_2\phi^{7/2} - \frac{1}{225}h_2^2\phi^{9/2}. \quad (4.23)$$

As seen in the equations above, the matter evolution equation is a slower changing function near the origin than the dilaton evolution function. The effect this has on numerical stability is remarkable and is evident by the number of echoing periods observed in this case. As discussed in the previous section, however, this effect only occurs for ($n = 2$, $\Lambda = 0$). In fact, it was this numerical stability that provided the motivation in [28] to define the matter function h instead of using χ (as is done here as well).

Nevertheless, one can parameterize the matter field to a more general function which stabilizes the numerical evolution at the origin for space-time dimensions other than four [53]. As seen in Section 2.2.2, an example of this function was presented for the case of six space-time dimensions. The general matter function is defined by

$$h = \frac{(m-1)!}{(2m-1)!}r^{1-m}\left(\frac{\partial}{\partial r}\right)^m\left(r^{2m-1}\chi\right), \quad (4.24)$$

where $m = n/2$. The new matter function h, defined in this way, not only

satisfies the wave equation but is constant along ingoing light waves in flat space-time. As a result, the numerical procedure is greatly stabilized near the origin.

There are, however, considerations for defining the matter function in this way. First, (4.24) is only valid in even space-time dimensions. Second, a separate set of code would need to be written for each dimension analyzed. This would impede the basic objective of developing a single code which accepts space-time dimension as an input parameter. Third, in order to evaluate (4.24), one would require additional higher order derivatives as one analyzed higher dimensional space-times. From a more pragmatic standpoint, the numerical accuracy of differentiation falls off substantially as the order of differentiation is increased, hence the gains made in stability come at the expense of accuracy. For these reasons, only the auxiliary scalar field given by (3.114) was used in the collapse simulations.

Figure 4.2 shows the horizon radius scaling observed in four dimensional collapse. The graph is equally spaced in $\log(a-a_*)$. To determine the slope, a least squares fit to the function $\log(r_{AH}) = \gamma \log(a - a_*) + c_F$ was performed as described in the previous subsection. The value of the slope of the graph is given in Table 4.1.

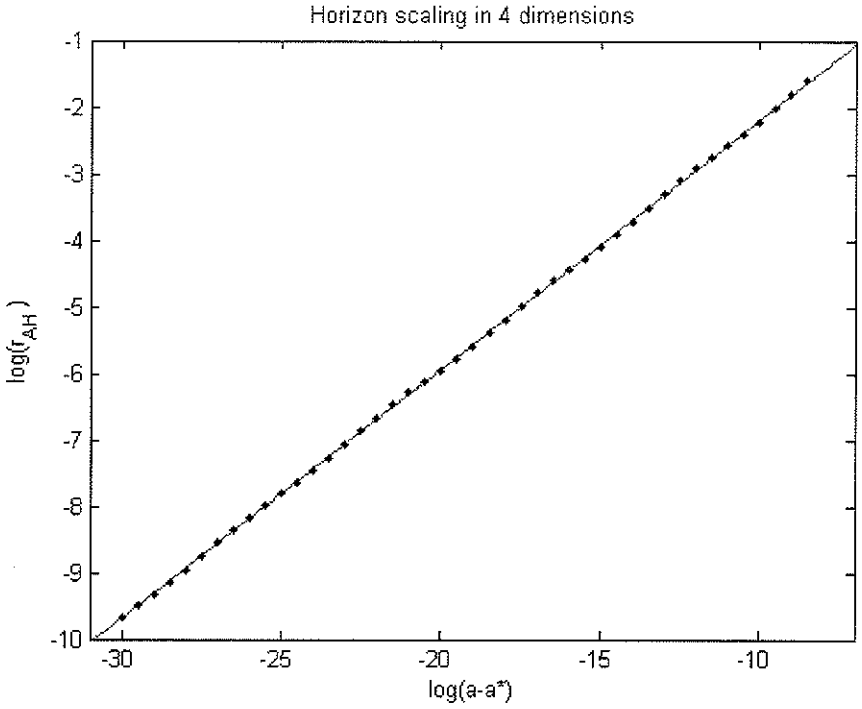

Fig. 4.2: Supercritical collapse in four space-time dimensions. The graph shows one of the first results obtained using space-time dimension as an input parameter. The high number of complete echoing periods—in this case four and evidenced by the deviation of the data from a line—are attributed to the unique stability in the evolution equations. The initial surface contained 12,000 grid points. The critical exponent was estimated to be $\gamma = 0.374 \pm 0.002$, in excellent agreement with earlier findings [29, 48].

a_*	γ	R^2
a_*^+	0.3723	0.99983
a_*	0.3744	0.99993
a_*^-	0.3767	0.99983

Tab. 4.1: Mass scaling in four dimensional scalar field collapse. In the table, a_* corresponds to the maximum value of R^2 in a least squares fit to a line. a_*^- is the lowest value of the amplitude that did not produce a reflection solution or a black hole by direct observation. a_*^+ is the largest value of the amplitude which reduced the maximum value of R^2 in the fit by 0.0001. The critical exponent was estimated to be $\gamma = 0.374 \pm 0.002$, in excellent agreement with earlier findings [29, 48].

During the numerical calculations the spacing between u slices was decreased prior to collapse. This was done if one of a few basic conditions were met and the effect of doing this was found to increase the accuracy of the final result. In most cases, a particular sequence of Δu divisions were essential for the code to remain stable. It was also essential to ensure that the same set of conditions were used for all the data points used to calculate γ.

If one of the following conditions were met then Δu would be decreased: i) if the number of grid points passing the origin in a single iteration exceeded some small amount; ii) if a relative minima formed in σ_{AH}; iii) if a minima that did form in σ_{AH} fell below a certain value; and iv) after a pre-determined amount of u coordinate time.

In order to determine the discrete self-similarity in the critical solution Δ, one needs to examine the periodic wiggle in the power law behaviour of the black hole mass. Recall, from (2.90) that the period of the wiggle is related to Δ by

$$\delta = \frac{\Delta}{2\gamma}.$$

To calculate δ, the periodicity of the residuals in the $\log(a - a_*)$ graph were calculated. Figure 4.3 shows a sine wave fit to the residuals in the $\log(a - a_*)$ graph. The period of the residuals was analyzed by KaleidaGraph Demo which uses a Levenberg-Marquardt algorithm. The fit to the residuals is the three parameter function:

$$y = A \sin\left[T \log\left(a - a_*\right) + B\right], \tag{4.25}$$

where $y = \log\left(r_{AH}\right) - c_F - \gamma \log\left(a - a_*\right)$. The period was determined to be

$$T = \frac{2\pi}{\delta} = 1.3682 \pm 0.0070. \tag{4.26}$$

The error in T represents the standard error as calculated by KaleidaGraph

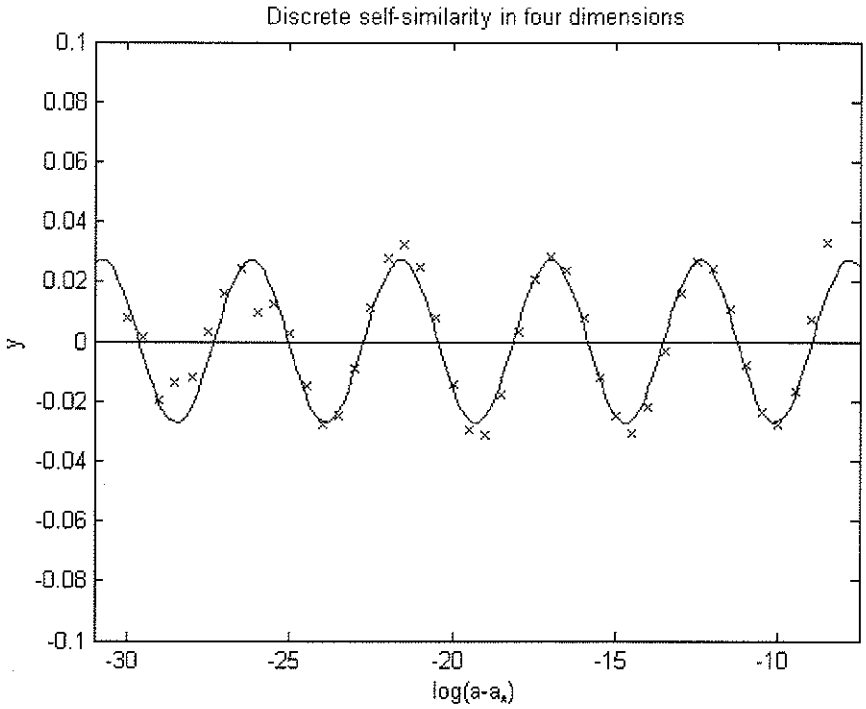

Fig. 4.3: Discrete self-similarity in four dimensions. A line is subtracted from the $\log(a-a_*)$ graph and KaleidaGraph Demo is used to fit a sine wave to the residuals. It was estimated that $\Delta = 3.44 \pm 0.02$, in excellent agreement with earlier findings [29, 48].

Demo. The r-squared goodness of the fit was $R^2 = 0.91362$. The low value of R^2 (relative to other fits in this analysis) clearly shows that the residuals are not likely to be sine functions (which is also evident by visual inspection), nevertheless, one expects the oscillation of the residuals to have the same period of a sine function with the same approximate shape. In the lower dimensional studies (presented below), the discrepency between the fitted data and a sine function becomes even more evident and, as a result, only using R^2 as an indicator of the quality of the fit can be misleading in these cases.

Scalar curvature in subcritical collapse

An alternative method of determining the critical phenomena in gravitational collapse is to examine the maximum scalar curvature at the origin in subcritical collapse. It had already been shown that the scalar curvature in subcritical collapse scaled during gravitational collapse and that the scaling constant was the same as the black hole mass scaling constant in supercritical collapse [27]. From (3.146), the Ricci curvature scalar at the origin with

$d = 4$ and $\Lambda = 0$ is given by

$$R_0^{(4)} = -8\dot{\chi}_0\chi_0', \tag{4.27}$$

where

$$\dot{\chi}_0 = \frac{d\chi}{d\phi}\frac{d\phi}{dr}\dot{r}|_{r=0} \tag{4.28}$$

$$\chi_0' = \frac{d\chi}{d\phi}\frac{d\phi}{dr}r'|_{r=0}. \tag{4.29}$$

For the subcritical collapse calculations the matter function h was fit to a linear function of r near the origin

$$h = h_0 + h_1\phi^{1/2}. \tag{4.30}$$

This gives the small ϕ approximation to χ

$$\chi = h_0 + \frac{1}{2}h_1\phi^{1/2}. \tag{4.31}$$

Therefore, with $l = 1$,

$$\frac{1}{2}R_0^{(4)} = h_1^2. \tag{4.32}$$

The above relation shows that the Ricci curvature scalar is simply proportional to the square of the gradient of the matter field at the origin. For a subcritical collapse ($a < a_*$) the absolute value of the gradient will steadily increase to a maximum where the density of matter near the origin is greatest. Let u_{MAX} represent the value of u when $R_0^{(4)}$ is maximized[7]. As the parameter a approaches a_* from the subcritical region, u_{MAX} approaches u_* from below, where, u_* is the value of u at criticality. If the collapse is subcritical, the matter will disperse to spatial infinity for $u > u_{MAX}$, a black hole will not form, and $R_0^{(4)}$ will then decrease to zero as $u \to \infty$.

Let us define a new variable

$$x = \begin{cases} -\log(u_* - u) + \log(u_* - u_{MAX}) & \text{if } u \leq u_{MAX} \\ \log(u_* + u - 2u_{MAX}) - \log(u_* - u_{MAX}) & \text{if } u > u_{MAX}. \end{cases}$$

Figure 4.4 shows the logarithm of (4.32) as a function of x for a near critical collapse simulation in four dimensions.

The initial null hypersurface contained 8000 grid points with a spacing of $\Delta v = 0.0003$. To refine Δu during the collapse, a different method is used then for the four dimensional supercritical collapse. In the supercritical

[7] Recall that we assigned $u = 0$ on the initial null hypersurface, therefore, $u_{MAX} > 0$.

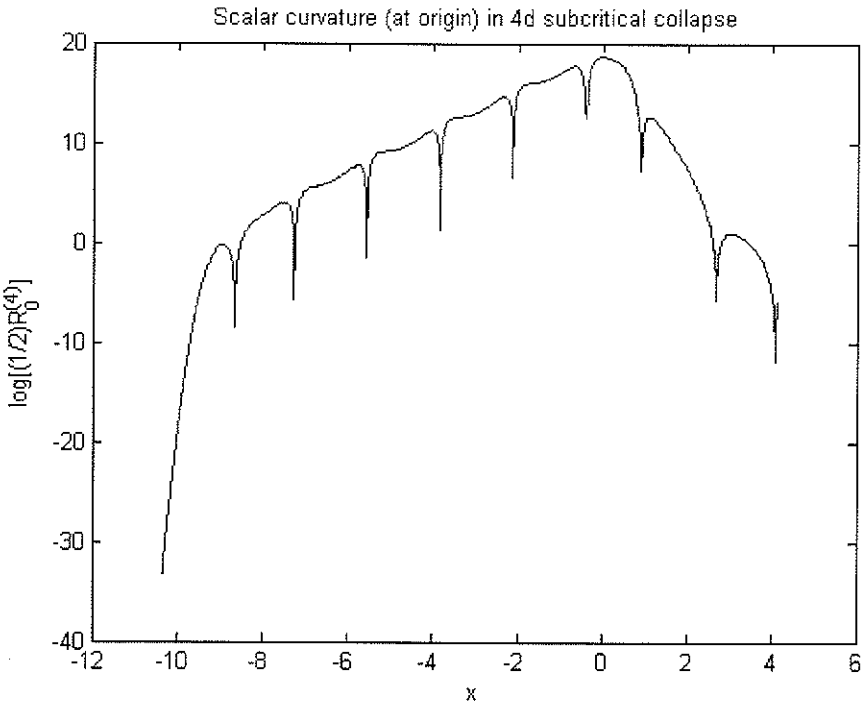

Fig. 4.4: Scalar curvature at the origin in four dimensional subcritical collapse. The curvature maximizes at $x = 0$ and decreases to zero as $u \to \infty$. For $x < 0$, $\log\left(\frac{1}{2}R_0^{(4)}\right)$ oscillates at a period that approaches $\Delta/2$ as $x \to 0$.

case, the grid spacing was decreased in the u direction in discrete steps. For example, if one of the conditions described above were met during a supercritical collapse, Δu was decreased by as much as a factor of 10 (in some cases by factors of 2 or 5). In the subcritical collapse calculations the spacing in u was decreased using the smooth function

$$\Delta u_i = (1 - a_u)\,\Delta u_0 \exp\left[-\left(\frac{u_i - u_*}{b_u}\right)^2\right], \tag{4.33}$$

where, a_u and b_u were adjusted to maximize resolution while keeping overall computing time to a manageable level. For the subcritical collapse data, $a_u = 0.999$, $b_u = 0.2$, and $\Delta u_0 = 0.001$ (the u spacing on the initial surface). The parameter u_* was determined through iteration. Using these values, a typical subcritical run would involve roughly $24,000$ iterations and require approximately 7 minutes of computing time.

Let us define the maximum curvature for a subcritical amplitude as

$$R^{(4)}_{MAX} = \frac{1}{2} R^{(4)}_0|_{u=u_{MAX}}. \tag{4.34}$$

It is then expected that

$$\log\left(R^{(4)}_{MAX}\right) = c_F - 2\gamma \log\left(a_* - a\right) + \Psi\left[\log\left(a_* - a\right)\right]. \tag{4.35}$$

Figure 4.5 shows $\log(R^{(4)}_{MAX})$ as a function of $\log(a_* - a)$. KaleidaGraph

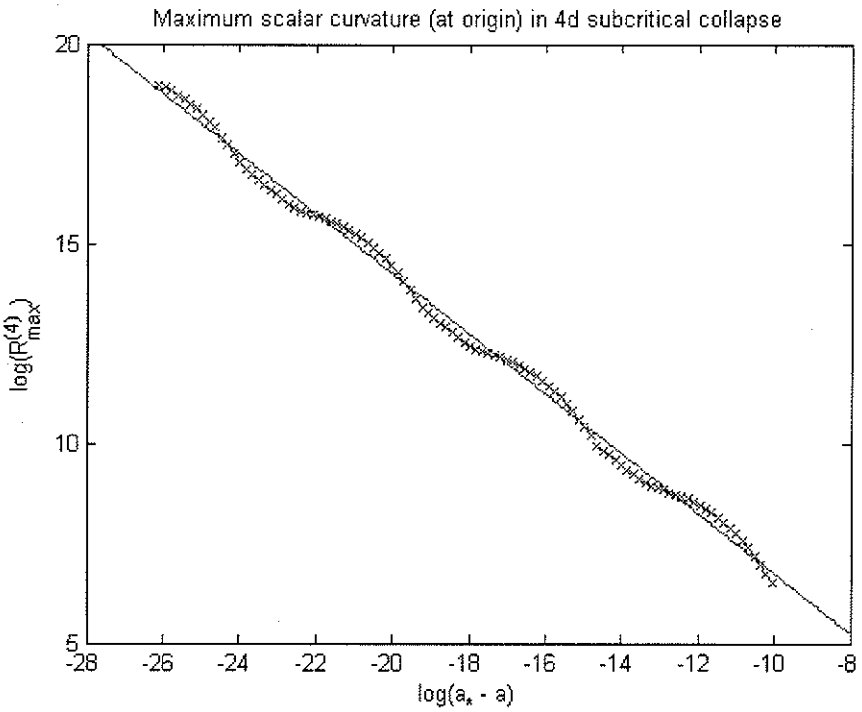

Fig. 4.5: Scaling of curvature in four dimensional subcritical collapse. The maximum value of the curvature at the origin obeys a power law with the same scaling constant as apparent horizon radius in supercritical collapse. The scaling exponent was estimated to be $\gamma = 0.374 \pm 0.002$, in excellent agreement with earlier findings [29, 48].

Demo was used to fit the data to the five parameter function

$$\log\left(R^{(4)}_{MAX}\right) = c_F - 2\gamma \log\left(a_* - a\right) + A\sin\left[T\log\left(a_* - a\right) + B\right]. \qquad (4.36)$$

Table 4.2 lists the results of the fitting procedure. Figure 4.6 shows the

γ	Δ	R^2
0.3743 ± 0.0024	3.448 ± 0.024	0.9999

Tab. 4.2: Critical phenomena in four dimensional subcritical collapse. The r-squared goodness of fit was maximized by varying a_* within the range of possible critical values of a. The mean values of the fit parameters were calculated at the maximum of R^2. The uncertainty in Δ includes contributions from the standard error in the fit and the relative error in γ added in quadrature.

residual of the curvature scaling after a linear fit is subtracted. A sine wave fit is shown on the graph. We estimate $\Delta = 3.45 \pm 0.02$, and $\gamma = 0.374 \pm 0.002$, both in excellent agreement with earlier supercritical collapse calculations.

Discrete self-similarity in supercritical collapse

An alternative method of measuring the period of self-similarity is by measuring the periodicity of the matter field at the origin. For these data, the numerical code was run with the function $\tilde{h}$ in the evolution equations (that is, performing the integration by parts procedure). The code used an initial

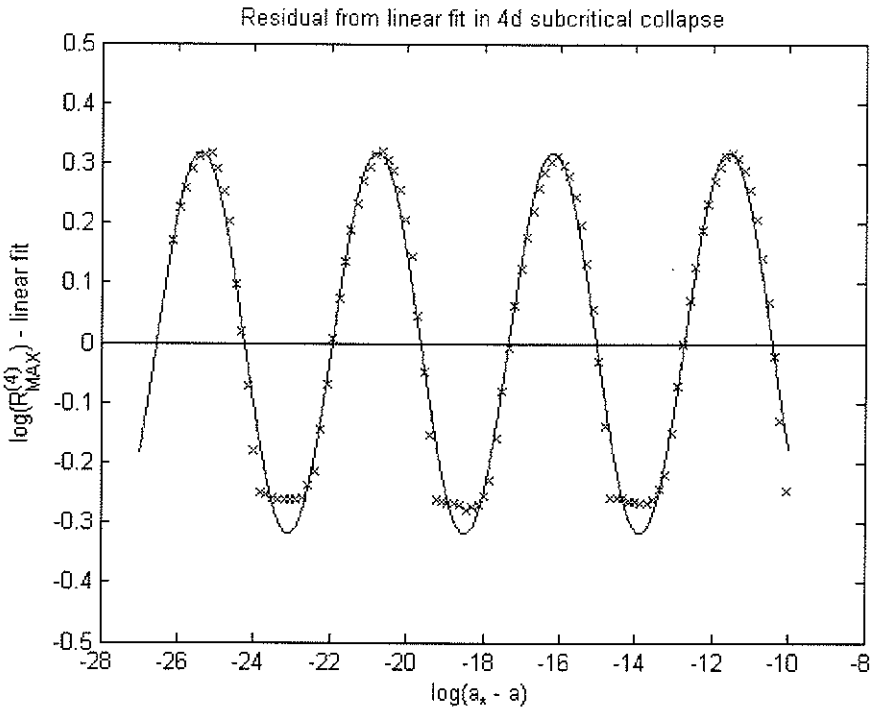

Fig. 4.6: Discrete self-similarity of the maximum curvature in four dimensional subcritical collapse. The discrete self-similar period was estimated to be $\Delta = 3.45 \pm 0.02$, in excellent agreement with earlier findings [29, 48]. The flat bottoms on the graph were also observed by Garfinkle in [27]. What causes this effect is unknown.

grid size of 7000 with spacing $\Delta v = 0.00034$. The spacing between u-slices was calculated using the function (4.33).

Figure 4.7 shows the periodicity of the matter field at the origin for a nearly critical collapse in four dimensions. The data were fit to a sine wave

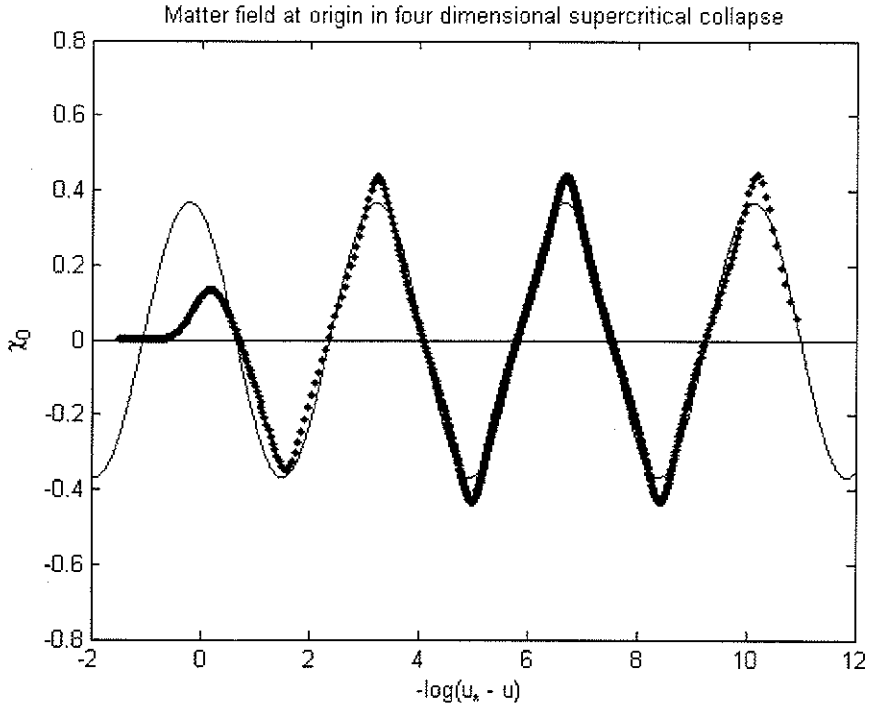

Fig. 4.7: Matter field at the origin in four dimensional supercritical collapse. The solid line represents the best estimate of a sine wave fit to the data. The discrete self-similarity period was estimated to be $\Delta = 3.44 \pm 0.01$, in excellent agreement with earlier findings [29, 48].

function using KaleidaGraph Demo.

For the purposes of the fitting, data were excluded with $-\log(u_* - u) <$

2.5. These data were excluded because they represent the state of the matter field early in the evolution. This is typically before the evolution begins to approximate the critical solution. One should expect a near critical evolution to approximate the critical solution only for intermediate times. After inspecting matter field ringing data, it was determined that the transition from "early" to intermediate times occurs around $-\log(u_* - u) < 2.5$.

The discrete self-similarity constant was determined to be $\Delta = 3.445 \pm 0.013$. The same error procedure was used as described above. That is, the unknown critical value (in this case u_*) was varied until R^2 was maximized. The error in Δ corresponds to the range found by allowing the maximum in R^2 to fall by 0.0001.

4.2.2 *Critical Collapse in Higher Dimensions:* $4 < d \leq 14$

In each dimension in the range $4 < d \leq 14$, an initial grid size of $6,000$ was used with spacing $\Delta v = 0.0005$. Supercritical collapse was observed for $d = 4.5$ as well as the remaining integer dimensions between 5 and 14, inclusive. In addition to the same procedure used for the $d = 4$ supercritical scaling results, the formalism included the integration by parts for these data.

The numerical solution became increasingly unstable as the dimension in-

creased above four. As a result, considerable care was needed in determining the sequence of Δu divisions for each dimension. In all cases, the parameter values of $\phi_0 = 1$ and $\sigma = 0.3$ were used for the Gaussian initial data and the amplitude a was allowed to vary in order to determine a range for the critical amplitude a_* separating supercritical and subcritical collapse. The cosmological constant was tuned to zero and the length scale set at $l = 1$. Table 4.3 summarizes the results of the study.

d	Δ	γ
4.5	3.30 ± 0.1	0.3984 ± 0.0014
5	3.10 ± 0.1	0.4119 ± 0.0037
6	2.98 ± 0.1	0.4302 ± 0.0042
7	2.96 ± 0.1	0.4405 ± 0.0058
8	2.77 ± 0.1	0.4459 ± 0.0054
9	2.63 ± 0.1	0.4524 ± 0.0054
10	2.50 ± 0.1	0.4562 ± 0.0060
11	2.46 ± 0.1	0.4588 ± 0.0053
12	2.44 ± 0.1	0.4616 ± 0.0067
13	2.40 ± 0.1	0.4639 ± 0.0089
14		0.4645 ± 0.0052

Tab. 4.3: Critical phenomena for $4 < d \leq 14$. The results presented here are found by using the same data reported in Bland et al. [48]. In this table, however, the error bars were recalculated and include an additional digit for γ. The code was optimized for the determination of the scaling constant γ on a case by case basis. As a result, the relative error in estimates of γ are much lower than for Δ. The self-similarity constants were determined by analyzing the periodicity in the scaling graphs. This method of determining Δ is highly sensitive to γ and, therefore, lead to a larger relative uncertainty.

As described above, the data were fit to a line (with slope γ) and the maximum of R^2 was found within the direct observation range of critical values of a. This procedure is further complicated by the appearance of multiple relative minima in the apparent horizon function. Figure 4.8 shows an example of the complex structure of σ_{AH} near a typical collapse in ten space-time dimensions. It was found that just prior to the moment of collapse,

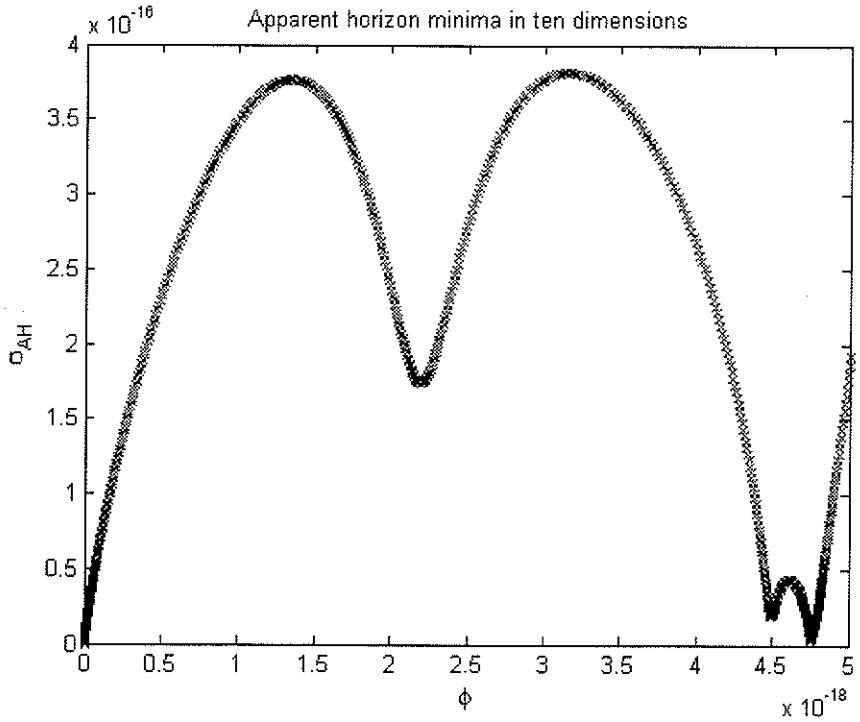

Fig. 4.8: Multiple relative minima near collapse in ten dimensions. The rightmost minimum (largest ϕ value) corresponds to the apparent horizon position at the moment of collapse. The appearance of multiple minima in σ_{AH} can lead to additional uncertainty when estimating r_{AH}.

new minima in σ_{AH} would appear ever closer to ϕ_{AH}. This can be seen in the figure. The new structure in the solution would also be accompanied by increasing numerical instability in the evolution equations, however, even if the code crashed prior to $\sigma_{AH} = 0$, the position of the outermost minimum would asymptotically approach ϕ_{AH}. As a result, if the code could be made to remain stable long enough during a given collapse then a fairly accurate estimate of r_{AH} could be determined.

Moreover, it was observed that the relative minima would also possess the critical scaling behaviour seen in r_{AH}. Thus, it was found that one could approximate the critical phenomena observed in gravitational collapse by tracking a particular relative minimum in σ_{AH}. In fact, it was determined that the scaling constant calculated in this way agreed very well with γ calculated using the last surviving outermost minimum at collapse. Figure 4.9 shows the comparison of the two calculations in the case of 10 dimensions. In Table 4.3, calculations of γ are calculated based on graphs of the type shown on the upper right of Figure 4.9.

The periodicity of the residuals in the scaling graphs can provide a rough estimate of the discrete self-similarity constant. Over the range of dimensions studied, data was obtained which contained between 1.5 and 3 periods

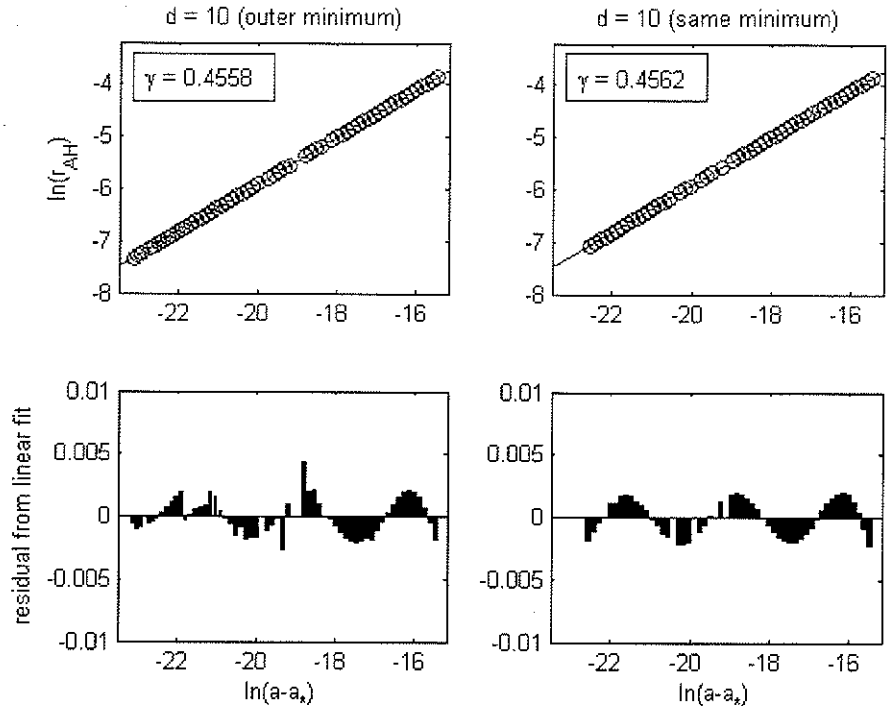

Fig. 4.9: Comparing relative minima in σ_{AH}. The left hand graphs show the scaling exponent (upper) and residuals (lower) from a linear fit using the best estimates of r_{AH}. As the critical amplitude is approached the code becomes unstable leaving points scattered about the linear fit. The right graphs track a particular minimum over the same range of amplitudes. The estimates of γ for both cases are in strong agreement but the graph on the right displays the self-similarity of the solution and can therefore provide a rough estimate of Δ.

of oscillations in the residuals of the linear fit graphs. In order to obtain the most reliable estimates for Δ (as in the $d = 4$ case above and in the $d < 4$ cases presented below) one requires about 4 periods for a given dimension. Because the code was originally optimized for the scaling study, I attempted to compensate for the lack of accuracy in Δ by increasing the relative uncertainty in the final calculations for Δ by 1%.

In [48], the period of oscillations of the residuals were estimated at the optimal value of a_*. Calculating the period of the wiggle lead to an uncertainty in δ of roughly 1%. To calculate Δ we also required an accurate estimate of γ, however, γ is known to roughly 1% in the higher dimensional study. To determine a conservative estimate of the total uncertainty in Δ, all three error contributions were added linearly. This leads to an estimate of a 3% relative error in Δ. For simplicity, the error is estimated to one digit (± 0.1) for all the higher dimension estimates of Δ.

As a diagnostic during the numerical collapse runs, the matter field was consistently examined near the origin to ensure our fitting procedure remained accurate. Figure 4.10 shows the matter field near the origin for a typical collapse run in eight dimensions. The matter field is shown at a late time just prior to $\sigma_{AH} = 0$. In the following subsections, the collapse results

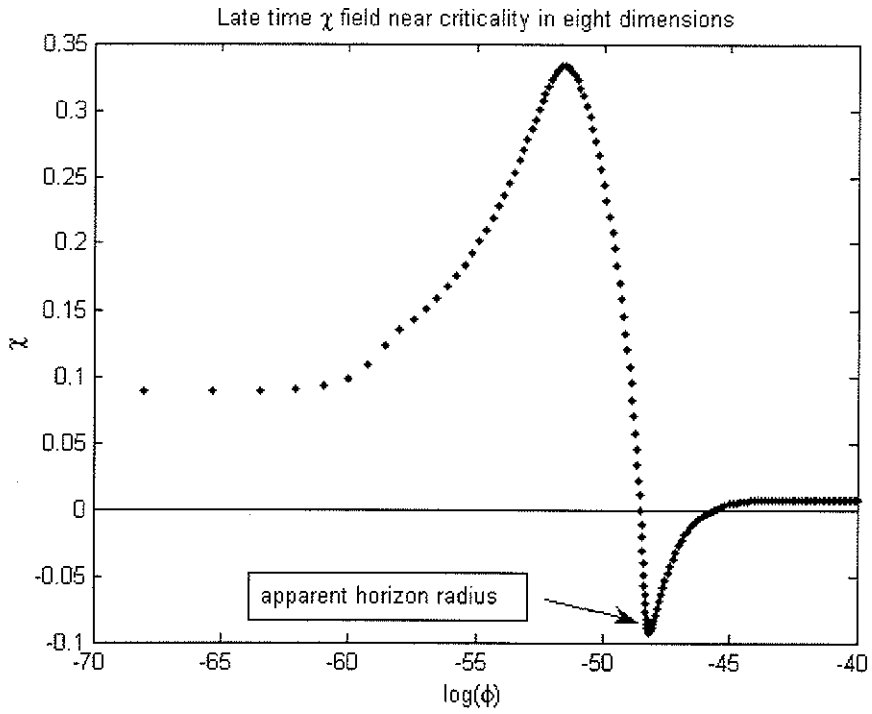

Fig. 4.10: Matter field near the origin in eight dimensional supercritical collapse. The graph indicates that, for this particular collapse run, a significant amount of matter remains behind the apparent horizon position.

from the lower dimensional study and an attempt to determine the functional dependence of critical phenomena on space-time dimension will be presented.

4.2.3 Critical Collapse in Lower Dimensions: $3 < d \leq 4$

The numerical code was modified to carry out the lower dimensional study. As had been done for the four dimensional subcritical collapse calculations, the u spacing between iterations was calculated using the smooth function (4.33). After running the collapse code through several iterations for each dimension, the critical parameters u_* and a_* were simultaneously determined within a small range. The parameters a_u and b_u were adjusted, along with Δv, to maximize resolution in the final result for a given value of N. For the results quoted below, initial grid sizes of between $8,000$ and $12,000$ grid points were used.

This method of numerical calculation, coupled with a greater numerical stability in lower dimensions, enabled determination of very accurate estimates of the critical amplitude. The numerical accuracy obtained was at or near the level of machine code precision for the lower dimension results quoted here. Once a rough estimate of the critical parameters was determined the collapse code was run over a range of amplitudes and the results

(a, r_{AH}) collated.

The self-similarity period was determined for each dimension by observing the periodic behaviour of the matter field at the origin. This method considerably decreases the uncertainty in determining the discrete self-similarity constant. Consistent with the 4-dimensional study, data was excluded for which $-log(u_* - u) < 2.5$ and the remaining data fit to a sine wave function using KaleidaGraph Demo. For these calculations, a stable collapse run with a supercritical amplitude closest to a_* was used. Table 4.4 summarizes the results of the low dimension study.

d	Δ	γ
3.02	2.083 ± 0.024	0.1379 ± 0.0042
3.05	2.526 ± 0.025	0.1628 ± 0.0008
3.1	2.783 ± 0.015	0.1989 ± 0.0014
3.2	3.097 ± 0.011	0.2495 ± 0.0010
3.3	3.254 ± 0.019	0.2853 ± 0.0024
3.4	3.354 ± 0.016	0.3053 ± 0.0027
3.5	3.411 ± 0.017	0.3235 ± 0.0018
3.7	3.451 ± 0.013	0.3476 ± 0.0015
3.9	3.453 ± 0.014	0.3672 ± 0.0023
4.0	3.445 ± 0.013	0.3744 ± 0.0022

Tab. 4.4: Critical phenomena for $3 < d \leq 4$. The critical amplitude was determined to a higher degree of accuracy than for the high dimension study by modifying the collapse code. As a result, the estimates of the critical constants have a lower relative uncertainty.

Figure 4.11 shows an example of the ringing of the matter field at the

origin in $d = 3.5$. The period of the ringing was estimated to be $\Delta = 3.411 \pm 0.017$.

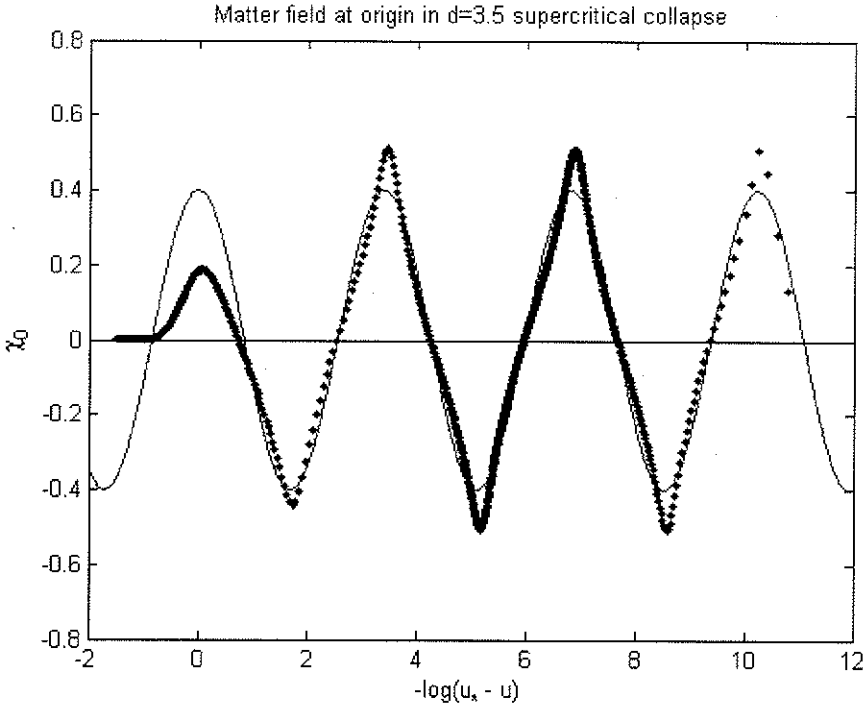

Fig. 4.11: Matter field at the origin in $d = 3.5$ supercritical collapse. The period was estimated to be $\Delta = 3.41 \pm 0.02$.

It was desired to determine the functional relationship between the critical constants and space-time dimension in order to predict their value at $d = 3$. Recall from above that the field equations become singular at $d = 3$ and so it is not possible to run collapse simulations for that value of d. Moreover, the dilaton field becomes negative for $d < 3$. For these reasons, the lower

dimension collapse calculations were limited to the range $3 < d \leq 4$.

A weighted fit to the data for two classes of functions using KaleidaGraph Demo was performed. The data was fit to the following forms

$$\left\{\Delta^{(d)}, \gamma^{(d)}\right\} = m_1 \log\left(d - m_2\right) - m_3 \log\left(d\right) + m_4, \tag{4.37}$$

$$\left\{\Delta^{(d)}, \gamma^{(d)}\right\} = m_4 - \frac{m_3}{\left(d - m_2\right)^{m_1}}. \tag{4.38}$$

The question of whether the data are well fit by other forms remains open. Nevertheless, in [48] it was suggested that γ could be described by a function either of the form (4.38) or of the form

$$\gamma^{(d)} = m_1 - m_2 \exp\left(-m_3 d\right). \tag{4.39}$$

Fitting the low dimension data to the form (4.39) did not yield results with a high degree of confidence. The results of the best fit (corresponding to the lowest χ^2) are shown in Table 4.5.

Function	m_1	m_2	m_3	R^2	χ^2_ν
$\gamma = m_1 - m_2 \exp\left(-m_3 d\right)$	0.376 ± 0.002	$(6 \pm 1) \times 10^3$	3.35 ± 0.07	0.9992	6.1

Tab. 4.5: Poor quality fit for γ with $3 < d \leq 4$. As a result of the fit, the function (4.39) was excluded as a likely form of $\gamma^{(d)}$. Even so, if one uses this function to predict the critical exponent, one finds $\gamma^{(3)} = 0.12 \pm 0.07$.

In the lower dimensional study, it was found that Δ and γ were very well fit by functions of the form given by (4.37) and (4.38). The results of several fits to these functions are shown in Table 4.6. In these fits, the data

Fit	Function	m_1	m_2	m_3	m_4	R^2	χ^2_ν
1	$\gamma = \frac{1}{2} - \frac{m_3}{(d-m_2)^{m_1}}$	0.62	2.80	0.1408		0.9999	0.54
2	$\gamma = m_4 - \frac{m_3}{(d-m_2)^{m_1}}$	0.6	2.80	0.14	0.50	0.9999	0.63
3	$\gamma = m_4 - \frac{m_3}{d-m_2}$		2.70	0.099	0.449	0.9998	0.64
4	$\gamma = \frac{1}{2} - \frac{m_3}{d-m_2}$		2.551	0.167		0.9948	> 15
5	$\gamma = \log\left[\frac{(d-m_2)^{m_1}}{d^{m_3}}\right] + m_4$	0.14	2.90	0.3	0.8	0.9998	0.89
6	$\gamma = m_1 \log\left(\frac{d-m_2}{d}\right) + m_4$	0.107	2.939		0.518	0.9996	1.59
7	$\gamma = \log\left[\frac{(d-m_2)^{m_1}}{d^{m_3}}\right] + \frac{1}{2}$	0.105	2.942	0.094		0.9995	1.74
8	$\gamma = m_1 \log\left(\frac{d-m_2}{d}\right) + \frac{1}{2}$	0.0962	2.959			0.9987	4.36
9	$\Delta = \log\left[\frac{(d-m_2)^{m_1}}{d^{m_3}}\right] + m_4$	0.63	2.987	2.8	7.4	0.9988	1.08
10	$\Delta = \log\left[\frac{\sqrt{d-3}}{d^2}\right] + m_4$				6.234	0.9969	1.82
11	$\Delta = \log\left[\frac{(d-3)^{m_1}}{d^{m_3}}\right] + m_4$	0.51		2.1	6.4	0.9970	2.25

Tab. 4.6: Fits of the functional form of the critical phenomena in massless scalar field collapse for $3 < d \leq 4$. Only the significant digits in the fitted values of the coefficients have been included.

is weighted and the fit parameters determined using KaleidaGraph Demo. In the table, the goodness of fit R^2 and the reduced chi-squared χ^2_ν [101] of the fits are included, and the fits have been ranked according to the latter.

The scaling constant γ was best fit to a function which had the form (4.38). If the functional form for Fit 1 is indeed a good representation of the data then the low value of χ^2_ν could be an indication that the uncertainty in γ has been over-estimated. This can be interpreted as verification that the

method of determining uncertainties presented here is, in fact, conservative.

Perhaps the most interesting aspect of the fit result is that the additional constraint of forcing the data to asymptote to a value of $1/2$ at large d did not deteriorate the quality of the fit even though the data is being extrapolated over a such a large range in d. Indeed, as can be seen by the result of Fit 2, the most likely value of m_4 overlaps with the value of $1/2$. Therefore, any increase in χ^2 due to the additional constraint is more than compensated for by the extra degree of freedom recovered.

Figure 4.12 is a graph of the critical scaling data with Fit 1 and Fit 5 shown with the data. Using the coefficients of Fit 1 to predict the value of γ at $d = 3$ and $d \to \infty$ gives

$$\begin{aligned} \gamma^{(3)} &= 0.11 \pm 0.02 \\ \gamma^{(\infty)} &= \frac{1}{2}. \end{aligned}$$

It is also desired to determine the form of Δ as a function of d. From the lower dimension data, Δ appears to reach a maximum around $d = 3.7$ which rules out the form (4.38). The results of the fitting procedure are included in Table 4.6. In this case, the self-similarity constant appears to diverge very

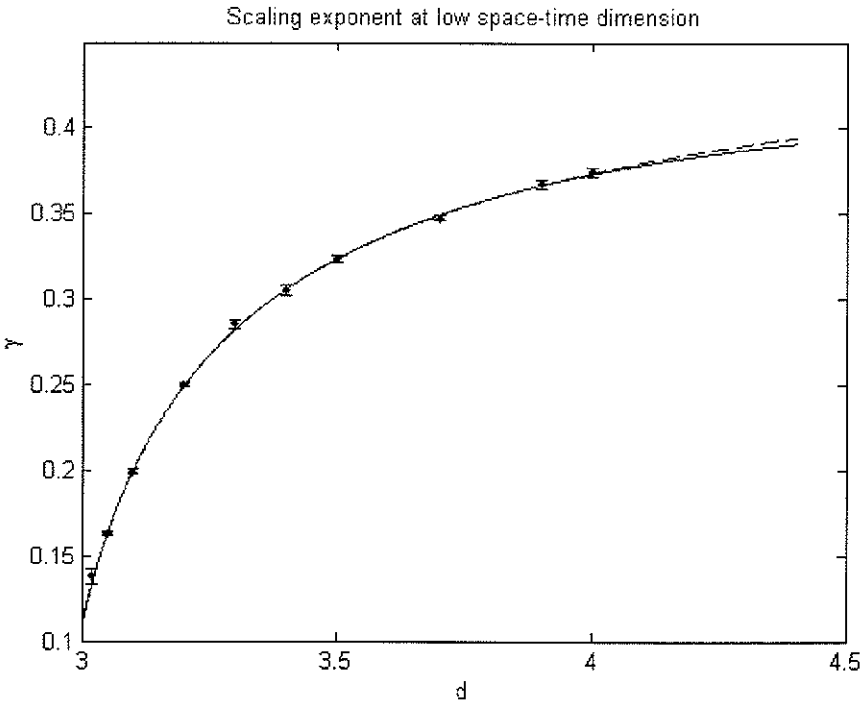

Fig. 4.12: Fits of the critical scaling constant for $3 < d \leq 4$. The solid line is Fit 5 with a quality of fit given by $\chi^2_\nu = 0.89$. The dashed line is the best fit function, Fit 1, with a quality of fit given by $\chi^2_\nu = 0.54$. Both functions extrapolate to a value of approximately 0.1 at $d = 3$.

near $d = 3$, however, the best fit result indicates that Δ is still finite at $d = 3$. If the fit is constrained by forcing the divergence at $d = 3$, the quality of the fit is noticeably degraded (Fit 11).

Figure 4.13 is a graph of the discrete self-similarity with Fit 9 and Fit 10 shown with the data. If one uses the coefficients of Fit 9 to predict the value

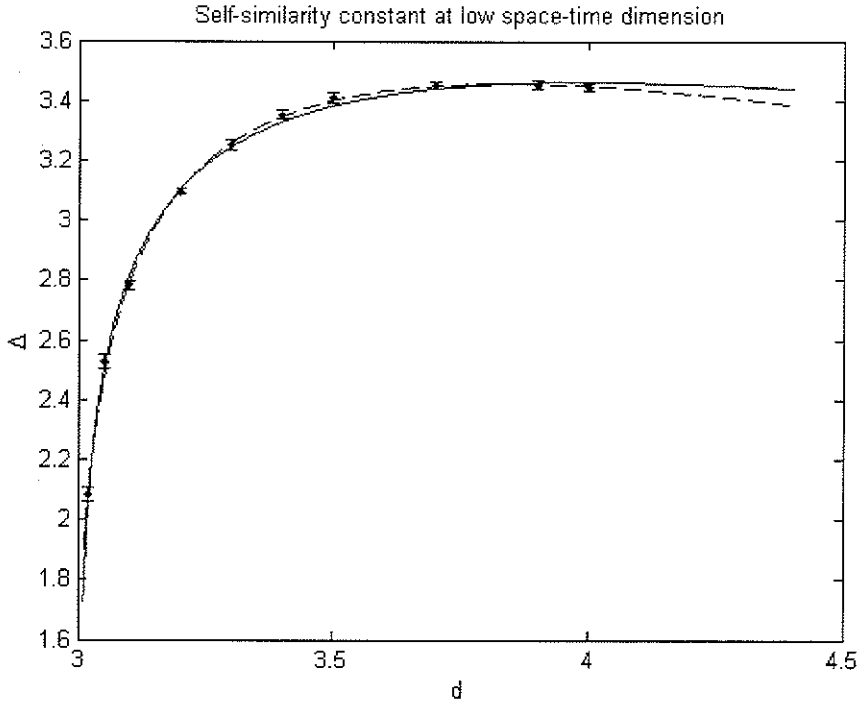

Fig. 4.13: Fits of the critical self-similarity constant for $3 < d \leq 4$. The solid line is Fit 10 with a quality of fit given by $\chi^2_\nu = 1.82$. The dashed line is the best fit function, Fit 9, with a quality of fit given by $\chi^2_\nu = 1.08$. Fit 9 extrapolates to a value of 1.5 ± 0.6 at $d = 3$, whereas, Fit 10 diverges at this value of d.

of Δ at $d = 3$ and $d \to \infty$ it is found

$$\begin{aligned} \Delta^{(3)} &= 1.5 \pm 0.6 \\ \Delta^{(\infty)} &\to -\infty. \end{aligned}$$

The prediction of Δ in 3 space-time dimensions is still not very accurate and, strictly based on the fit results, it may not be prudent to assume Δ does not diverge at $d = 3$. If indeed Δ diverges in three space-time dimensions how might one interpret that?

If one examines the definition of a discretely self-similar space-time given by (2.83), it is seen that the diffeomorphism is entirely suppressed if $\Delta \to -\infty$. One might, therefore, conclude from the results presented here that the critical solution in spherically symmetric gravitational collapse of scalar field in three space-time dimensions is, at most, continuously self-similar and not discretely self-similar. This conclusion could be consistent with the findings of Pretorius and Choptuik [51] and Husain and Olivier [52] for the case of scalar field collapse in $2 + 1$ AdS, see Section 2.2.1. In the model studied here, however, different boundary conditions are used.

In the following subsection, both sets of results (for all d) will be used

to develop a hypothesis of the functional form of the critical phenomena observed in gravitational collapse of scalar field.

4.2.4 Dimension Dependence of Critical Phenomena

The results in Tables 4.3 and 4.4 were combined and a weighted fit to functions of the form (4.37) and (4.38) was performed in order to determine the functional dependence of the critical constants on the full range of d. The results of those fits are given in Table 4.7.

Fit	Function	m_1	m_2	m_3	m_4	R^2	χ^2_ν
12	$\gamma = m_4 - \frac{m_3}{(d-m_2)^{m_1}}$	0.66	2.80	0.134	0.493	0.9999	0.23
13	$\gamma = \frac{1}{2} - \frac{m_3}{(d-m_2)^{m_1}}$	0.61	2.813	0.1407		0.9999	0.29
14	$\gamma = m_4 - \frac{m_3}{d-m_2}$		2.658	0.118	0.464	0.9992	2.06
15	$\gamma = \frac{1}{2} - \frac{m_3}{d-m_2}$		2.518	0.177		0.9921	> 20
16	$\gamma = \log\left[\frac{(d-m_2)^{m_1}}{d^{m_3}}\right] + m_4$	0.110	2.938	0.137	0.556	0.9998	0.99
17	$\gamma = m_1 \log\left(\frac{d-m_2}{d}\right) + \frac{1}{2}$	0.0962	2.958			0.9994	3.28
18	$\gamma = m_1 \log\left(\frac{d-m_2}{d}\right) + m_4$	0.095	2.960		0.499	0.9994	3.43
19	$\gamma = m_1 - m_2 \exp(-m_3 d)$	0.416	280	2.31		0.9926	> 40
20	$\Delta = \left(\log\left[\frac{\sqrt{d-3}}{d^2}\right] + m_1\right) \exp\left[-m_2 (d - m_3)\right] + m_4$	3.7	0.05	3.9	2.5	0.9951	1.68
21	$\Delta = \log\left[\frac{\sqrt{d-3}}{d^2}\right] + m_4$				6.233	0.9934	1.91
22	$\Delta = \log\left[\frac{(d-3)^{m_1}}{d^{m_3}}\right] + m_4$	0.504		2.05	6.30	0.9936	2.06
23	$\Delta = \log\left[\frac{(d-m_2)^{m_1}}{d^{m_3}}\right] + m_4$	0.52	2.998	2.09	6.36	0.9938	2.11

Tab. 4.7: Fits of the functional form of the critical phenomena in massless scalar field collapse for $3 < d \leq 14$. Only the significant digits in the fitted values of the coefficients have been included. A damping term was added to Fit 20.

The data and best fits of the self-similarity constant are shown in Figure 4.14. Even though the higher dimensional results are less accurate, Δ does appear to approach a constant at large dimension. If so, the previous fits

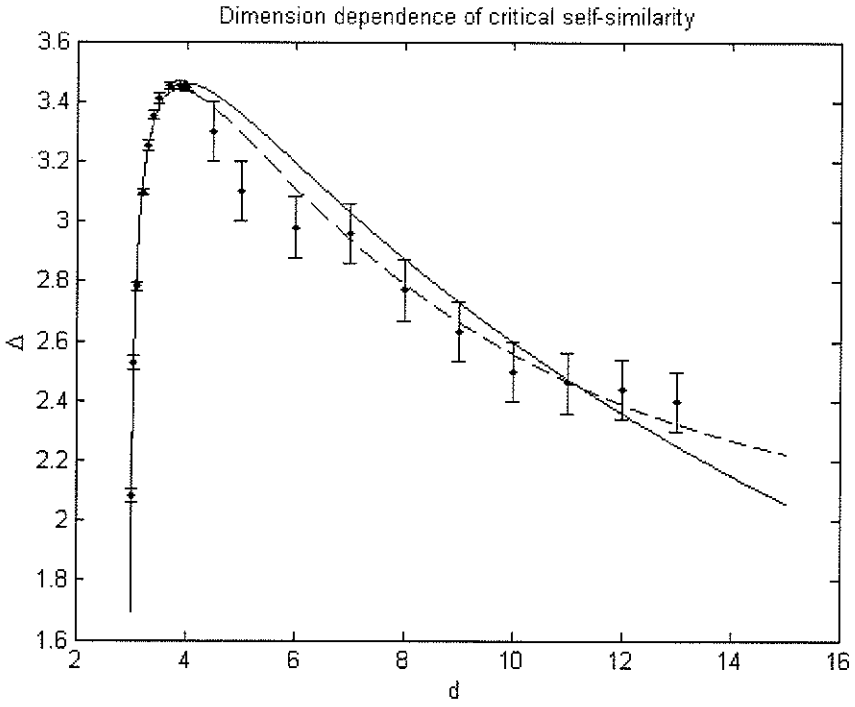

Fig. 4.14: Fits of the critical self-similarity constant for $3 < d \leq 14$. The solid line is Fit 21 with a quality of fit given by $\chi^2_\nu = 1.91$. The dashed line is the best fit function, Fit 20, with a quality of fit given by $\chi^2_\nu = 1.68$. Fit 20 asymptotes to a positive constant at large d whereas Fit 21 diverges to $-\infty$.

would not be valid to describe Δ at large d. To include this consideration, a damping term was added to Fit 20. The fit was noticeably improved. Using the results of Fit 20, it is hypothesized that

$$\Delta^{(d)} = \left[\log\left(\frac{\sqrt{d-3}}{d^2}\right) + 3.7\right] \exp\left[-0.05\,(d-3.9)\right] + 5/2 \quad (4.40)$$

$$\Delta^{(3)} = -\infty \quad (4.41)$$

$$\Delta^{(\infty)} = \frac{5}{2}. \quad (4.42)$$

The data and best fits of the scaling exponent are shown in Figure 4.15. Including the higher dimension results did not affect the qualitative aspect of the apparent functional dependence of the critical scaling exponent on space-time dimension. Similar to the findings given in the previous subsection, the data were better fit to a function of the form (4.38) which asymptotes to a positive constant at large d. The only difference being that constraining the fit to asymptote to a value of 1/2 slightly reduces the quality of the fit. Even so, the standard error of the fit parameter m_4 in Fit 12 overlaps with 1/2: that is, $m_4 = 0.493 \pm 0.007$. Moreover, the relative errors for the remaining parameters of Fit 12 are considerably larger compared to Fit 13 as is seen when the fit is extrapolated to $d = 3$. Using the results of Fit 12,

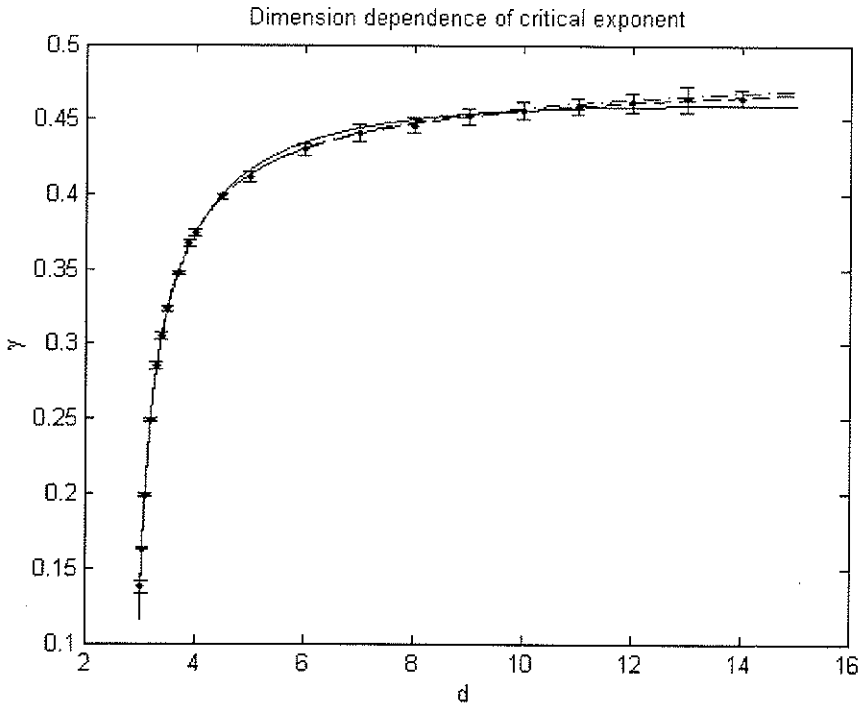

Fig. 4.15: Fits of the critical scaling constant for $3 < d \leq 14$. The solid line is Fit 16 with a quality of fit given by $\chi^2_\nu = 0.99$. The dashed line is the best fit function, Fit 12, with a quality of fit given by $\chi^2_\nu = 0.23$. Fit 13 ($\chi^2_\nu = 0.29$) has also been included in the graph (the dash-dot line). Fit 12 and 13 asymptote to positive constants at large d whereas Fit 16 diverges to $-\infty$.

it is predicted that

$$\begin{aligned}
\gamma^{(d)} &= 0.493 + \frac{-0.134}{(d-2.80)^{0.66}} \\
\gamma^{(3)} &= 0.11 \pm 0.04 \\
\gamma^{(\infty)} &= 0.493 \pm 0.007.
\end{aligned}$$

In order to reduce the uncertainty in the extrapolation, it is hypothesized that the functional form of γ (using the results of Fit 13) is, instead, given by

$$\gamma^{(d)} = \frac{1}{2} - \frac{0.1407}{(d-2.813)^{0.61}} \tag{4.43}$$

$$\gamma^{(3)} = 0.11 \pm 0.01 \tag{4.44}$$

$$\gamma^{(\infty)} = \frac{1}{2}. \tag{4.45}$$

5. CONCLUSIONS

In this thesis, I have analyzed the dependence on space-time dimension of the critical phenomena observed in gravitational collapse. The matter field analyzed is a d-dimensional, spherically symmetric, massless, minimally coupled scalar field. I have numerically calculated the properties of the critical solution of this matter field in the context of dilaton gravity over the finite range $3 < d \leq 14$ and shown that the results agree qualitatively with previous studies. The critical solutions in these dimensions exhibit power law scaling, universality, and discrete self-similarity analogous to that originally seen by Choptuik in the case of $3 + 1$.

A single computer code, written in C, which has been designed to carry out the simulations, uses space-time dimension as an input parameter. In practice there are no impediments in either the field equations, or the numerical code, which prevents the user to input a fractional dimension in the calculation. As a result, I have analyzed both integer d and non-integer d

cases. In each case, I calculated the black hole horizon radius power law scaling constant γ and discrete self-similarity constant Δ in supercritical collapse. I also analyzed these constants in $3+1$ subcritical collapse.

Once the values of the critical phenomena were estimated, the results were collated as a function of d. I find that γ and Δ are accurately described by general smooth functions of d and, in both cases, developed a hypothesis for the particular form of both functions. Using these forms, the data were extrapolated to $d = 3$ and $d \to \infty$. I predict that γ approaches a finite positive constant at both extremes, whereas, Δ asymptotes to a finite constant as $d \to \infty$ and probably diverges to $-\infty$ as $d \to 3$.

Figure 5.1 shows the results for the scaling exponent as a function of d along with my prediction of the form of γ. The graph also shows known results from earlier studies. Included on the graph are the results of Sorkin and Oren [63], Garfinkle, Cutler and Duncan [53], and Gundlach [29].

Figure 5.2 shows the results for the discrete self-similarity constant as a function of d along with my prediction of the form of Δ. The graph also shows known results from earlier studies. Included on the graph are the results of Sorkin and Oren [63], Garfinkle, Cutler and Duncan [53], and Gundlach [29].

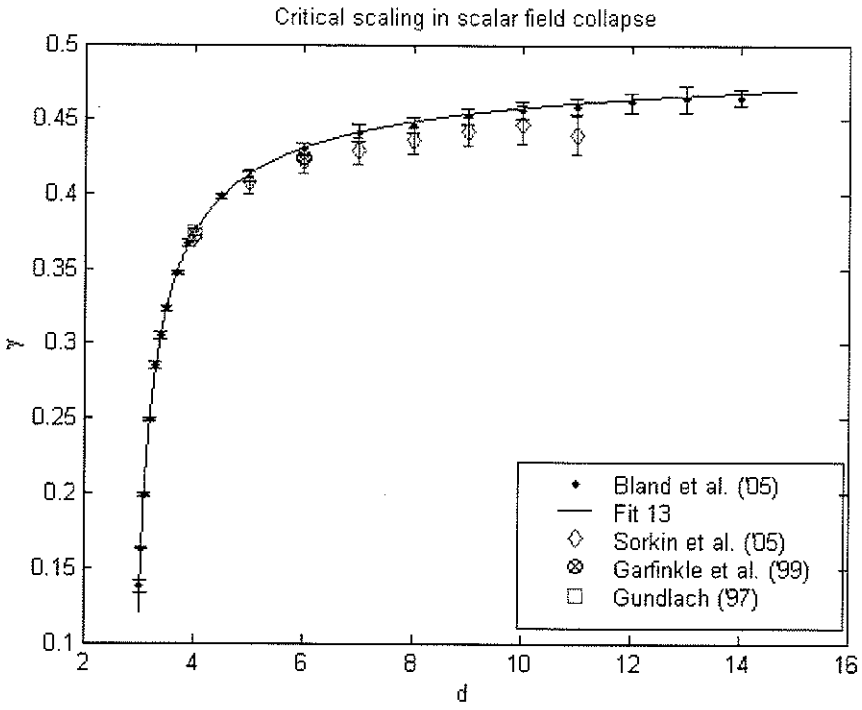

Fig. 5.1: Final values of the scaling constants. The graph also shows known results from earlier studies and the hypothetical form for $\gamma^{(d)}$.

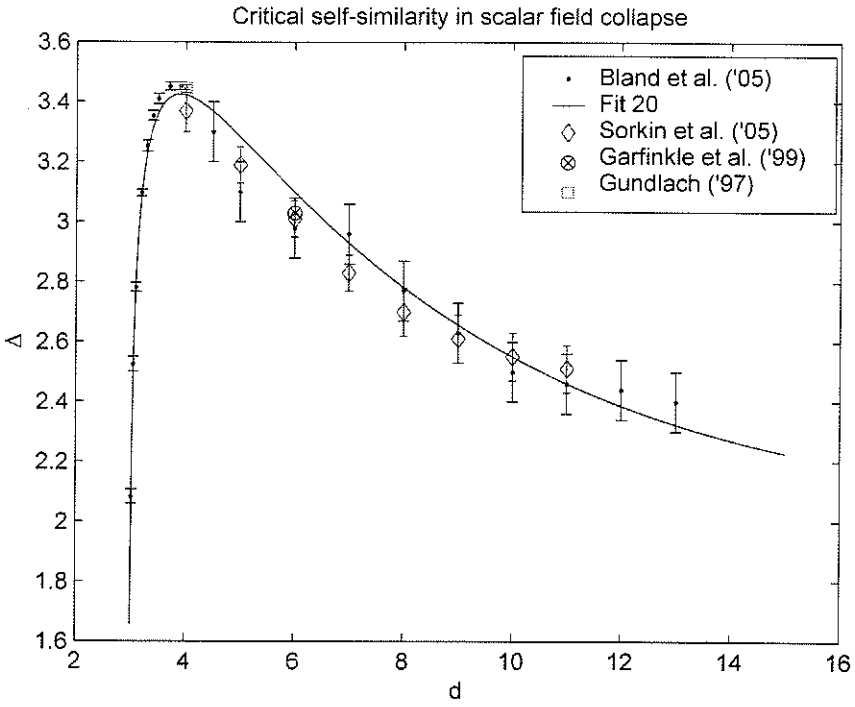

Fig. 5.2: Final values of the self-similarity constant. The graph also shows known results from earlier studies and the hypothetical form for $\Delta^{(d)}$.

5.1 Properties of the critical solution at $d = 3$

I have hypothesized, based on extrapolation, that the critical solution in gravitational collapse of spherically symmetric minimally-coupled massless scalar field in three space-time dimensions with vanishing cosmological constant is a Type II critical solution without a discrete self-similarity. It has also been predicted that in supercritical collapse, the black hole horizon radius approaches the power law given by

$$r_{AH} = c_F (a - a_*)^\gamma , \tag{5.1}$$

where a is a one parameter family of initial data, a_* is the critical value of a, c_F is a family dependent constant, and $\gamma = 0.11 \pm 0.01$.

In our coordinate system (3.83), the matter field equation (3.80) in three dimensions becomes

$$r'\dot{\chi} + \dot{r}\chi' + 2r\dot{\chi}' = 0. \tag{5.2}$$

The metric function is given by

$$g(u, v) = C_1(u) \exp\left[\int \frac{r(\chi')^2}{r'} dv\right]. \tag{5.3}$$

Following the work of Garfinkle [47], we now impose a css ansatz on the field equations by defining the new coordinates

$$T = -\log(-u) \tag{5.4}$$

$$R = \frac{1 - v/u}{2}, \tag{5.5}$$

where, the u coordinate has been shifted so that u increases to the central critical singularity at $u = 0$. The matter field will take the form [47]

$$\chi = cT + \psi(R), \tag{5.6}$$

which requires us to assume the space-time is approximately flat. Therefore,

$$r = \frac{1}{2}(v - u). \tag{5.7}$$

Inserting (5.6) into (5.2) and using (5.7) we find for the wave equation [47]

$$R(1 - 2R)\psi'' + (1 - 3R)\psi' - c = 0. \tag{5.8}$$

Garfinkle finds the solution to this equation, which in our coordinates is given

by

$$g(u,v) = C_1(u)\left(\frac{u+v+2\sqrt{uv}}{4\sqrt{uv}}\right)^{2c^2}. \tag{5.9}$$

In [69], a perturbation analysis of the css solution given above was carried out in an attempt to determine the scaling constant in three dimensional collapse. Using regularity conditions at the origin and a Minkowksi background near the origin, several perturbative modes were found. The perturbation with one unstable mode gave a scaling constant of $\gamma = 4/3$. Unfortunately, this mode did not reproduce the numerical results at intermediate times as reported by Pretorius and Choptuik [51]. As stated above, Pretorius and Choptuik reported a scaling constant of 1.2 ± 0.05. In their numerical analysis, however, Pretorius and Choptuik used a background AdS space-time and Dirichlet boundary conditions. Husain and Olivier [52] numerically analyzed the same system using a double null parameterization and a background AdS space-time. They reported a scaling constant $\gamma \sim 0.81$. In our analysis we have used a Minkowski background with $\Lambda = 0$ for $d > 3$ and estimated the properties of the critical solution at $d = 3$. It is, therefore, not clear whether we should expect to see a continuously self-similar critical solution as well.

Clément and Fabbri [102] analyzed the Garfinkle result and derived, by a limiting process, a new css solution which can be extended to the full

$\Lambda < 0$ equations. The equations they derived will describe collapse to a null central singularity and they find no curvature singularities in the space-time. Nevertheless, they performed an perturbation analysis using the methods of Frolov [103] and Hayward [104] to estimate the scaling constant in the critical solution. These authors estimate $\gamma = 0.4$. As one can now see, it is important to continue analysis of three dimensional collapse as there remains several unresolved issues in the problem.

Table 5.1 summarizes the various predictions of the scaling constant in three dimensional collapse of spherically symmetric scalar field. Clearly there

Author	Method	γ
Pretorius and Choptuik [51]	Numerical, $\Lambda \neq 0$	1.2 ± 0.05
Husain and Olivier [52]	Numerical, $\Lambda \neq 0$	0.81
Garfinkle and Gundlach [69]	Perturbation, $\Lambda \neq 0$	4/3
Clement and Fabbri [102]	Perturbation, $\Lambda \neq 0$	0.4
Bland and Kunstatter [99]	Extrapolation, $\Lambda = 0$	0.11 ± 0.01

Tab. 5.1: Comparing predictions for γ in three dimensional collapse.

is discrepancy on the nature of the critical solution in three dimensional collapse. It would be useful to continue work on this case until an analytic solution could be obtained which matches the numerical observations.

5.2 Properties of the critical solution in the large d limit

Assuming γ and Δ can be described by smooth functions of d I have predicted, using an extrapolation argument, that both critical quantities asymptote to finite positive constants as $d \to \infty$. This suggests that they are the critical phenomena of a limiting theory at large d. This limiting theory appears to contain a Type II discretely self-similar critical solution.

In order to study the $d \to \infty$ case, let us recall the evolution equations with $\Lambda = 0$ in the large d limit:

$$\begin{aligned} \tilde{g} &= \frac{ng\phi^{(n-1)/n}}{Cl^2(n-1)} - \frac{\tilde{h}}{C} \\ \tilde{g}_\infty &= \frac{g\phi}{Cl^2} - \frac{\tilde{h}_\infty}{C} \\ \dot{\phi} &= -\frac{l\tilde{g}}{2}. \end{aligned}$$

In the limit of large d, the dilaton potential becomes

$$V = \frac{1}{l^2}, \tag{5.10}$$

and the total action is, therefore, given by

$$S = \frac{1}{2G}\int d^2x\sqrt{-g}\left[\phi R + \frac{1}{l^2} - \phi\left(\nabla\chi\right)^2\right]. \tag{5.11}$$

One can now see that in vacuum, the action is equivalent to the CGHS action in the form (3.13). The total action in the current form differs from that of CGHS in the coupling to the matter field. Interestingly, however, Peleg, Bose and Parker [105] numerically examined the classical CGHS action and observed Choptuik mass scaling $M_{BH} \propto |a - a_*|^\gamma$ with $\gamma = 0.53 \pm 0.01$. This value of γ is suspiciously similar to our extrapolated value at the limit of large d. It would be interesting to see whether a connection exists between the two theories.

In the computer code written for this thesis, the dilaton field at constant v is evolved using discrete steps in u. Hence, the evolved field to first order is given by

$$\begin{aligned}\phi\left(u+\Delta u, v\right) &= \phi\left(u,v\right) + \dot{\phi}\left(u,v\right)\Delta u \\ &= \phi - \left(\frac{nC_1\left(u\right)\phi^{(n-1)/n}}{2Cl(n-1)} - \frac{l\tilde{h}}{2C}\right)\Delta u.\end{aligned} \tag{5.12}$$

With $l = 1$ and $C_1(u) = 1$, grid points very near the origin are approximately

given by

$$\phi^i_{j+1} = \phi^i_j - \left(\frac{n \left(\phi^i_j\right)^{(n-1)/n}}{2(n-1)} \right) \Delta u_j. \tag{5.13}$$

As stated in the previous chapter, if $\phi^i_{j+1} < 0$ then the position of the origin in the grid is shifted and the corresponding grid point is removed. Therefore, the condition for lost grid points at small ϕ is given by

$$\phi^{1/n} = r < \frac{n\epsilon}{2(n-1)}, \tag{5.14}$$

where $\Delta u_j = \epsilon$. We notice from (5.14) that as n grows, the demand for numerical accuracy grows to the power of n, otherwise, grid points will begin to pile up at the origin and the stability of the numerical code breaks down. In practice, we found that for $n > 12$ ($d > 14$) the code could no longer be made stable enough to extract useful data. Moreover, if we examine the condition for losing grid points in the limit of large d we find the unacceptable result

$$\phi < \exp\left[-n \left(1 - \frac{n\epsilon}{2(n-1)} \right) \right].$$

Our current parameterization would not be capable of performing calcula-

tions at the limit of large d and as we have seen in the previous section the parameterization also breaks down at the $d = 3$ limit.

In conclusion, the critical phenomena in the gravitational collapse of spherically symmetric minimally-coupled massless scalar field in finite dimensions greater than three has been studied. General forms for the scaling constant γ and discrete self-similarity constant Δ in this range of dimensions have been found and an extrapolation of these results has been carried out in order to predict the values of these constants at $d = 3$ and the limit $d \to \infty$. It has also been shown that the current parameterization breaks down at these two extremes and so numerical confirmation of these predictions is not possible at present. It would be interesting to find a new parameterization, in the context of dilaton gravity, so that one can investigate these two extremes and attempt to verify the predictions for γ and Δ.

APPENDIX

A. DERIVATION OF THE FIELD EQUATIONS

We wish to examine the first line of (3.72). Formally,

$$\delta\left(\sqrt{-g}R\right) = \sqrt{-g}\left(R_{\mu\nu} - \frac{1}{2}g_{\mu\nu}R\right)\delta g^{\mu\nu} + \sqrt{-g}g^{\mu\nu}\delta R_{\mu\nu}. \tag{A.1}$$

However, as discussed in chapter 3, the Riemann curvature tensor has only one independent component in two dimensions. In fact, in exactly two dimensions (from 3.3),

$$R_{\mu\nu} = \frac{1}{2}g_{\mu\nu}R, \tag{A.2}$$

which simplifies (A.1) to

$$\delta\left(\sqrt{-g}R\right) = \sqrt{-g}g^{\mu\nu}\delta R_{\mu\nu}. \tag{A.3}$$

The variation of the Ricci tensor is given by the Palatini identity [106]

$$\delta R_{\mu\nu} = \nabla_\nu \left(\delta\Gamma^\lambda_{\mu\lambda}\right) - \nabla_\lambda \left(\delta\Gamma^\lambda_{\mu\nu}\right), \tag{A.4}$$

where $\delta\Gamma^\lambda_{\mu\nu}$ is the change in the affine connection. Explicitly,

$$\delta\Gamma^\lambda_{\mu\nu} = -g^{\lambda\rho}\delta g_{\rho\sigma}\Gamma^\sigma_{\mu\nu} + \frac{1}{2}g^{\lambda\rho}\left[\frac{\partial\delta g_{\rho\mu}}{\partial x^\nu} + \frac{\partial\delta g_{\rho\nu}}{\partial x^\mu} - \frac{\partial\delta g_{\mu\nu}}{\partial x^\rho}\right]. \tag{A.5}$$

The variation in the affine connection can also be expressed as the tensor [3]

$$\delta\Gamma^\lambda_{\mu\nu} = \frac{1}{2}g^{\lambda\rho}\left[\nabla_\nu\left(\delta g_{\rho\mu}\right) + \nabla_\mu\left(\delta g_{\rho\nu}\right) - \nabla_\rho\left(\delta g_{\mu\nu}\right)\right]. \tag{A.6}$$

We insert (A.6) into (A.4) and use (3.70) to obtain

$$\begin{aligned}\delta R_{\mu\nu} &= -\frac{1}{2}g^{\lambda\rho}\left[\nabla_\nu\nabla_\mu\left(\delta g_{\lambda\rho}\right) + \nabla_\lambda\nabla_\rho\left(\delta g_{\mu\nu}\right)\right] \\ &\quad + \frac{1}{2}g^{\lambda\rho}\left[\nabla_\lambda\nabla_\nu\left(\delta g_{\rho\mu}\right) + \nabla_\lambda\nabla_\mu\left(\delta g_{\rho\nu}\right)\right].\end{aligned} \tag{A.7}$$

Therefore,

$$g^{\mu\nu}\delta R_{\mu\nu} = \left(\nabla^\mu\nabla^\nu - g^{\mu\nu}\Box\right)\delta g_{\mu\nu} = -\left(\nabla_\mu\nabla_\nu - g_{\mu\nu}\Box\right)\delta g^{\mu\nu}, \tag{A.8}$$

where we have made use of the definition (1.14) and of the identity [3]

$$\delta g^{\mu\nu} = -g^{\mu\rho} g^{\nu\sigma} \delta g_{\rho\sigma}. \tag{A.9}$$

Hence, we re-express (A.1) as

$$\delta \left(\sqrt{-g} R \right) = -\sqrt{-g} \left(\nabla_\mu \nabla_\nu - g_{\mu\nu} \Box \right) \delta g^{\mu\nu}. \tag{A.10}$$

REFERENCES

[1] A. Einstein, The Foundation of the General Theory of Relativity, in *The Collected Papers of Albert Einstein Volume 6: The Berlin Years: Writings, 1914-1917: English Translation of Selected Texts*, A. Engel, translator, Princeton University Press, New Jersey (1997). Originally published in Annalen der Physik **49**, 769 (1916).

[2] S. W. Hawking and G. F. R. Ellis, *The Large Scale Structure of Space-Time*, Cambridge University Press, Cambridge (1973).

[3] S. Weinberg, *Gravitation and Cosmology: Principles and Applications of the General Theory of Relativity*, Wiley, New York (1972).

[4] K. Schwarzschild, On the Gravitational Field of a Mass Point according to Einstein's Theory, Gen. Rel. Grav. **35**, 951 (2003). English translation by S. Antoci and A. Loinger. Originally published in Sitzungsberichte der Königlich Preußische Akademie der Wissenschaften, 189 (1916).

[5] P. Painlevé, La Méchanique classique et la théorie de la relativité, C. R. Acad. Sci. (Paris) **173**, 677 (1921).

[6] A. Gullstrand, Allegemeine Lösung des statischen Einkörper-problems in der Einsteinschen Gravitations theorie, Ark. Mat., Astron. Fys. **16**, 1 (1922).

[7] K. Martel and E. Poisson, Regular coordinate systems for Schwarzschild and other spherical spacetimes, Am. J. Phys. **69**, 476 (2001).

[8] P. Kraus and F. Wilczek, Some applications of a simple stationary line element for the Schwarzschild geometry, Mod. Phys. Lett. **A9**, 3713 (1994).

[9] R. Penrose, Gravitational Collapse and Space-Time Singularities, Phys. Rev. Lett. **14**, 57 (1965).

[10] J. R. Oppenheimer and H. Snyder, On Continued Gravitational Contraction, Phys. Rev. **56**, 455 (1939).

[11] P. C. W. Davies, S. A. Fulling and W. G. Unruh, Energy-momentum tensor near an evaporating black hole, Phys. Rev. **D13**, 2720 (1976).

[12] S. W. Hawking, Particle Creation by Black Holes, Commun. Math. Phys. **43**, 199 (1975).

[13] C. Gundlach, Critical phenomena in gravitational collapse, Phys. Rep. **376**, 339 (2003); Critical Phenomena in Gravitational Collapse, Living Rev. Relativity **2**, 4 (1999). URL: http://www.livingreviews.org/lrr-1999-4

[14] L. Lehner, Numerical relativity: a review, Class. Quantum Grav. **18**, R25 (2001).

[15] D. S. Goldwirth and T. Piran, Gravitational collapse of massless scalar field and cosmic censorship, Phys. Rev. **D36**, 3575 (1987).

[16] R. M. Wald, Gravitational Collapse and Cosmic Censorship, unpublished report, April 1997 APS meeting, gr-qc/9710068.

[17] G. Rein and A. D. Rendall, Global Existence of Solutions of the Spherically Symmetric Vlasov-Einstein System with Small Initial Data, Commun. Math. Phys. **150**, 561 (1992).

[18] A. D. Rendall, Theorems on Existence and Global Dynamics for

the Einstein Equations, Living Rev. Relativity **8**, 6 (2005). URL: http://www.livingreviews.org/lrr-2005-6

[19] M. W. Choptuik, Universality and Scaling in Gravitational Collapse of a Massless Scalar Field, Phys. Rev. Lett. **70**, 9 (1993).

[20] R. Penrose, Singularities and time-asymmetry, in *General Relativity: An Einstein Centenary Survey*, eds. S. W. Hawking and W. Isreal, Cambridge University Press, New York (1979).

[21] V. Moncrief and D. M. Eardley, The Global Existence Problem and Cosmic Censorship in General Relativity, Gen. Rel. Grav. **13**, 887 (1981).

[22] S. L. Shapiro and S. A. Teukolsky, Formation of Naked Singularities: The Violation of Cosmic Censorship, Phys. Rev. Lett. **66**, 994 (1991).

[23] D. Christodoulou, Examples of Naked Singularity Formation in the Gravitational Collapse of a Scalar Field, Ann. Math. **140**, 67 (1994).

[24] D. Christodoulou, The Instability of Naked Singularities in the Gravitational Collapse of a Scalar Field, Ann. Math. **149**, 183 (1999).

[25] D. Christodoulou, The Problem of a Self-Gravitating Scalar Field, Commun. Math. Phys. **105**, 337 (1986).

[26] R. S. Hamadé and J. M. Stewart, The spherically symmetric collapse of a massless scalar field, Class. Quantum Grav. **13**, 497 (1996).

[27] D. Garfinkle and G. C. Duncan, Scaling of curvature in subcritical gravitational collapse, Phys. Rev. **D58**, 064024 (1998).

[28] D. Garfinkle, Choptuik scaling in null coordinates, Phys. Rev. **D51**, 5558 (1995).

[29] C. Gundlach, Understanding critical collapse of a scalar field, Phys. Rev. **D55**, 695 (1997).

[30] D. Garfinkle, Choptuik scaling and the scale invariance of Einstein's equation, Phys. Rev. **D56**, 3169 (1997).

[31] A. M. Abrahams and C. R. Evans, Critical Behaviour and Scaling in Vacuum Axisymmetric Gravitational Collapse, Phys. Rev. Lett. **70**, 2980 (1993).

[32] C. R. Evans and J. S. Coleman, Critical Phenomena and Self-Similarity in the Gravitational Collapse of Radiation Fluid, Phys. Rev. Lett. **72**, 1782 (1994).

[33] T. Koike, T. Hara and S. Adachi, Critical Behavior in Gravitational

Collapse of Radiation Fluid: A Renormalization Group (Linear Perturbation) Analysis, Phys. Rev. Lett. **74**, 5170 (1995).

[34] D. Maison, Non-universality of critical behaviour in spherically symmetric gravitational collapse, Phys. Lett. **B366**, 82 (1996).

[35] R. S. Hamadé, J. H. Horne and J. M. Stewart, Continuous self-similarity and S-duality, Class. Quantum Grav. **13**, 2241 (1996).

[36] D. W. Neilsen and M. W. Choptuik, Critical phenomena in perfect fluids, Class. Quantum Grav. **17**, 761 (2000).

[37] T. Harada and H. Maeda, Convergence to a self-similar solution in general relativistic gravitational collapse, Phys. Rev. **D63**, 084022 (2001).

[38] M. W. Choptuik, T. Chmaj and P. Bizoń, Critical Behavior in Gravitational Collapse of a Yang-Mills Field, Phys. Rev. Lett. **77**, 424 (1996).

[39] P. R. Brady, C. M. Chambers and S. M. C. V. Gonçalves, Phases of massive scalar field collapse, Phys. Rev. **D56**, 6057 (1997).

[40] G. Rein, A. D. Rendall and J. Schaeffer, Critical collapse of collisionless matter: A numerical investigation, Phys. Rev. **D58**, 044007 (1998).

[41] I. Olabarrieta and M. W. Choptuik, Critical phenomena at the threshold of black hole formation for collisionless matter in spherical symmetry, Phys. Rev. **D65**, 024007 (2001).

[42] E. W. Hirschmann and D. M. Eardley, Universal scaling and echoing in the gravitational collapse of a complex scalar field, Phys. Rev. **D51**, 4198 (1995).

[43] E. W. Hirschmann and D. M. Eardley, Critical exponents and stability at the black hole threshold for a complex scalar field, Phys. Rev. **D52**, 5850 (1995).

[44] S. Hod and T. Piran, Critical behavior and universality in gravitational collapse of a charged scalar field, Phys. Rev. **D55**, 3485 (1997).

[45] D. J. Rowan and G. Stephenson, The massive scalar meson field in a Schwarzschild background space, J. Phys. **A9**, 1261 (1976).

[46] D. J. Rowan and G. Stephenson, Solutions of the time-dependent Klein-Gordon equation in a Schwarzschild background space, J. Phys. **A9**, 1631 (1976).

[47] D. Garfinkle, Exact solution for (2+1)-dimensional critical collapse, Phys. Rev. **D63**, 044007 (2001).

[48] J. Bland, B. Preston, M. Becker, G. Kunstatter and V. Husain, Dimension-Dependence of the Critical Exponent in Spherically Symmetric Gravitational Collapse, Class. Quantum Grav. **22**, 5355 (2005).

[49] M. Bañados, C. Teitelboim and J. Zanelli, Black Hole in Three-Dimensional Spacetime, Phys. Rev. Lett. **69**, 1849 (1992).

[50] S. Carlip, The (2+1)-dimensional black hole, Class. Quantum Grav. **12**, 2853 (1995).

[51] F. Pretorius and M. W. Choptuik, Gravitational collapse in 2+1 dimensional AdS spacetime, Phys. Rev. **D62**, 124012 (2000).

[52] V. Husain and M. Olivier, Scalar field collapse in three-dimensional AdS spacetime, Class. Quantum Grav. **18**, L1 (2001).

[53] D. Garfinkle, C. Cutler and G. Comer Duncan, Choptuik scaling in six dimensions, Phys. Rev. **D60**, 104007 (1999).

[54] F. R. Tangherlini, Schwarzschild Field in N Dimensions and the Dimensionality of Space Problem, Nuovo Cimento **27**, 636 (1963).

[55] R. C. Myers and M. J. Perry, Black Holes in Higher Dimensional Space-Times, Ann. Phys. **172**, 304 (1986).

[56] X. Dianyan, Exact solutions of Einstein and Einstein-Maxwell equations in higher-dimensional spacetime, Class. Quantum Grav. **5**, 871 (1988).

[57] R. Arnowitt, S. Deser and C. W. Misner, in *Gravitation: An Introduction to Current Research*, ed. L. Witten, Wiley, New York (1962).

[58] B. C. Xanthopoulos and T. Zannias, Einstein gravity coupled to a massless scalar field in arbitrary spacetime dimensions, Phys. Rev. **D40**, 2564 (1989).

[59] A. V. Frolov, Self-similar collapse of a scalar field in higher dimensions, Class. Quantum Grav. **16**, 407 (1999).

[60] M. Birukou, V. Husain, G. Kunstatter, E. Vaz and M. Olivier, Spherically symmetric scalar field collapse in any dimension, Phys. Rev. **D65**, 104036 (2002).

[61] V. Husain, G. Kunstatter, B. Preston and M. Birukou, Anti-de Sitter gravitational collapse, Class. Quantum Grav. **20**, L23 (2003).

[62] G. Kunstatter, "Dimension dependence of the critical exponent in spherical black hole formation", contributed talk given at *GR17*, Dublin (2004).

[63] E. Sorkin and Y. Oren, Choptuik's scaling in higher dimensions, Phys. Rev. **D71**, 124005 (2005).

[64] L. Landau and E. Lifshitz, *Statistical Physics*, Oxford University Press, London (1938).

[65] M. Plischke and B. Bergersen, *Equilibrium Statistical Physics*, Prentice Hall, New Jersey (1989).

[66] T. Koike, T. Hara and S. Adachi, Renormalization group and critical behaviour in gravitational collapse, unpublished report, gr-qc/9607010.

[67] M. E. Cahill and A. H. Taub, Spherically Symmetric Similiarity Solutions of the Einstein Field Equations for a Perfect Fluid, Commun. Math. Physics **21**, 1 (1971).

[68] E. W. Hirschmann, A. Wang and Y. Wu, Collapse of a scalar field in 2 + 1 gravity, Class. Quantum Grav. **21**, 1791 (2004).

[69] D. Garfinkle and C. Gundlach, Perturbations of an exact solution for (2+1)-dimensional critical collapse, Phys. Rev. **D66**, 044015 (2002).

[70] J. Soda and K. Hirata, Higher dimensional self-similar spherical symmetric scalar field collapse and critical phenomena in black-hole formation, Phys. Lett. **B387**, 271 (1996).

[71] S. Hod and T. Piran, Fine structure of Choptuik's mass scaling relation, Phys. Rev. **D55**, 440 (1997).

[72] C. Teitelboim, Gravitation and Hamiltonian Structure in Two Spacetime Dimensions, Phys. Lett. **B126**, 41 (1983); in *Quantum Theory of Gravity*, ed. S. Christensen, Adam Hilger, Bristol (1984); R. Jackiw in *Quantum Theory of Gravity*, ed. S. Christensen, Adam Hilger, Bristol (1984).

[73] T. Banks and L. Susskind, Canonical Quantization of 1+1 Dimensional Gravity, Int. J. Theor. Phys. **23**, 475 (1984).

[74] A. Achúcarro and M. E. Ortiz, Relating black holes in two and three dimensions, Phys. Rev. **D48**, 3600 (1993).

[75] C. G. Callan, S. B. Giddings, J. A. Harvey and A. Strominger, Evanescent black holes, Phys. Rev. **D45**, 1005 (1992).

[76] G. W. Gibbons, Antigravitating Black Hole Solitons with Scalar Hair in $N = 4$ Supergravity, Nucl. Phys. **B207**, 337 (1982); G. W. Gibbons and K. Maeda, Black Holes and Membranes in Higher-Dimensional Theories with Dilaton Fields, *ibid.* **B298**, 741 (1988).

[77] D. Garfinkle, G. Horowitz and A. Strominger, Charged black holes in string theory, Phys. Rev. **D43**, 3140 (1991); G. Horowitz and A. Strominger, Black Strings and p-Branes, Nucl. Phys. **B360**, 197 (1991).

[78] E. Witten, String theory and black holes, Phys. Rev. **D44**, 314 (1991).

[79] S. Bose, L. Parker and Y. Peleg, Semi-infinite throat as the end-state geometry of two-dimensional black hole evaporation, Phys. Rev. **D52**, 3512 (1995).

[80] S. Bose, J Louko, L. Parker and Y. Peleg, Hamiltonian thermodynamics of two-dimensional vacuum dilatonic black holes, Phys. Rev. **D53**, 5708 (1996).

[81] S. Bose, L. Parker and Y. Peleg, Hawking Radiation and Unitary Evolution, Phys. Rev. Lett. **76**, 861 (1996).

[82] S. Bose, L. Parker and Y. Peleg, Predictability and semiclassical approximation at the onset of black hole formation, Phys. Rev. **D53**, 7089 (1996).

[83] S. Bose, L. Parker and Y. Peleg, Validity of the semiclassical approximation and back reaction, Phys. Rev. **D54**, 7490 (1996).

[84] S. Bose, L. Parker and Y. Peleg, Lorentzian approach to black hole thermodynamics in the Hamiltonian formulation, Phys. Rev. **D56**, 987 (1997).

[85] W. G. Unruh, Notes on black-hole evaporation, Phys. Rev. **D14**, 870 (1976).

[86] P. Thomi, B. Isaak and P. Hajicek, Spherically symmetric systems of fields and black holes. I. Definition and properties of apparent horizon, Phys. Rev. **D30**, 1168 (1984).

[87] J. Gegenberg and G. Kunstatter, The Conformal Anomaly and One-

Loop Effective Action in a Midisuperspace Model, Phys. Lett. **B233**, 331 (1989).

[88] J. Gegenberg and G. Kunstatter, Quantum theory of black holes, Phys. Rev. **D47**, 4192 (1993).

[89] R. B. Mann, Conservation laws and two-dimensional black holes in dilaton gravity, Phys. Rev. **D47**, 4438 (1993).

[90] D. Louis-Martinez and G. Kunstatter, Birchoff's theorem in two-dimensional dilaton gravity, Phys. Rev. **D49**, 5227 (1994).

[91] D. Louis-Martinez, *Dirac's Constrained Systems: Two-Dimensional Gravity and Spinning Relativistic Particle*, Ph. D. thesis (unpublished), University of Manitoba, Winnipeg (1994).

[92] J. Gegenberg, D. Louis-Martinez and G. Kunstatter, Observables for two-dimensional black holes, Phys. Rev. **D51**, 1781 (1995).

[93] T. Banks and M. O'Laughlin, Two-Dimensional Quantum Gravity in Minkowski Space, Nucl. Phys. **B362**, 649 (1991).

[94] D. Zwillinger ed., *Standard Mathematical Tables and Formulae 30th Ed.*, CRC Press, Boca Raton (1996).

[95] R. M. Wald, *General Relativity*, The University of Chicago Press, Chicago (1984).

[96] D. Louis-Martinez and G. Kunstatter, Two-dimensional dilaton gravity coupled to an Abelian gauge field, Phys. Rev. **D52**, 3494 (1995).

[97] D. Christodoulou, A Mathematical Theory of Gravitational Collapse, Commun. Math. Phys. **109**, 613 (1987).

[98] G. Kunstatter, R. Petryk and S. Shelemy, Hamiltonian thermodynamics of black holes in generic 2D dilaton gravity, Phys. Rev. **D57**, 3537 (1998).

[99] J. Bland and G. Kunstatter, Asymptotic Behaviour of Choptuik Scaling and Scale Echoing in Spherically Symmetric Gravitational Collapse of Scalar Field, in preparation.

[100] R. L. Burden and J. D. Faires, *Numerical Analysis 4th Ed.*, Prindle, Weber & Schmidt, Boston (1988).

[101] P. R. Bevington and D. K. Robinson, *Data Reduction and Error Analysis in the Physical Sciences 3rd Ed.*, McGraw-Hill, New York (2002).

[102] G. Clément and A. Fabbri, Analytical treatment of critical collapse in

(2+1)-dimensional AdS spacetime: a toy model, Class. Quantum Grav. **18**, 3665 (2001).

[103] A. V. Frolov, Perturbations and critical behavior in the self-similar gravitational collapse of a massless scalar field, Phys. Rev. **D56**, 6433 (1997).

[104] S. Hayward, An extreme critical spacetime: echoing and black-hole perturbations, Class. Quantum Grav. **17**, 4021 (2000).

[105] Y. Peleg, S. Bose and L. Parker, Choptuik scaling and quantum effects in 2D dilaton gravity, Phys. Rev. **D55**, 4525 (1997).

[106] A. Papapetrou, *Lectures on General Relativity*, D. Reidel Publishing Company, Holland (1974).